Charles University

Faculty of Science

Ph.D. study program: Cell and Developmental Biology

M.Sc. QING ZHAO

The role of *Xenopus tropicalis* Immature Sertoli Cells in *Xenopus tropicalis* Tadpole Muscle Regeneration and Adult Frog Heart Regeneration

Doctoral Dissertation

Supervisor:

doc. RNDr. Ing. Vladimír Krylov, Ph.D.

Prague, 2025

Univerzite Karlova

Přírodovědecká fakulta

Doktorský studijní program: Buněčné a vývojové biologie

M.Sc. QING ZHAO

Úloha nezralých Sertoliho buněk *Xenopus tropicalis* v regeneraci svalů pulců *Xenopus tropicalis* a regeneraci srdce dospělých žab

Disertační práce

Školitel:

doc. RNDr. Ing. Vladimír Krylov, Ph.D.

Praha, 2025

Declaration of Authorship

I, Qing Zhao, declare that this dissertation titled, "*The role of Xenopus tropicalis Immature Sertoli Cells in Xenopus tropicalis Tadpole Muscle Regeneration and Adult Frog Heart Regeneration*" and the work presented in it are my own. All the literature is properly cited, and I have not been yet awarded any other academic degree or diploma for this thesis or its substantial part.

Signed:

Date: 22.05.2025

Acknowledgments

First and foremost, I would like to express my sincere gratitude to Charles University, Faculty of Science, for granting me the opportunity to study and conduct research in Prague. For me, Prague is an incredible place to live and work, and it holds many cherished memories from my PhD journey.

I am deeply thankful to my family for their unconditional love and unwavering support throughout this long and challenging process. I could not have come this far without their constant encouragement.

I would also like to express my heartfelt appreciation to my supervisor, Dr.Vladimir Krylov, for offering me the opportunity to join his research group and for his dedicated guidance throughout my doctoral studies. His enthusiasm for science and his logical approach to scientific thinking were a great source of inspiration. Despite his busy schedule with both administrative duties and research responsibilities, he always found time to support our work—be it through hands-on experiments, troubleshooting, or project discussions. Specifically, I want to highlight that, with his help, I made significant improvements: I developed my own logical approach to gene cloning, mastered microinjection techniques, and became proficient in scientific writing.

He also provided me with many opportunities to grow professionally, including a three-month internship at King's College London in the laboratory of Professor Peter Zammit, where I gained valuable experience in techniques related to human muscle cells. I am equally grateful to Professor Peter Zammit and his team for offering me the opportunity to expand my skill.

Lastly, I would like to extend my sincere thanks to Dr. Tereza Tlapáková for her generous help and support in all aspects of my PhD work. I also wish to thank two master students I worked with in the beginning two years of my project: Světlana Žabková, Irem Mertová , our lab manager: Jiří Vávra and all the other staff at our laboratory and at the Department of Cell Biology, Charles University, for their assistance and kindness throughout my research

Prague, May 22nd, 2025

Abstract

Overcoming immune rejection is always a trending topic in regenerative medicine and transplantation research. Sertoli cells (SCs), which possess immunoprotective properties provide a fascinating study point in cell-based therapy in regenerative medicine.

Xenopus tropicalis immature Sertoli cells (XtiSCs), derived from juvenile testes, retain the hallmark morphological and genetic signatures of Sertoli cells. *Xenopus tropicalis* (*X. tropicalis*) is a perfect model for both tail regeneration and heart regeneration research. In tadpole tail regeneration model, we discovered the novel role of XtiSCs in promoting muscle regeneration post tail amputation through mechanisms of interaction with macrophages which are crucial for regeneration success. Besides, XtiSCs have remarkable viability and homing capabilities. XtiSCs injection led to significant muscle fibre preservation and regeneration.

In adult frog heart regeneration model, XtiSCs also exhibit excellent viability that they could survive at the implantation site for over three weeks following hind limb muscle bed injection. Besides, we successfully developed a protocol for adult frog macrophage depletion via administration of clodronate liposomes into frog dorsal lymph sac. We found XtiSCs treatment significantly improved the morphology of the regenerated apex after its cutting and increased cardiac muscle regeneration.

Due to the current limitations in available antibodies for frog-specific studies, further exploration at the molecular level remains restricted. To address this, we initiated the development of transgenic *X. tropicalis* lines. Using CRISPR/Cas9-mediated homologous recombination, we successfully constructed two GFP knock-in plasmids targeting the *Pax7* and *MMP7* genes, and conducted preliminary experiments toward generating stable knock-in frog lines.

Overall, our study not only underscores the therapeutic potential of SCs in regenerative medicine but also offers valuable insights into immunomodulatory strategies that can enhance tissue repair and transplantation outcomes.

Key words: Immature Sertoli cells, *Xenopus tropicalis*, Tadpole, Tail Regeneration, Frog, Heart Regeneration, Macrophages, Transgene line, CRISPR/Cas9, Knock-in

Abstrakt

Překonání imunitní rejekce štěpu je stále aktuálním tématem v oblasti regenerativní medicíny a výzkumu transplantací. Sertoliho buňky (SCs), které vykazují imunoprotektivní vlastnosti, představují fascinující nástroj v oblasti studia buněčných terapií v rámci regenerativní medicíny.

Nezralé Sertoliho buňky druhu *Xenopus tropicalis* (XtiSCs), získané z juvenilních varlat, si zachovávají charakteristické morfologické a genetické znaky Sertoliho buněk. *Xenopus tropicalis* je ideálním modelem pro výzkum regenerace ocasu i srdce. V modelu regenerace ocasu pulců jsme objevili novou roli XtiSCs při podpoře svalové regenerace po amputaci ocasu prostřednictvím interakce s makrofágy, které jsou pro úspěšnou regeneraci zásadní. Kromě toho vykazují XtiSCs pozoruhodnou životaschopnost a schopnost cílené migrace. Injekce XtiSCs vedla k výrazné ochraně svalových vláken a podpoře jejich regenerace.

V modelu regenerace srdce dospělých žab XtiSCs rovněž prokázaly výbornou životaschopnost – přežívaly v místě implantace více než tři týdny po injekci do svalového lůžka v zadní končetině. Navíc jsme úspěšně vyvinuli protokol pro depleci makrofágů u dospělých žab pomocí aplikace klodronátových liposomů do lymfatického vaku dospělce *X. tropicalis*. Zjistili jsme, že aplikace XtiSCs významně zlepšila morfologii regenerovaného srdečního hrotu po jeho předchozí amputaci a zvýšila poměr srdečních svalových vláken oproti vazivu v rámci regenerace.

Vzhledem k omezené dostupnosti protilátek specifických pro drápatky je další výzkum založený na imunofluorescenci zatím omezen. Abychom tuto překážku překonali, zahájili jsme vývoj transgenních linií *X. tropicalis*. Pomocí homologní rekombinace zprostředkované CRISPR/Cas9 jsme úspěšně vytvořili dva knock-in plazmidové konstrukty s reportérovým genem GFP a cílenými na geny *Pax7* a *MMP7*. Zároveň jsme provedli předběžné experimenty směřující k vytvoření stabilních knock-in linií drápatky tropické.

Naše studie nejenže zdůrazňuje terapeutický potenciál Sertoliho buněk v regenerativní medicíně, ale také poskytuje cenné poznatky o imunomodulačních strategiích, které mohou zlepšit regeneraci tkání a výsledky transplantací.

Klíčová slova: Juvenilní Sertoliho buňky, *Xenopus tropicalis*, pulci, regenerace ocasu, žába, regenerace srdce, makrofágy, transgenní linie, CRISPR/Cas9, knock-in

Content

1 ABBREVIATIONS

XtiSCs: *Xenopus Tropicalis* Immature Sertoli cells

***X. tropicalis*:** *Xenopus tropicalis*

X. leavis: *Xenopus leavis*

SCs: Sertoli Cells

hCG: Human Chorionic Gonadotropin

MSCs: Mesenchymal Stem Cells

TGF-β: Transforming Growth Factor Beta

CCL2: Chemokine (C-C motif) ligand 2

CXCL12: C-X-C Motif Chemokine Ligand 12

NO: Nitric Oxide

LLC: Lewis Lung Carcinoma

BTB: Blood Testis Barrier

TIB: Testicular Immunological Barrier

FACS: Fluorescence-Activated Cell Sorting

DAPI: 4′,6-diamidino-2-phenylindole

FITC: Fluorescein Isothiocyanate

ECM: Extracellular Matrix

ROS: Reactive Oxygen Species

IL10: Interleukin-10

TALENs: Transcription Activator-like Effector Nucleases

CRISPR-Cas: Clustered Regularly Interspaced Short Palindromic Repeats-CRISPR Associated

TALE: Transcription Activator-like Effectors

GFP: Green Fluorescent Protein

IVF: In Vitro Fertilization

TNF-α: Tumor Necrosis Factor-α

P55: Tumor Necrosis Factor (TNF) Receptor Type 1

GSK3: Glycogen Synthase Kinase 3

Wnt: Wingless-Type MMTV Integration Site Family

dpf: Days Post-fertilization

hpa: Hours Post-amputation

dpa: Days Post-amputation

IFNγ: Interferon Gamma

ROCs: Re-Organisation Cells

EF: Electric Field

JI: Electric Current Density

TEP: Transepithelial Potential.

BMP: Bone Morphogenetic Protein

FGF: Fibroblast Growth Factor

Shh: Sonic Hedgehog

MI: Myocardial Infarction

CI: Cryoinjury

FGF: Fibroblast Growth Factors

PDGF: Platelet-Derived Growth Factor

VEGF: Vascular Endothelial Growth Factor

MLC2: Myosin Light Chain 2

DSB: Double-Strand Break

RVD: Repeat Variable Di-Residue

NHEJ: Non-Homologous End Joining

3UTR: 3'-Untranslated Region

mRNA: Messenger RNA

gRNAs: Guide RNAs

PBS: Phosphate buffered saline

MMR: Marc's Modified Ringer's Solution

MCS: Multiple Cloning Site

γCry: γ-Crystallin

PCR: Polymerase Chain Reaction

2 INTRODUCTION

Sertoli cells (SCs), the essential somatic components of the testis, play a dual role by not only nurturing developing germ cells but also safeguarding them from the immune system. As immune-privileged cells, SCs are integral to the formation of the blood-testis barrier and are uniquely equipped to modulate immune responses within their environment. Numerous studies have demonstrated that SCs can survive long-term following co-transplantation, both allogeneic and xenogeneic, enhancing graft survival and function in the absence of immunosuppressive therapy. Their immunoprotective properties have shown therapeutic potential in various pathological conditions, including diabetes (Dufour et al., 2003; Luca et al., 2016), ischemic injury (Milanizadeh et al., 2018), and Duchenne muscular dystrophy (Chiappalupi et al., 2016). These findings underscore the regenerative potential of SCs and support their continued exploration as a tool in cell-based therapies.

XtiSCs is a somatic cell line isolated from juvenile *Xenopus tropicalis* (*X. tropicalis*) testes, exhibiting morphological and gene expression characteristics of Sertoli cells (Tlapakova et al., 2016). XtiSCs underwent full epithelial-mesenchymal transition (EMT) upon EMT inducer CHIR99021 treatment, exhibiting differentiation capacity and migration potential towards Hela cells *in vitro* and towards the injury site *in vivo* in wounded tadpoles (Nguyen et al., 2019).

The two key events during muscle regeneration is muscle stem cells (namely satellite cells) activation, and the immune response. The inflammatory response after injury is coupled tightly with stages of myogenesis. Of them, inflammatory macrophages are recruited to the injury site within 24 hours after injury and later polarize toward anti-inflammatory macrophages (Arnold et al., 2007; Varga et al., 2016). Recent findings revealed that macrophages provided a niche for muscle stem cells during muscle regeneration (Ratnayake et al., 2021). Interestingly, Xenopus tadpoles are similar with mammals in muscle regeneration process, both in terms of $Pax7^{+}$satellite cell activation (Chen et al., 2006) and inflammatory response (inflammatory myeloid cells and reparative myeloid cells' activation) (Aztekin et al., 2020). Using *X. tropicalis* tadpoles as our experiment model, we investigated the effects of XtiSCs on tadpole muscle regeneration after its amputation and we found that XtiSCs could promote muscle regeneration in amputated tadpole tail through regulating macrophage numbers/possibly their phenotype, at the injection site and the regenerated tail. Collectively, this work investigated the role of

Sertoli cells on muscle regeneration as an immunoregulator for macrophage response, which provides basis for Sertoli cell therapy clinical research in the regeneration filed.

Heart disease is one of the leading causes of death worldwide, making the study of cardiac regeneration a critical area of research. The mammalian heart has very limited regenerative capacity upon injury, which was reported to be able to regenerate heart tissue within 1-6 days after birth, but this capacity is lost as they mature (Porrello et al., 2011). Interestingly, recent studies demonstrated that mammalian cardiogenesis continues throughout adult life, although the proliferation frequency is less than 1% in humans (Bergmann et al., 2009; Ali et al., 2014).

Different from mammals, lower vertebrates such as teleost fish and urodele amphibians (newts and axolotls) have an excellent capacity to regenerate cardiac tissue without scarring, and restore complete function. (Becker et al., 1974; Flink, 2002; Poss et al., 2002; Lepilina et al., 2006; Piatkowski et al., 2013). Anuran amphibians can fully regenerate the heart before metamorphosis, but this ability is reported to graduall diminishes as they transit from larvae to adult frogs in *Xenopus laevis (X. laevis)* (Marshall et al., 2019). In Xenopus frogs, it is notable to mention that Marshall et al. (2019) found that *X. laevis* frogs' hearts were unable to regenerate following endoscopy-based heart apex resection, while Liao et al. found that *X. tropicalis* frogs' hearts were capable of near scar-free regeneration following approximately 10% heart apical resection (Liao et al., 2017). *X .laevis* and *X. tropicalis* are two commonly used model organisms within the genus Xenopus, sharing huge similarities in morphology, developmental staging systems, and physiological pathways, etc. (P.d and J, 1994; Kashiwagi et al., 2010; Zahn et al., 2017; Phipps et al., 2020). The reported differences in heart regeneration capacity between the two species may be owing to species-specific factors, animal age, differences in resection protocols (such as the size of the resected tissue), and other variables (Liao et al., 2018). In the meantime, an intriguing question arises as to why *X. tropicalis* adults possess such extraordinary heart regeneration potential.

The immune response is closely associated with the heart regeneration process as well (Simões and Riley, 2022). Multiple immune cell types are active to establish an inflammatory and reparative immune state essential for tissue regeneration and recovery (Nahrendorf et al., 2007). Proinflammatory macrophages play a crucial role in clearing cell debris through releasing of pro-inflammatory cytokines, proteolytic enzymes, and ROS.

Anti-inflammatory macrophages become predominant as heart regeneration progresses. These cells produce anti-inflammatory and pro-fibrotic cytokines, such as IL-10 and TGF-β, which can ultimately lead to either successful regeneration or permanent fibrosis (Voll et al., 1997; Wan et al., 2013). A prolonged pro-inflammatory response can result in adverse tissue remodeling (Tripathi et al., 2020) and attenuation of the inflammatory response can cause impaired phagocytosis of dead cardiomyocytes, etc (Bujak et al., 2008).

By transplanting XtiSCs into adult frogs followed by apex resection of the frog heart, we investigated the role of XtiSCs in *X. tropicalis* heart regeneration. Our findings indicate that XtiSCs possess a remarkable ability to promote cardiac cell proliferation and reduce scar formation in both wild-type and macrophage-depleted frogs.

These study not only highlights the beneficial role of Sertoli cells in tadpole tail regeneration and frog heart regeneration, but also provides a theoretical basis for Sertoli cell-based therapeutic strategies in regenerative medicine.

Transgenic animals play a pivotal role in biology research. They are important tools for human disease research in terms of gene function study, disease intervention, etc. The two common used Xenopus strains, allotetraploid *X. laevis* and diploid *X. tropicalis* are tolerant with high efficiency of gene editing, and together with their accurate genome sequences (Hellsten et al., 2010; Session et al., 2016; Fisher et al., 2023;), make them an ideal model for transgene frog trials. CRISPR/Cas9 is revealed to be a highly efficient and easy-to-operate genome editing tool in the past years. The studies of injection of Cas9 mRNA, together with single guide RNA (gRNA), into fertilized eggs are reported to have successfully constructed gene-mutated frogs or knocked in frogs (Aslan et al., 2017; Mao et al., 2018; Naert and Vleminckx, 2018a; Mochii et al., 2024). Of them, one study applied CRISPR/Cas9-mediated knock-in strategy via utilizing ‘2 baits’ sequences which successfully integrated Green Fluorescent Protein (GFP) to the 3UTR region of targeted genes (Mao et al., 2018).

Pax7 is an important gene expressed in satellite cells (Seale et al., 2000; Halevy et al., 2004). Studies revealed that *Pax7* expressed in quiescent and newly activated muscle satellite cells and downregulated upon myogenic differentiation (Zammit et al., 2004; Collins et al., 2005;). In frogs, the *Pax7* activation during tadpole muscle regeneration is akin to the tissue repair events of mammals (Chen et al., 2006). *MMP7* is reportedly associated with macrophage function in inflammation (Parks et al., 2004; Paré et al., 2017; Jobin et al.,

2019). By utilizing the CRISPR/Cas9-mediated knock-in approach mentioned above, we successfully constructed *Pax7* and *MMP7* donor plasmid and injected Cas9 mRNA, gRNA and donor plasmid into 1-cell stage *X. tropicalis* embryos. F0 positive tadpoles were selected and raised to frogs. Validation was performed using genomic PCR and by breeding F0 frogs to obtain F1 offspring. While no F0 frogs carrying the knock-in construct were identified, the overall workflow provides an important foundational step toward the successful generation of transgenic knock-in *X. tropicalis* lines in our laboratory.

3 GENERAL BACKGROUND

3.1 Sertoli Cells and their Role in Spermatogenesis

Sertoli cells are the essential somatic cells within the seminiferous tubules (Fig.1), which which play key regulatory roles in ensuring testis development, normal spermatogenesis, and overall male fertility (França et al., 2016). In addition to their role in nourishing developing germ cells throughout spermatogenesis, Sertoli cells also function as phagocytes by engulfing residual cytoplasm and apoptotic germ cells during this process (Sertoli cell - Wikipedia).

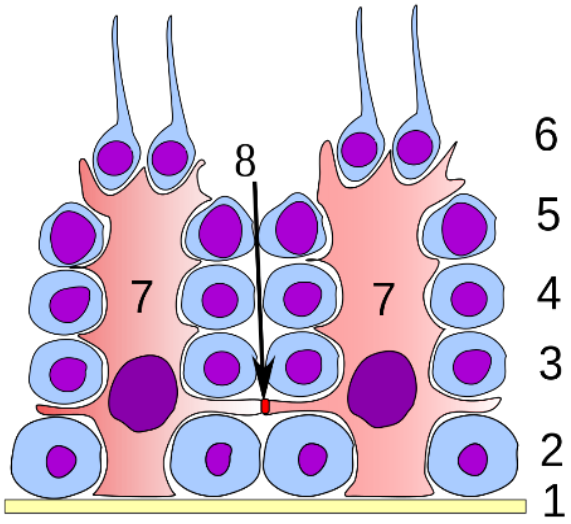

Figure 1. Germinal epithelium of the testicle.
1:basal lamina; 2-6:spermatogenic cells; 7: Sertoli cells; 8: tight junction (blood testis barrier); (Sertoli cell - Wikipedia)

Moreover, the occluding junctions of Sertoli cells form the blood-testis barrier (BTB), a structure that partitions the blood vessels and the seminiferous tubules of the testes (Fig. 2). Together with local immune suppression, provide an immunoprivileged microenvironment for the completion of meiosis (Fijak and Meinhardt, 2006; Mruk and Cheng, 2015).

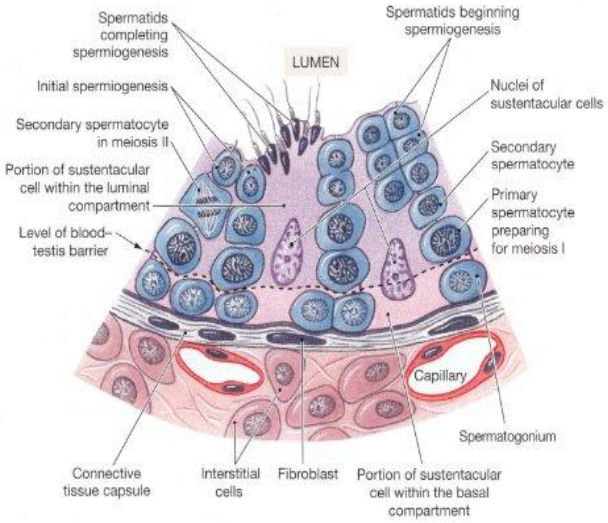

Figure 2. Schematic view of the seminiferous epithelium.
The germinal epithelium is divided by the Sertoli cell into two compartments: the basal and adluminal compartments. The basal compartment contains spermatogonium and newly formed primary spermatocytes, while the adluminal compartment contains meiotic primary spermatocytes and other spermatogenic cells. Fully formed spermatozoa are released into the lumen. The blood testis barrier is in the dashed line (J. Gordon Betts et al., 2022).

3.2 Sertoli Cells Used As Potential Clinical Treatment Approach

It was thought that the somatic cell populations within testes including Sertoli cells, Leydig cells, and peritubular myoid cells form a spermatogonial stem cell (SSC) niche which helps maintain stem cell phenotype and stimulate spermatogenic cell differentiation (Oatley and Brinster, 2012).

3.2.1 In Reproductive Dysfunction

Many reports reveal that Sertoli cells can be used for therapeutic treatment to male reproductive dysfunction. Massimo Menegazzo et al. revealed that *in vitro* co-culture of porcine Sertoli cells with human sperm increased its quality after 7 days (Menegazzo et al., 2011). Similarly, Mingming Wang et al. revealed that Sertoli cells co-culture with sperm improved in vitro fertilization (IVF) outcomes in mice by increasing sperm motility (Wang et al., 2021a).

3.2.2 In Improving Transplantation Outcomes

Early since 1980s, many studies have demonstrated that the immunoprotective environment of testes made it a promising host organ of transplants. Selawry et al. demonstrated that allogeneic islets transplanted to rats' surgically created cryptorchid testis made diabetic rats

normoglycemic after 24h and insulin was secreted from the islets (Halberstadt et al., 2004). Subsequent studies repeated and extended these findings, for example, neonatal porcine islets grafted into dog testes proliferated and secreted insulin and glucagon 2-3 month later, both in immunosuppressants group and non-immunosuppressants group (Gores et al., 1999).

Further experiments revealed that the somatic cell populations from testes (referred as Sertoli cells in general, with Sertoli cells as majorities for example, ~95% Sertoli cells, 5% myoid cells and others) were carrying this immuno-protective role. The isolation principle is to remove interstitial cells (mainly the Leydig cells outside of seminiferous tubules) by enzyme digestion and then make single cell suspension of seminiferous tubules while removing as much as possible the spermatogenic cells through centrifuge. Sertoli cells will adhere at the final cell culture step. Co-transplantation of Sertoli cells with islets showed much longer cure than islets-only control (Selawry and Cameron, 1993) in rats. Francesca Fallarino and Giovanni Luca et al. reported that neonatal microencapsulated porcine Sertoli cells injection alone led to diabetes prevention and reversion in overtly diabetic (nonobese diabetic [NOD]) mice through inducing neogenesis of beta-cells (Fallarino et al., 2009; Luca et al., 2010).

Besides diabetes research, Sertoli cells are reported to function in treatment of many other diseases. Sara Chiappalupi et al. found that microencapsulated Sertoli Cells injection to dystrophic mice significantly reduced chronic DMD conditions in Mdx mouse model and showed protection effect when conducted presymptomatic treatment. Further, they revealed that microencapsulated Sertoli Cells injection restored muscle morphology and performance in dystrophic mice and Sertoli Cells had promyogenic and antifibrotic effects on dystrophic myoblasts (Chiappalupi et al., 2015; Chiappalupi et al., 2016; Salvadori et al., 2021). P R Sanberg et al. demonstrated that Sertoli Cells had trophic effect on dopamine neurons and alleviated hemiparkinsonism in rats (Sanberg et al., 1997). Alpa A Trivedi et al. revealed that Sertoli cells could be used as a carrier of ex vivo gene in the injured spinal cord (Trivedi et al., 2006).

The mechanism of Sertoli cells' immunological protection is widely addressed (Selawry et al., 1991; Lynch et al., 1995; Suarez-Pinzon et al.,; 2000 Kaur et al., 2020). Here we put three researches about the possible physical interaction between Sertoli cells and immune cells. First, Sertoli cells express the p55 TNF-α receptor, while testicular macrophages under stress can secret TNF-α, which hints the possible interaction between Sertoli cells and macrophages (Moore and Hutson, 1994; Mauduit et al., 1996). Second, co-culture of Sertoli

cell line derived from *X. tropicalis* (XtiSCs) with murine macrophages showed that there were significant increase of interleukin (IL)10 and significant decrease of Lymphocytes Expressing Interferon-gamma (IFN-γ) compared to both unstimulated cells and xenogeneic control (Vegrichtova et al., 2022). Third, Hassan Kabbesh et al. revealed that Sertoli Cells are the main constituent of the testicular immunological barrier (TIB) by transmigration experiment of LeukoTracker-labeled M0, M1, and M2 macrophages through mono- and co-cultures of Sertoli cells (Kabbesh et al., 2023).

3.3 *Xenopus Tropicalis* Immature Sertoli Cells (XtiSCs)

Our laboratory has successfully established a somatic cell line from testes of juvenile *X. tropicalis* frogs exhibiting morphological and gene expression characteristics of Sertoli cells (referred as XtiSCs). Long-term cultivation promotes the formation of colonies which resemble embryonic stem cells (ESCs). Katushka RFP under CAG promoter was then transfected into the cell line to trace the cell movement (Tlapakova et al., 2016). XtiSCs underwent full epithelial-mesenchymal transition (EMT) upon EMT inducer CHIR99021 treatment. After a three-day treatment with CHIR99021, XtiSCs exhibited a morphological transition from a cobblestone-like shape to an elongated, rod-like form (Nguyen et al., 2019). All of these characteristics of XtiSCs are illustrated in Fig. 3.

Microinjection to the peritoneal cavity of two days old tadpoles showed that the RFP signal was enriched mainly in heart, pronephros and intestine (Tlapakova et al., 2016). We also found limited differentiation of XtiSCs primarily into osteocytes and less frequently into adipocytes and chondrocytes. Interestingly, cell treatment with GSK3 inhibitor CHIR99021 (activator of Wnt signaling pathway) enhances their differentiation potential towards cardiomyocytes in microinjection experiments into the peritoneal cavity in 2 days post-fertilization (dpf) tadpoles (Nguyen et al., 2019).

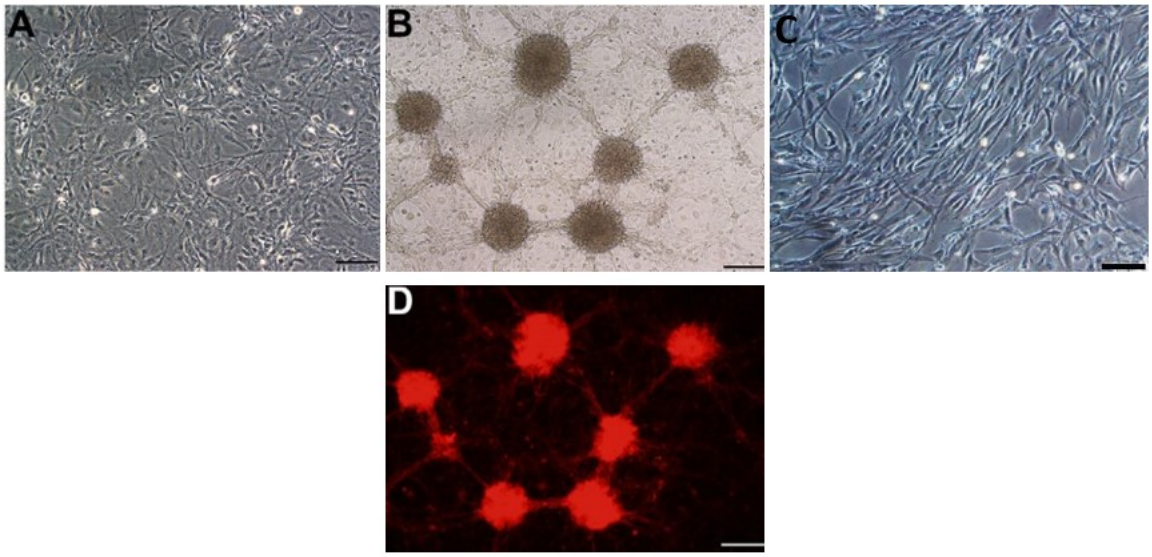

Figure 3. XtiSCs cell culture characterization.
(A) XtiSCs cell culture in monolayer in short term culture. (B) Formation of cell colonies in long term cultivation of XtiSCs. (C) XtiSCs after GSK-3 inhibitor CHIR 99021 treatment in 3 days, with morphological changes into fibroblast-like shape. (D) RFP-positive cell colonies of XtiSCs. Scale bar A,C: 100 µm; B,D: 200 µm (Tlapakova et al., 2016)

3.4 Muscle Regeneration

The regeneration potential in lower vertebrates is robust throughout life, while in higher vertebrates such as mammals, particularly humans, is limited or absent (Iismaa et al., 2018). Muscle regeneration shares common features with muscle development because the molecular pathways that underlines prenatal development is reactivated when tissue reconstruction after injury (Hawke and Garry, 2001; Chargé and Rudnicki, 2004).

The most important two events during muscle regeneration is muscle stem cells (namely satellite cells) activation, and the immune environment response. As illustrated in Fig. 4, satellite cells located beneath the basal lamina surrounding individual myofibres which are mitotically quiescent until exposed to physiological stimuli (such as exercise) and pathological conditions (such as injury and degenerative diseases) (Gayraud-Morel et al., 2009). *Pax7* is a canonical biomarker of most quiescent and proliferating satellite cells as it is expressed across multiple species, including human, mouse, monkey, salamander, frog, and zebrafish, et al. (Seale et al., 2000; McLoon and Wirtschafter, 2003; Chen et al., 2005; Relaix et al., 2005; Morrison et al., 2006; Hammond et al., 2007). After satellite cell activation, *MyoD*, *Myf5*, Myogenin and *MRF4* are expressed to initiate myoblast differentiation and proliferation (Musarò, 2014). Certain satellite cell populations then downregulate muscle

specific markers and return back into quiescent state to maintain the stem cell pool (Zammit et al., 2004).

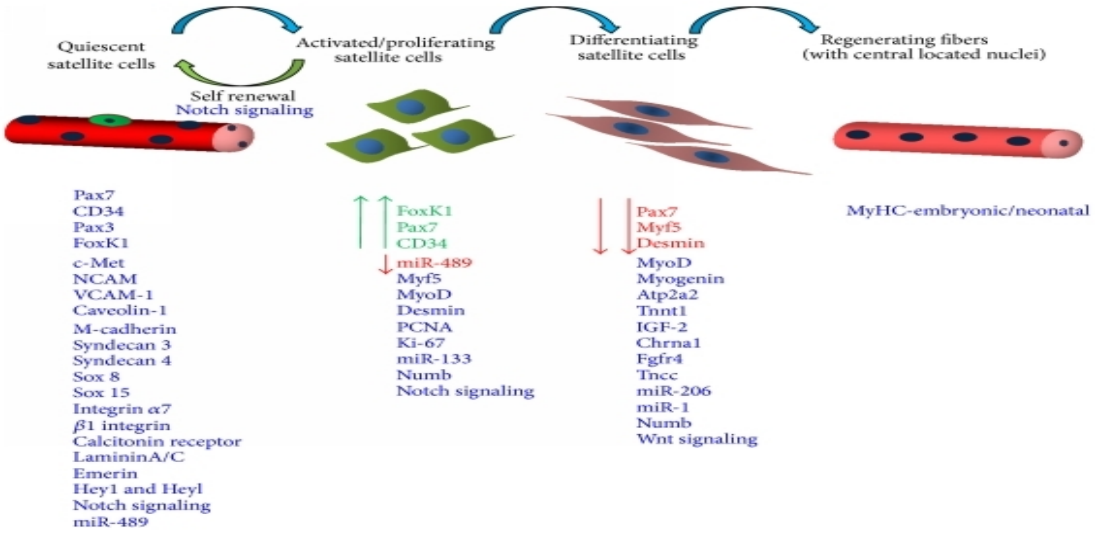

Figure 4. The diagram of Satellite Cells' quiescence, activation, proliferation, differentiation. (Musarò, 2014)

The inflammatory response after injury is coupled tightly with stages of myogenesis (Fig. 5). Early after injury, neutrophils are the first inflammatory myeloid cells that invade the injury site, decrease after 24h and disappear after 36–48h (Belcastro et al., 1996). Ly6Chi monocytes/macrophages rapidly increase within 24h after injury and secrete proinflammatory cytokines such as interferon-γ (IFNγ) and tumour necrosis factor (TNF) as well as nitric oxide (NO) which promote myoblast proliferation and inhibit differentiation. 2–3 days after, Ly6Clo macrophages become the predominant subsets and release anti-inflammatory cytokines such as IL-4 and IL-13 as well as transforming growth factor-β (TGF-β) which inhibit myoblast proliferation and stimulates their differentiation and fusion (Arnold et al., 2007; Cordani et al., 2014). The inflammatory vs. reparative capacity of macrophages are often referred to as M1 or M2 macrophages, while an *in vivo* muscle injury induced by cardiotoxin showed that Ly6Chi and Ly6Clo macrophages partially overlap with M1 and M2 gene expression patterns, respectively (Varga et al., 2016).

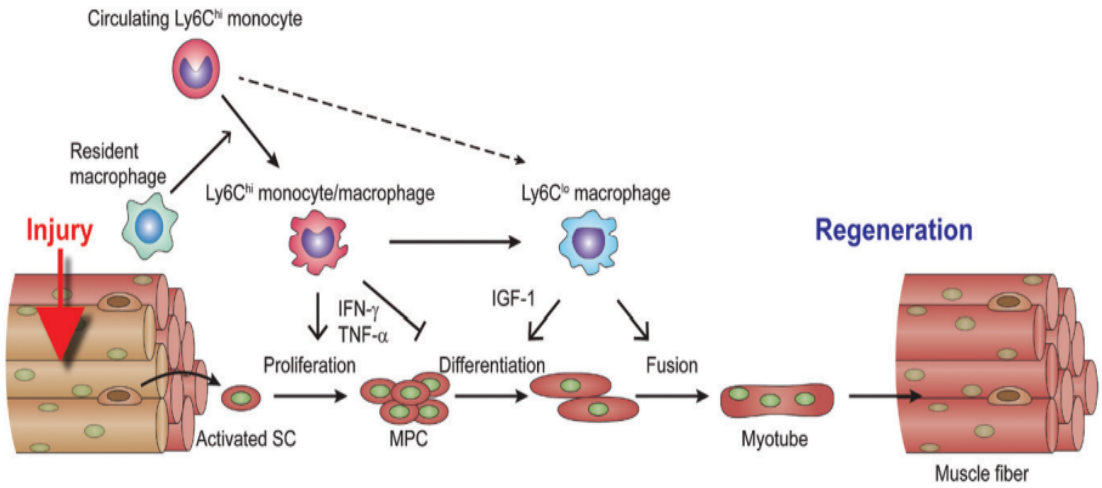

Figure 5. Macrophages and regulators in muscle regeneration.(Oishi and Manabe, 2018)

3.5 Tail Regeneration Study in Xenopus

Xenopus tadpoles possess the remarkable ability to regenerate their tails, including all major tissue types such as the spinal cord, blood vessels, muscle, and fin (Fig. 6A), from early tailbud stages (Deuchar, 1975) through to pre-metamorphosis (Deuchar, 1975; Nieuwkoop, 1994; Love et al., 2011; Gaete et al., 2012a; Phipps et al., 2020). Interestingly, this regenerative capacity is transiently lost during the onset of feeding stages in *X. laevis*, a phase referred to as the "refractory period" (Beck et al., 2003). In contrast, *X. tropicalis* does not exhibit this refractory period and retains the ability to regenerate the tail throughout all pre-metamorphic stages (Wang and Shi, 2021).

Regeneration proceeds through three stages: (1) an initial phase involving wound closure and an inflammatory response during 0–1 days post-amputation (dpa); (2) the formation of a blastema-like regenerative bud at approximately 1–2 dpa; and (3) a subsequent outgrowth and overt regeneration phase beginning around 2–3 dpa (Love et al., 2011).

The initiation of a regenerative programme is regulated by a variety of molecular mechanisms, including key developmental signaling pathways such as Notch, bone morphogenetic protein (BMP), Wnt, fibroblast growth factor (FGF), transforming growth factor β (TGFβ), and Sonic hedgehog (Shh) (Beck et al., 2003; Ho and Whitman, 2008; Lin and Slack, 2008; Love et al., 2011; Lin et al., 2012; Taniguchi et al., 2014; Aztekin et al., 2019). In addition to these pathways, further studies have underscored the importance of cellular processes and components, such as apoptosis, the extracellular matrix (ECM), and regeneration-organizing cells (ROCs), in orchestrating successful tissue regeneration (Tseng et al., 2007; Contreras et al., 2009; Aztekin et al., 2019).

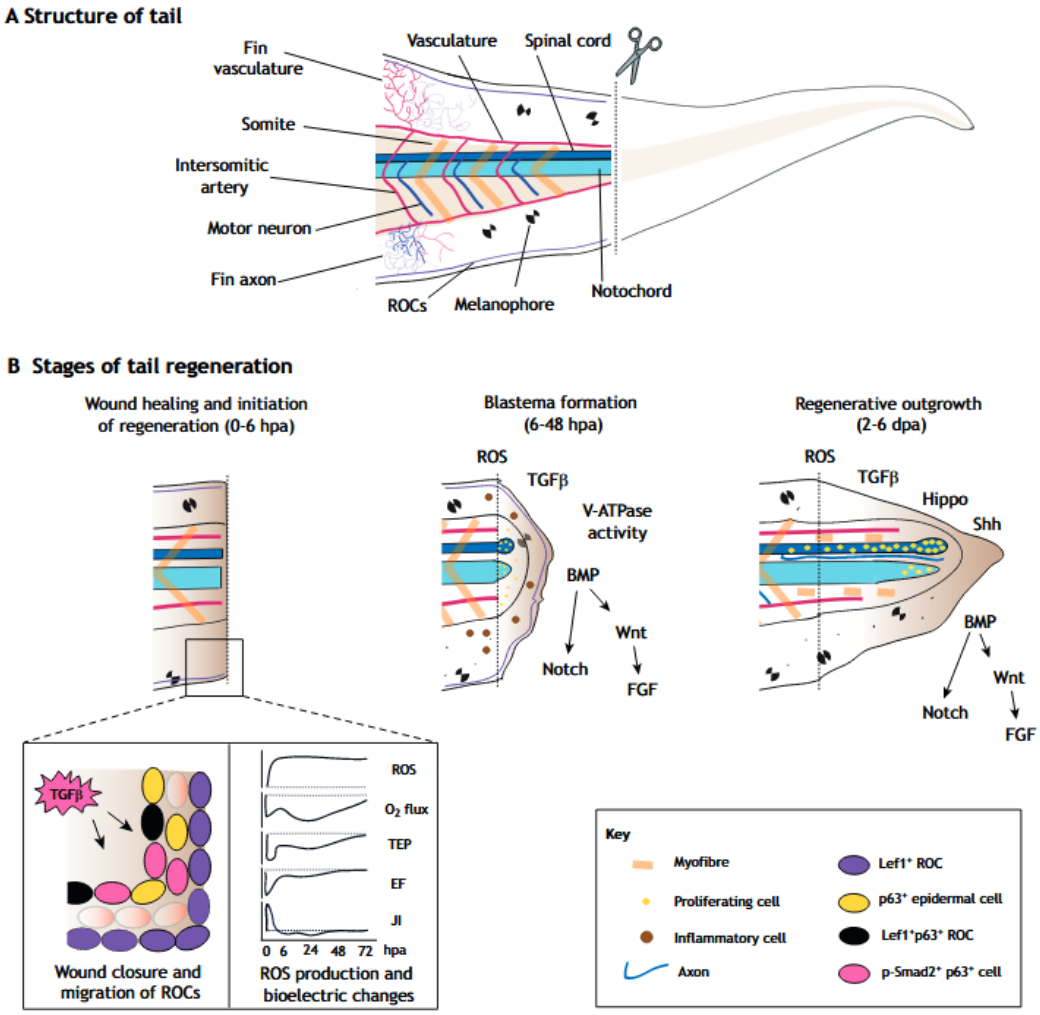

Figure 6. Tail regeneration.
(A) The image illustrates the anatomy of an intact Xenopus tadpole tail, which comprises somitic muscle (orange), a notochord (light blue), vasculature (red), and epidermal cells. It also includes recently identified regeneration-organizing cells (ROCs, purple), melanophores (black), a spinal cord (dark blue), and motor neurons. (B) The key stages of Xenopus tail regeneration are depicted. Wound healing initiates immediately after amputation, with the first 0–6 hours post-amputation (hpa) marking the onset of regeneration. This early phase involves bioelectrical changes and the upregulation of key signaling molecules, including reactive oxygen species (ROS) and transforming growth factor β (TGFβ). Between 6–48 hpa, a blastema forms, comprising proliferative cells and early regenerative structures such as the spinal cord and notochord. From 2 days post-amputation (dpa), regenerative outgrowth commences, with the regenerate extending along neuronal axons from the rostral spinal cord and accompanying outgrowth of the spinal cord, notochord, and vasculature. Concurrently, existing myofibres undergo degeneration and are replaced by newly formed myofibres derived from Pax7+ satellite cells. Melanophores reappear in the regenerate from melanophore precursors. Several major signaling pathways active during regeneration are depicted in the accompanying schematic, including those involving the electric field (EF), current density (JI), and transepithelial potential (TEP) (Phipps et al., 2020).

3.5.1 *Xenopus Tropicalis* and *Laevis* Are Favorable Models for Muscle Regeneration Study

Xenopus (*X. laevis* and *X. tropicalis*) are one of the most commonly used experimental organisms, featured in their large quantity and easy to manipulate embryos, rapid embryo growth and development, fully sequenced and well annotated genome as well as remarkable structural similarity with the human genome (Nenni et al., 2019). Xenopus can achieve both scar-free healing and tissue regeneration during its larval stages, while it loses these abilities during metamorphosis and adulthood in most tissues (Stocum, 1992).The regeneration mainly includes three phases: (1) Early phase: inflammatory-like phase by 6hpa; (2) Intermediate phase: cell proliferation beginning at 24 hpa; (3) Late phase: regrowth phase of differentiated tissues, such as neurons, notochord, muscle and vasculature by 48 and 72 hpa (Love et al., 2011). Intriguingly, Xenopus shares many common features with humans in both satellite cell activation process and inflammatory response after injury. Ying Cheng et al. revealed that the muscle regeneration in Xenopus tails was similar to muscle repair in mammals, through which process $Pax7^+$ satellite cells were activated to repair the damaged muscle (Chen et al., 2006). Roberto Paredes et al. demonstrated that the inflammatory response in Xenopus larvae was similar to that seen in human patients following injury (Paredes et al., 2015).

3.6 Heart Regeneration

The regeneration process restoring tissue architecture was built through a sequential events including cellular proliferation, differentiation and dedifferentiation and coordinated morphogenic rearrangements (Uygur and Lee, 2016).

The heart regeneration capacity differs a lot among different species upon injury. As depicted in Fig. 7 and 8, in vertebrates, adult mammalian heart could not regenerate including human, mouse, etc. While urodele amphibians and teleost fish have remarkable cardiac regeneration capacity throughout life (Oberpriller and Oberpriller, 1974; Poss et al., 2002; Witman et al., 2011; Gamba et al., 2014). Specifically, zebrafish is able to fully regenerate their hearts with minimal scarring and fully restore cardiac function (Poss et al., 2002). Interestingly, two commonly used anuran amphibians animal models *X. laevis* and *X. tropicalis* behaves differently when it comes heart regeneration: both species are able to regenerate its heart before metamorphosis, while it was reported that *X. laevis* didn't retain

the ability to regenerate its heart and *X. tropicalis* could fully regenerate its heart after apical resection(Liao et al., 2017; Liao et al., 2018; Marshall et al., 2019).

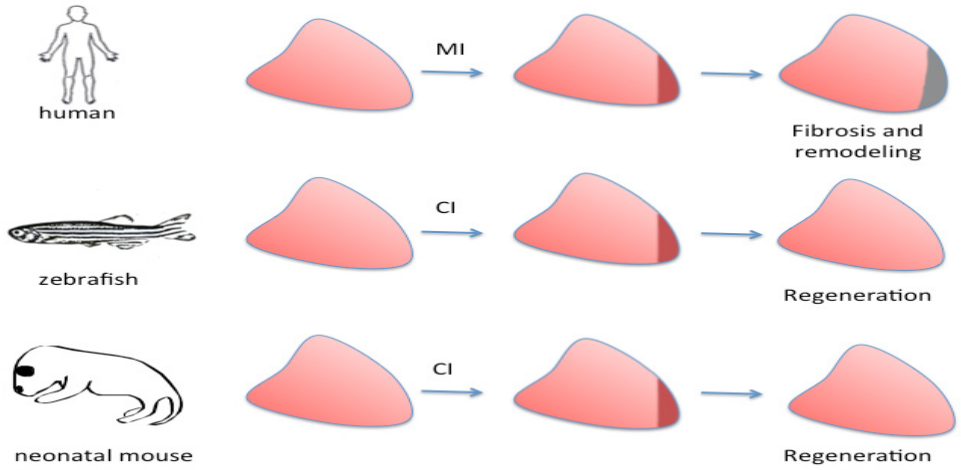

Figure 7. Different regenerative capacities of the hearts of adult humans, adult zebrafish and neonatal mice.
In adult humans, myocardial infarction (MI) leads to irreversible loss of cardiomyocytes, which are subsequently replaced by fibrotic tissue (brown), resulting in the formation of a permanent scar (grey). In contrast, zebrafish possess a remarkable capacity for cardiac regeneration; following cryoinjury (CI), they form a transient fibrotic scar (brown) that is eventually resolved, allowing for complete myocardial regeneration. Similarly, neonatal mice exhibit regenerative potential, capable of restoring myocardium after cryoinjury or ventricular resection, but this ability is limited to the first week of postnatal life (Sanchez-Iranzo et al., 2013).

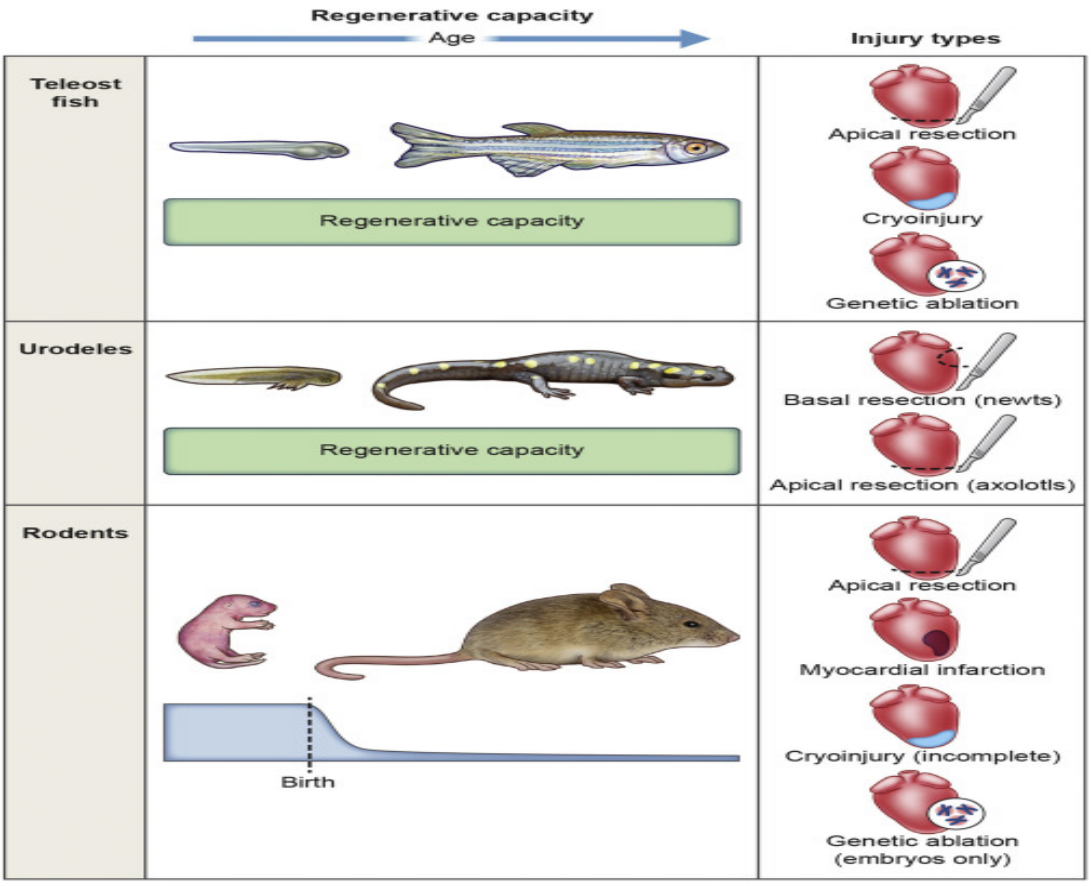

Figure 8. Heart Regeneration across Model Organisms.
Regenerative capacity is conserved in adult teleost fish and urodeles but undergoes developmental loss in anurans and mammals. (Uygur and Lee, 2016)

3.6.1 Heart Regeneration Mechanisms

Heart regeneration is an orchestrated process, of which cardiomyocyte proliferation plays a central role (Fig. 9). The immune response is tightly coupled with the proliferation process and extracellular matrix deposition which is controlled by signals from the epicardium following injury creates a permissive environment for cellular proliferation. Angiogenesis which is triggered by FGF and PDGF signaling can provide oxygen and nutrients to regrow the tissue. Nerves also play an indispensable role in heart regeneration including direct cellular interactions, secretion of signaling molecules, and modulation of the microenvironment.

Cardiomyocyte proliferation is considered as the central mechanism during heart regeneration. It was considered for many years that the postnatal human heart was not able to do cell renewal which caused the non-regenerative capacity of human heart upon injuries. However, this view was overturned over the last decades, revealing that mammalian

cardiogenesis occurs during adult life, including in humans (Bergmann et al., 2009; Bergmann et al., 2015).

Clinical reports of infant heart surgeries (Fratz et al., 2011) and a case study of a newborn with myocardial infarction (Haubner et al., 2016) suggest that the human neonatal heart possesses a notable regenerative capacity and can functionally recover from injury. Similarly, in neonatal mice, a regenerative response is observed immediately after birth. Porrello et al. demonstrated enhanced cardiomyocyte proliferation and robust angiogenic growth following resection or myocardial infarction (MI) in neonatal mice, but only within a narrow postnatal window (Porrello et al., 2011; Porrello et al., 2013). Upon injury, the neonatal mouse heart exhibits rapid hemostasis, infiltration of inflammatory cells, epicardial activation, and cardiomyocyte proliferation—features reminiscent of the regenerative responses seen in teleost fish and axolotls. Importantly, the newly formed cardiomyocytes predominantly originate from pre-existing cardiomyocytes that re-enter the cell cycle (Porrello et al., 2013; Haubner et al., 2016), as also observed in zebrafish (Lepilina et al., 2006; Jopling et al., 2010). Notably, this regenerative capacity diminishes rapidly, as it is absent by postnatal day 7 or 14, indicating a swift loss of cardiac regenerative potential in mammals after birth.

The inflammatory system responds immediately to heart injury in all vertebrate species studied so far (Kyritsis et al., 2012; Xin et al., 2013). Macrophage regulation is pivotal for cardiac regeneration, with their polarization states (pro-inflammatory M1 vs. reparative M2) affecting outcomes such as fibrosis resolution or scar formation. Macrophages could promote angiogenesis, clear apoptotic cells, and secrete regenerative factors for example VEGF and IL-10, and the imbalances between M1 and M2 macrophages activity can drive pathological remodeling (Aurora et al., 2014; Lavine et al., 2014). Neonatal hearts, which retain regenerative capacity, exhibit temporally coordinated macrophage recruitment and phenotype switching, which is lost in adults (Haubner et al., 2016; Pinto et al., 2016). Non-regenerating species resolve inflammation via fibrotic scarring, whereas regenerating animals achieve tissue restoration through cellular repopulation.

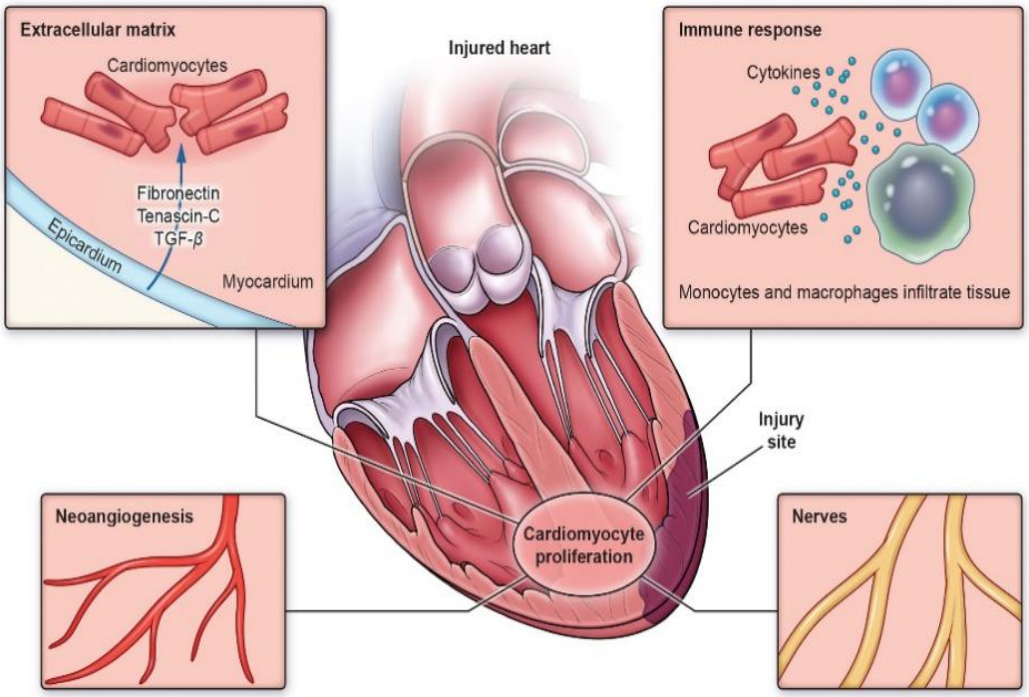

Figure 9. Evolutionarily Conserved Mechanisms of Cardiac Regeneration.
Cardiomyocyte proliferation is a fundamental component of cardiac regeneration. The inflammatory response plays a pivotal role in orchestrating the balance between cellular proliferation and tissue repair. Following injury, the deposition of extracellular matrix (ECM) establishes a supportive microenvironment conducive to regeneration, which is modulated by paracrine signals from the epicardium. Concurrently, neoangiogenesis, mediated by fibroblast growth factor (FGF) and platelet-derived growth factor (PDGF) signaling pathways, facilitates the delivery of oxygen and nutrients essential for tissue regrowth. Additionally, emerging evidence indicates that proper innervation is a critical factor for the successful regeneration of cardiac tissue (Uygur and Lee, 2016).

3.6.2 *X. tropicalis and X. laevis* In Frog Heart Regeneration Study

Both *X. tropicalis and X. laevis* larvae possess a remarkable capacity for complete heart regeneration following injury. However, their regenerative potential diverges dramatically in adulthood. In *X. laevis*, the adult heart loses this regenerative ability and instead responds to injury with fibrotic scarring, similar to the mammalian response (Marshall et al., 2019). In contrast, studies using *X. tropicalis* have shown that the adult heart can regenerate following ventricular apex resection without forming scar tissue (Liao et al., 2017).

Further insights into the regenerative mechanisms in *X. tropicalis* were gained through the use of a transgenic reporter line, Tg(mlc2:H2C), which expresses mCherry in cardiomyocyte nuclei under the control of the myosin light chain 2 (mlc2) promoter. This model demonstrated that cardiomyocyte proliferation contributes to heart regeneration in the adult *X. tropicalis* following injury (Xiao-Lin Lin et al., 2024).

Discrepancies in the regenerative outcomes between *X. laevis* and *X. tropicalis* have been the subject of insightful discussions between the research groups leading these studies (Liao

et al., 2018; Marshall et al., 2018). Several factors likely contribute to the observed differences. Similar variability in regenerative potential has been noted in other vertebrate groups. For example, within teleost fish, zebrafish exhibit robust and lifelong cardiac regeneration (Poss et al., 2002), whereas this ability is absent in medaka (Ito et al., 2014). One major factor is the age of the animals used in the studies: Marshall et al. employed 5-year-old *X. laevis*, whereas Liao et al. used 1-year-old *X. tropicalis*. Age-related decline in regenerative capacity is well documented in multiple models. Additionally, differences in surgical technique may influence regeneration outcomes. Endoscopic resection used in the *X. laevis* study resulted in larger clot formation compared to the smaller clots observed after apical resection in *X. tropicalis*. The specific site of injury also plays a role in the regenerative outcome, as different cardiac regions may differ in their ability to regenerate.

During metamorphosis, Xenopus undergoes significant immune system maturation, a process that correlates with the loss of regenerative capacity (Godwin and Rosenthal, 2014). While inflammation is essential for initiating regenerative responses, it can also inhibit regeneration under certain conditions. In salamanders, for example, Godwin et al. (Godwin et al., 2017) demonstrated that macrophage depletion at early time points following cardiac injury leads to regeneration failure, suggesting that heart regeneration is dependent on a properly timed innate immune response. Together, these studies in amphibians highlight the critical role of inflammation and immune system dynamics in governing regenerative capacity.

3.7 Transgenic Lines in Xenopus

Among the two main Xenopus species (*X. laevis* and *X. tropicalis*) used in biomedical research, *X. laevis* has been predominantly used since the 1950s due to its large size and experimental robustness. But due to its allotetraploid genome and relatively long generation time (10-12 months), its genetic tractability is poor. Recent years, *X. tropicalis* was frequently used as a genetic model because of its shorter generation time (5-7 months) and genuine diploid genome.

Transgene frogs serve as an ideal model to study vertebrate development and human disorders. Commonly used genome-editing methodology which allows for the rapid creation of mutant frogs to model human diseases including ZFN transgenes, TALENs and CRISPR-Cas methods.

ZFNs (Sequence-specific zinc finger nucleases) are the fusion of the nonspecific cleavage domain of the type IIS restriction enzyme FokI with a zinc-finger protein which are designed to cleave predetermined genomic sites, generating targeted double-strand breaks (DSBs) that enable site-directed mutagenesis and genome editing(Gaj et al., 2012; Miller et al., 1985; Young et al., 2011).

TALE proteins contain a central domain with 33–35 amino acid repeats, termed repeat-variable diresidues (RVDs). These RVDs confer sequence-specific DNA binding, allowing TALEs to theoretically target virtually any predefined genomic locus (Bogdanove and Voytas, 2011). Two TALEN arms recognize and bind the DNA sequence with a small 15-25 base spacer region in between which allows the dimerization of fused Fok1 endonuclease and activate its catalytic domain, to create site-specific DNA double-strand breaks (DSBs) (Christian et al., 2010; Li et al., 2011; Mahfouz et al., 2011; Miller et al., 2011). The TALEN-induced mutations was first introduced in *X. tropicalis*, resulting in efficient somatic and germline mutagenesis (Ishibashi et al., 2012; Lei et al., 2012) .

Another genome editing technique is CRISPR-Cas9, and it has been more widely used due to its simpler design. CRISPR (clustered regularly interspaced short palindromic repeats) comprises DNA sequences in prokaryotic genomes. These sequences originate from bacteriophage DNA fragments that previously infected the host prokaryote or its ancestors, forming an adaptive immune archive (Barrangou, 2015; Rath et al., 2015; Hille et al., 2018). Cas is CRISPR-associated genes that are adjacent to these elements. Cas9 endonuclease enzymes together with CRISPR sequences form the basis of a technology known as CRISPR-Cas9 to edit genes within living organisms (Bolotin et al., 2005; Jinek et al., 2012; Cong et al., 2013; Wright et al., 2016; Bak et al., 2018).

Till now, the applications in Xenopus is being exploited more and more (Blitz, 2012; Shi et al., 2022; Naert and Vleminckx, 2018b).

3.7.1 CRISPR-Cas9 Knock-In Strategy for Generating Transgenic *X. tropicalis*

CRISPR/Cas9-mediated knock-in using a donor plasmid and a homology-independent DNA repair mechanism has emerged as a powerful tool for generating reporter gene transgenic animals. To avoid the integration of unnecessary plasmid backbone sequences, Mao et al. developed an efficient and precise strategy using a donor plasmid flanked by two identical Cas9 target sites on both sides of the transgene cassette (Mao et al., 2018). When co-injected with Cas9 mRNA and guide RNAs (gRNAs) into one-cell stage fertilized *X. tropicalis*

embryos, simultaneous cleavage occurs at both the targeted genomic site and within the donor plasmid. This promotes the precise insertion of the cassette into the genome without plasmid backbone contamination.

In this system, the donor cassette contains a fluorescent reporter gene under a ubiquitous or tissue-specific promoter. For example, when the cassette is correctly integrated into the target locus, mCherry is expressed in the eyes (serving as a co-injection marker), and GFP is expressed in a tissue-specific manner, depending on the endogenous gene's expression. This strategy has been successfully applied to integrate EGFP into the *GAPDH* locus in human cells and the *Myh6* locus in *X. tropicalis*, demonstrating its cross-species applicability.

Following this two-guide CRISPR knock-in approach (Fig. 10), we constructed donor plasmids targeting the 3' UTR regions of *Pax7* and *MMP7* in *X. tropicalis*. These constructs were co-injected with Cas9 mRNA and gene-specific gRNAs into one-cell stage embryos. We obtained F0 tadpoles displaying KatushkaFP fluorescence in the eyes, along with GFP expression in putative target tissues, indicating preliminary success in targeted cassette integration.

These positive F0 tadpoles were raised to sexual maturity, and outcrosses were performed to generate F1 offspring. Unfortunately, no F1 tadpoles exhibiting reporter gene expression were obtained, suggesting that stable germline transmission was not achieved in this trial. Nevertheless, this work represents an important step toward establishing transgene knock-in techniques in *X. tropicalis* and provides valuable experience for future optimization.

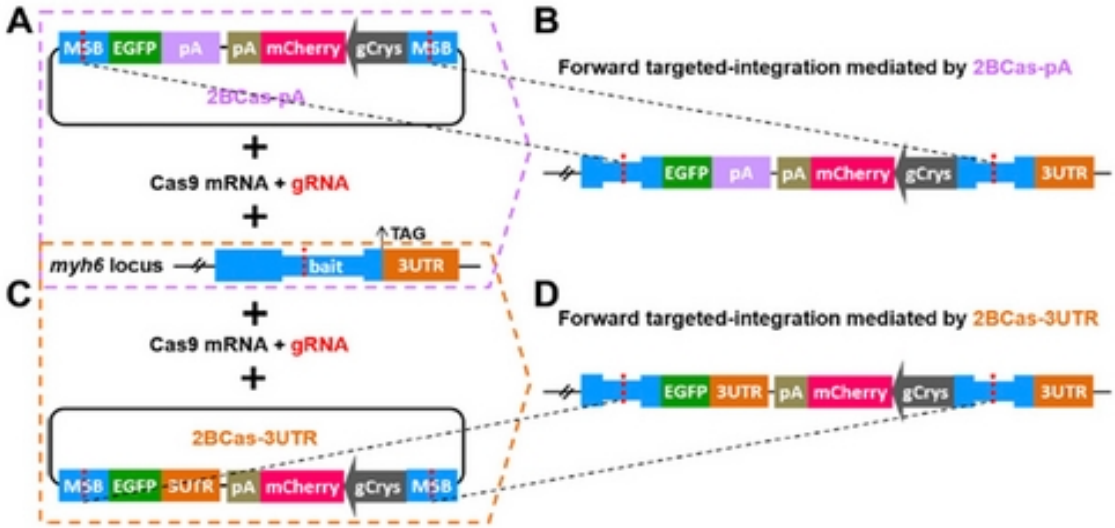

Figure 10. A diagram of the 2-bait Cas strategy

(A, B) The two-bait CRISPR/Cas9 strategy, based on a donor plasmid containing a transcriptional terminator, simultaneously cleaves the target genomic locus and dual bait sites in the donor construct,

generating coordinated DSBs to drive targeted integration. This facilitates targeted integration of the EGFP cassette into the *myh6* locus (an example from Mao et al. experiment) in the forward orientation, primarily utilizing the non-homologous end joining (NHEJ) pathway. (C, D) Similarly, a two-bait CRISPR/Cas9 approach using a donor plasmid harboring the 3′ untranslated region (3′UTR) of the *myh6* gene creates coordinated cleavages at the genomic target site and two baits of donor plasmid. This also promotes targeted forward integration of the EGFP reporter into the myh6 locus through the NHEJ pathway (Mao et al., 2018).

4 MATERIALS AND METHODS

4.1 Chemicals

β-mercaptoethanol, 55mM (Life Technologies)

Agarose (Lonza)

Ampicillin (Amresco)

Bovine serum albumin (Sigma-Aldrich)

Cysteine (Sigma-Aldrich)

Collagenase A (Roche)

Clodronate Liposomes (Liposoma Technology)

Control Liposomes (Liposoma Technology)

DNase I (Sigma Aldrich)

DAPI (Intimex s.r.o.)

Ethanol,absolute (Penta)

Ethidium bromid (Merck Life Science s.r.o.)

Ficoll (Sigma-Aldrich)

Fluorescent Dil Liposomes (Liposoma Technology)

Formaldehyde,37% (Penta)

Gentamicin, 50µl/mL (Gentaveto)

Horse Serum (Gibco)

Human chronic gonadotropin hormone, C1063 (Sigma-Aldrich)

Kanamycin (Sigma-Aldrich)

L-15 medium Leibovitz (Life Technologies)

L-glutamine, 200mM (Sigma-Aldrich)

Mowiol/DAPI (Sigma-Aldrich)

O.C.T.™Compound 4583 (Tissue-Tek)

Papain, 61.25 µg/ml (Biochrom AG)

RPMI 1640 medium (Life Technologies)

Saccharose (Penta)

SOC medium (Thermo Fisher Scientific)

Sodium pyruvate, 100mM (Sigma-Aldrich)

Tricaine Methanesulfonate (MS222) (Sigma-Aldrich)

Triton X-100 (Sigma-Aldrich)

4.2 Instruments

Countess® Automated Cell Counter (Invitrogen)

Cryotome CM3050 S (Leica)

Flow box EM Box 120 (Scholler Instruments)

Fluorescence microscope Olympus BX40 (Olympus)

Fluorescence stereomicroscope Olympus SZX16 (Olympus)

Inversed microscope Olympus BX40F (Olympus)

Mini centrifuge ROTILABO® with butterfly rotor (ROTH)

Microinjector IM 400 with sucking module IM 400B (Narishige)

Micropipette puller PC-10 (Narishige)

Stereomicroscope Stemi 2000 (Zeiss)

Vortex Ika Works Minishaker MS1 (Ika Works)

Water bath Techne TE 10D Tempette (Techne)

Zeiss LSM 880 NLO confocal microscope (Zeiss)

4.3 Other materials

1.5ml Eppendorf tubes (Biologix)

2-0 multifilament silk suture with cutting needle (Ethicon)

Bel-Art® Disposable Pestles, BAF199230000 (Merck Group)

DNA Gel Loading Dye 6X (Thermo Fisher Scientific)

DH5α/dam- host Competent Cells: Kind gift from Dr. Marie Macůrková lab

E.Z.N.A Cycle pure kit (Omega)

Gene ruler DNA ladder, SM0333 (Thermo Fisher Scientific)

Glass capillary for microinjection (Drummond)

GeneArt™ CRISPR Nuclease mRNA, A29378 (Thermo Fisher Scientific)

Invitrogen™ TrueGuide™ gRNA (Thermo Fisher Scientific)

Insulin syringe 0.5ml/50 I.U. (Omnican)

PhusionTM High–Fidelity DNA Polymerase, F530L (Thermo Fisher Scientific)

pluriStrainer Mini 70 µm (pluriSelect)

Primer Synthesis (Integrated DNA Technologies, IDT)

QIAGEN Plasmid Midi Kit (QIAGEN)

Rapid DNA Ligation Kit (Roche)

SuperFrost Plus™ Adhesion slides (Epredia)

Sterile cotton (Hartmann)

Serological pipette (Biologix)

T2A sequence synthesis for gene cloning (Integrated DNA Technologies, IDT)

Taq DNA Polymerase (Thermo Fisher Scientific)

4.4 Antibodies

4.4.1Primary antibodies

Cat./Clone. No	Antigen	Species	Supplier	Dilution
CH1	Cardiac Tropomyosin	Mouse	Developmental Studies Hybridoma Bank	2 µg/ml
AB233	Red fluorescence	Rabbit	Evrogen	1:5000
F3648	Fibronectin	Rabbit	Sigma-Aldrich	1:500

Cat./Clone No.	Fluorophore Conjugation	Supplier	Dilution
Isolectin B4	Fluorescein	Vector Laboratories	1:200

4.4.2 Secondary antibodies

Cat./Clone No.	Antigen	Species	Supplier	Dilution
A11001	Mouse IgG-	Goat	Thermo Fisher	1:500

	Alexa Fluor® 488 conjugate		Scientific	
A11012	Rabbit IgG-Alexa Fluor® 594 conjugate	Goat	Thermo Fisher Scientific	1:500

4.5 Solutions

4.5.1 Phosphate buffered saline

10x Phosphate buffered saline (PBS) (pH=7.4) (stock solution)

79 g NaCl

29 g Na2HPO4.12H2O

3.1 g KH_2PO_4

1.1 g KCl

Add distilled H_2O to 1000 ml

1x PBS (pH=7.4)

50 ml 10x PBS

Add distilled H_2O to 500 ml

2/3 PBS (pH=7.4)

33.4 ml 10x PBS

Add distilled H_2O to 500 ml

Xenopus cells have different osmolarity (100mM) compared with mammalian cells (150mM).

4.5.2 Fixation solutions

4% Paraformaldehyde (pH=7.4)

4 g Paraformaldehyde

Add 2/3PBS to 100 ml

4.5.3 Medium for cell culture cultivation

Xenopus testicular cell 2/3 cultivation medium

150 ml L-15 Leibovitz

30 ml 5x RPMI 1640

45 ml Foetal bovine serum (FBS)

4.5 ml L-glutamine (200mM)

8 mL $NaHCO_3$ (7.5%)

450 µl Gentamicin(50mg/ml)

3 ml Sodium pyruvate (100 mM)

818 µl β-mercaptoethanol

Volume adjusted to 450 ml with steriled ddH_2O.

Papain solution

61.25 mg/l papain

0.5mM EDTA

1mM L-cysteine in PBS without $Ca2^+$ and $Mg2^+$

4.5.4 In vitro fertilization (IVF) solutions

20x Marc's Modified Ringer's Solution (MMR) (pH=7.5)

58.44 g NaCl

1.49 g KCl

2.03 g $MgCl_2$

11.92g HEPES (1M)

Add distilled H_2O to 500 ml

0.05x MMR (pH=7.7)

2.5 ml 20x MMR

Add distilled H_2O to 1000 ml

0.05x MMR + Gentamycin (pH=7.7)

2.5 ml 20x MMR

1.0 ml Gentamycin (50 mg/ml)

Add distilled H_2O to 1000 ml

1x MMR + Gentamycin (pH=7.7)

5 ml 20x MMR

100 µl Gentamycin (50 mg/ml)

Add distilled H_2O to 100 ml

2.2% Cysteine + 0,1x MMR (pH=7.7)

500 µl 20x MMR

2.2g L-Cysteine

Add distilled H_2O to 100 ml

L-15 Leibovitz + 10% FBS medium

10 g Foetal bovine serum

Add L-15 Leibovitz to 100ml

0.4% MS222 (pH=7) (Killing solution)

4 g MS222

4 g $NaHCO_3$

Add distilled H_2O to 1000 ml

1% Agarose (for Petri dish coating)

1 g Agarose

Add distilled H_2O to 100 ml, mix and microwave till agarose melting. Pour the solution to several Petri dishes and let it cool for 15 min.

4.5.4 Microinjection solution

0.2% MS222 (Sleeping solution)

0.2 g MS222

0.2 g $NaHCO_3$

Add distilled H_2O to 100ml

6% Ficoll

3 g Ficoll

Add 0.1x MMR + Gentamycin to 50ml

Adjust PH by adding NaOH

4.5.5 Cryotome solutions

20% Saccharose in 2/3 PBS

20 g Saccharose

Dissolve in 100ml H_2O

4.5.6 Immunofluorescence Solutions

0.1% PBT

100ul TritonX100

Dissolve in 100ml PBS

Immunofluorescence blocking solution (10% horse serum)

1ml horse serum

Diluted by 10ml 0.1% PBT

Whole mount Immunofluorescence blocking solution (1%BSA)

0.1 g BSA

Dissolve in 10ml 2/3PBS

4.5.7 DNA isolation using alkaline lysis method

Solution I (pH 8.0)

50mM glucose

25mM Tris-Cl

10mM EDTA

100ug/mL RNase A.

Filter sterilized and stored at 4ºC fridge.

Solution II

0.2M NaOH

1% SDS

This solution should be made up fresh on the day of use.

Solution III (PH4.8)

5M potassium acetate solution

Store at 4ºC fridge

4.5.8 DNA Cloning Solutions

10X TBE

108 g Tris base

55 g H3BO4

40 ml 0.5M EDTA (pH 8.0)

Add distilled H_2O to 1000ml

1X TBE

10ml 10X TBE

Add distilled H_2O to 100ml

4.6 Methods

4.6.1 Animal Handling and Tadpole Generation

Adult *X. tropicalis* (Ivory Coast strain; University of Portsmouth source) were maintained under standard conditions, with 24–26°C, 12h:12h light-dark cycles, in dechlorinated and filtered water supplemented with sea salt (2.5 g/10 L). Embryos were generated via standardized *in vitro* fertilization protocols (Geach and Zimmerman, 2011). Tadpoles in NF developmental Stage 48-50 were used for tail amputation experiments. 1-2 years old adult frogs were used for heart regeneration experiments.

4.6.2 In Vitro Fertilization

To induce ovulation in female *X. tropicalis*, a two-step human chorionic gonadotropin (hCG) injection protocol was employed. On the day prior to in vitro fertilization (IVF), a priming dose of 20 IU hCG was administered into the dorsal lymph sac at approximately 5:00 PM. On the following day, a booster dose of 180 IU hCG was injected at around 9:00–10:00 AM. When maintained at 25 °C, females typically begin ovulating within 4-6 hours after the booster injection. To ensure an adequate number of eggs, 2-3 females were routinely used per IVF attempt. One male was sacrificed by placing the frog in killing solution for 10-15 min till its leg reflexes were lost. Cervical spine section was performed with scissors and spike. Testes were isolated and put in 500 µl L-15 + 10% FBS medium in 1.5ml eppendorf tubes. The testes were homogenized using disposable pestles and mix by pipette.

When hormonally induced female frogs began laying eggs into water, they were deemed ready for in vitro fertilization (IVF). A single drop of 1x MMR + Gentamycin was placed at the center of a 90 mm Petri dish. Eggs were gently squeezed from the female and collected into the same area. Homogenized testes from a male were then distributed evenly over the eggs. During this process, eggs were carefully arranged into a monolayer using a pipette tip to facilitate uniform exposure to sperm. The mixture was left undisturbed for 5 minutes to allow sperm-egg interaction.

Subsequently, 0.05× MMR was gently poured into the dish until it was filled, initiating fertilization. After 20 minutes, the fertilization medium was replaced with 2.2% L-cysteine to remove the jelly coat surrounding the embryos. The eggs were transferred into a 250 ml beaker and gently swirled for approximately 5 minutes. Following jelly coat removal, embryos were rinsed four times with 0.05× MMR to eliminate residual L-cysteine. The

cleaned embryos were then transferred into agarose-coated Petri dishes containing 0.05× MMR+Gentamycin, with approximately 200–300 embryos per dish. Later when the majority of embryos reach the 8-cell stage, unfertilized eggs and abnormally developing embryos were carefully removed. On the second day, the culture medium was replaced with fresh 0.05× MMR +Gentamycin, and malformed or non-viable embryos were carefully removed. On the third day, the medium was replaced with 0.05× MMR to allow the embryos to begin acquiring their natural microbiota. On the fourth day, embryos were transferred to tadpole housing tanks, and feeding was initiated.

4.6.3 XtiSCs Cell Culture

The isolation and culture of XtiSCs were performed according to the protocol described by Tlapakova et al. (2016). Non-fluorescent XtiSCs were used for mitochondrial labeling experiments, while XtiSCs transfected with Katushka RFP were utilized for all transplantation studies. For the Katushka RFP-expressing XtiSCs, cells were sorted based on fluorescence using an inFlux v7 Sorter (BD Biosciences) and were used within three months of sorting.

4.6.4 Effect of XtiSCs in *X. tropicalis* Tadpole Tail Regeneration

4.6.4.1 XtiSCs transplantation into *X. tropicalis* tadpoles

XtiSCs were collected and rinsed three times with 2/3× PBS to remove eliminate media residue. Viable counts were obtained using a Countess Automated Cell Counter (Invitrogen). Two-week-old tadpoles were anesthetized in a sleeping solution containing 0.004% MS-222 for 5–10 minutes. Subsequently, 1,000 viable XtiSCs (2.5 × 10^7 cells/ml) were injected into the upper tail tissue. After injection, tadpoles were returned to 0.01× MMR supplemented with gentamicin. The medium was refreshed daily, and any deceased tadpoles were promptly removed to maintain optimal rearing conditions. On the same day as the injection, one-third of the tail was amputated, and tadpoles were monitored at 1, 3, 5, and 7 days post-amputation (dpa).

For mitochondrial labeling, XtiSCs were collected, washed three times with 2/3× PBS, and incubated with 100 nM MitoTracker® Red CMXRos (MiTT, Thermo Fisher Scientific) for 30 minutes at room temperature. Cells were then washed twice with 2/3× PBS, resuspended in 2/3× PBS, and kept on ice prior to injection. To confirm specificity, 50 nl of 100 nM

MitoTracker dye was injected into 4-week-old *X. tropicalis* tadpoles, which demonstrated that the dye alone was not specifically taken up by macrophages (Fig. 24).

Experimental procedures for macrophage depletion and XtiSC transplantation are illustrated in Fig. 15A. All figures use abbreviated group names, with complete explanations provided below.

Uninjected+2/3PBS: Uninjected (no liposomes injection) tadpoles were injected with 2/3PBS;

Uninjected +XtiSCs: Uninjected (no liposomes injection) tadpoles were injected with XtiSCs;

Control lipo+2/3PBS: Control liposomes-injected tadpoles were injected with 2/3PBS;

Control lipo+XtiSCs: Control liposomes-injected tadpoles were injected with XtiSCs;

Clodronate lipo+2/3PBS: Clodronate liposomes-injected tadpoles were injected with 2/3PBS;

Clodronate lipo+XtiSCs: Clodronate liposomes-injected tadpoles were injected with XtiSCs;

5.6.1.2 XtiSCs Migration Observation

Tadpoles were anesthetized in sleeping solution at a final concentration of 0.004% MS222 prior to observation. Katushka RFP fluorescence was observed under fluorescence stereomicroscope (Olympus SZX16).

5.6.1.3 Clodronate Liposomes-based Macrophage Depletion in *X. tropicalis* Tadpoles

Before injection, tadpoles were anesthetized in a solution containing 0.004% MS-222 (Sigma-Aldrich) and 0.004% $NaHCO_3$. Control liposomes (PBS) and clodronate liposomes (Liposoma Technology) were administered into the heart vein region of the tadpoles on two consecutive days, with 5.4 nl injected each time. To evaluate the distribution range of the liposomes and verify the injection procedure, fluorescent DiI liposomes (Liposoma Technology) were injected at 5.4 nl as a procedural control.

5.6.1.4 Tail Regeneration Statistics

Tail regeneration was evaluated using images of tadpole tails captured with a Leica TL3000 Ergo stereo microscope. Prior to observation, tadpoles were anesthetized in a solution containing 0.004% MS-222 (Sigma-Aldrich) and 0.004% $NaHCO_3$. Tail length measurements were taken from the snout to the point where the axis of the tail myotomes intersects with the body wall, as defined by Haas and Das (2011). The regeneration index was derived by dividing the regenerated tail length by the total tail length. Statistical analysis was performed using GraphPad, student's t-test ($P<0.05$) for the comparison between groups.

4.6.4.5 Whole Mount Hybridization

The whole-mount immunofluorescence staining protocol for isolectin B4 was adapted from Willsey (2021) with minor modifications. Tadpole samples were fixed overnight in 4% formaldehyde prepared in 2/3 PBS, followed by three washes in 2/3 PBS, each lasting 30 minutes. The bleaching step was omitted to preserve the Katushka RFP fluorescence of the XtiSCs. Samples were then permeabilized in 1% Triton X-100 for 1 hour at room temperature and washed three times with 2/3 PBS for 30 minutes each. Blocking was performed using 1% BSA at room temperature for 2 hours. Isolectin B4 staining (Vector Laboratories, Fluorescein-conjugated Isolectin B4) was carried out overnight at 4°C, followed by three 30-minute washes in 2/3 PBS. Finally, samples were immersed in 150–200 µL of 2/3 PBS, ensuring complete coverage, and nuclei were labeled by staining with DAPI at a final concentration of 1 µg/mL.

Similarly, whole-mount immunofluorescence staining of skeletal muscle was performed based on the protocol by Hamilton et al. (2021), with slight modifications. Tadpoles were fixed overnight in 4% formaldehyde in 2/3 PBS and washed three times for 30 minutes each with 2/3 PBS. To preserve Katushka RFP fluorescence, the bleaching step was omitted. Permeabilization was carried out using 1% Triton X-100 for 1 hour at room temperature, followed by three 30-minute washes in 2/3 PBS. Samples were blocked overnight at 4°C in 10% horse serum. The primary antibody 12/101 (Developmental Studies Hybridoma Bank, DSHB) was incubated with the samples for 2–3 days at 4°C, followed by three washes of 30 minutes each in 2/3 PBS. The secondary antibody (Alexa Fluor 488 anti-mouse) was

incubated overnight at 4°C, followed by three additional washes. Finally, nuclei were stained with DAPI (1 µg/mL) in 150–200 µL of 2/3 PBS.

Imaging for the whole tadpole tail was conducted using a Zeiss LSM 880 NLO confocal microscope, with z-stack settings (6-8µm thickness).

4.6.4.6 Macrophage Cells Counting

To count macrophages, a standard deviation Z-projection was generated for the green channel. Thresholding was performed using the Otsu method, and particles were filtered by size, retaining those between 38.8 pixels and infinity.

For area measurements, the transmitted light channel was used. Areas for measurement were manually selected using the polygon selection tool. In cases where the automated particle analysis did not accurately reflect macrophage numbers, manual counting was performed for those specific samples.

4.6.4.7 Analysis of Muscle Fibers Degradation and Growth

For samples at 1 day post-amputation (1 dpa), the amputation plane was defined as a line parallel to the fin cut, approximating the region where muscle fibers begin early degradation. The intact muscle region was delineated from the last clearly identifiable somite to the point where muscle fibers started to deteriorate. The baseline calibration area extended from the last complete somite to the amputation boundary. Muscle fiber regeneration at 3 and 5 days post-amputation (3 dpa and 5 dpa) was assessed following the methodology established by Laura N. Borodinsky's laboratory (Hamilton et al., 2021; Levin and Borodinsky, 2022), with slight modifications. Specifically, the analyzed area spanned from the newly regenerated muscle fibers to the most posterior visible end of the notochord, excluding the fin. All measurements were performed using ImageJ software. Z-stack images were flattened into maximum-intensity projections for analysis, with each individual z-slice examined to confirm the presence of regenerated muscle fibers.

4.6.4.8 Immunofluorescence

XtiSCs were collected, rinsed twice with 2/3 PBS, and seeded as a monolayer onto SuperFrost Plus™ Adhesion slides (Epredia), then air-dried overnight. For staining, cells

were fixed with 4% formaldehyde in 2/3 PBS for 10 minutes at room temperature, followed by three washes with 2/3 PBS, each lasting 10 minutes. Permeabilization was performed using 1% Triton X-100 for 30 minutes at room temperature, followed by three additional 10-minute washes with 2/3 PBS. Blocking was carried out with 1% BSA for 1 hour at room temperature. Primary antibodies were incubated overnight at 4°C, then washed three times for 10 minutes each with 2/3 PBS. Secondary antibodies were applied for 2 hours at room temperature, followed by three 10-minute washes with 2/3 PBS. For isolectin B4 staining, which requires a single incubation, samples were incubated for 2 hours at room temperature, then washed three times for 10 minutes each with 2/3 PBS. Slides were air-dried for 30 seconds to 1 minute until fully dry. DAPI was added to the mounting medium at the working concentration to stain nuclei. Coverslips were gently placed over the samples, and edges sealed with transparent nail polish. Secondary antibody incubation was also performed as a negative control. Imaging was performed using either a Zeiss LSM 880 NLO confocal microscope or a Leica DM6 FS fixed-stage fluorescence microscope.

4.6.4.9 Single Cell Suspension Preparation and Staining

Tadpoles were maintained in 2/3 PBS and euthanized using 0.2% MS-222. Tail segments exhibiting strong Katushka RFP fluorescence were excised under an Olympus SZX16 fluorescence stereomicroscope and collected into 1.5 ml Eppendorf tubes on ice. The segments were rinsed once with 2/3 PBS, then digested in a 200 µL solution containing 1 mg/mL Collagenase A (Roche) and 10 µg/µL DNase I (Sigma Aldrich), incubated at 30°C for 1 hour with gentle mixing every 5–10 minutes using a Pasteur pipette. Subsequently, a 1:50 dilution of papain solution was added, mixed thoroughly, and incubated at room temperature for 10 minutes. The enzymatic reaction was stopped by adding cold 2/3 PBS to fill the tubes. The cell suspension was filtered through a 70 µm cell strainer (pluriStrainer Mini) and centrifuged at 1000 × g for 5 minutes at 4°C. The resulting pellet was resuspended in 200 µL 2/3 PBS and incubated with fluorescein-conjugated isolectin B4 (Vector Laboratories) for 1 hour at room temperature to label endothelial and select immune cells. After staining, cells were washed twice with 2/3 PBS and centrifuged under the same conditions. The final pellet was resuspended in 20 µL 2/3 PBS and spread onto SuperFrost Plus™ adhesion microscope slides (Epredia) to form a monolayer. Slides were air-dried and imaged using a confocal microscope.

4.6.4.10 Data Analysis

Data analysis was conducted using GraphPad Prism software (version 9.5). Results were presented as the mean with the standard error of the mean (SEM). The data were obtained from at least three independent biological replicates. For comparing significant differences between two groups, where multiple variables were considered for statistical evaluation (e.g., no injection vs. control liposomes injection vs. clodronate liposomes injection; 2/3PBS injection vs. XtiSCs injection; various time points), Student's t-test was applied ($P<0.05$).

4.6.5 Effect of XtiSCs in *X. tropicalis* Heart Regeneration Study

4.6.5.1 XtiSCs Transplantation into *X. tropicalis* Frogs

XtiSCs expressing Katushka RFP were harvested by papain solution at room temperature incubation for 10 minutes, followed by centrifugation at 900 rpm for 5 minutes. The cell pellet was then washed with 2/3 PBS twice to remove residual culture medium and re-suspended in 2/3 PBS medium. The cell concentration was quantified using the Countess Automated Cell Counter (Invitrogen). Subsequently, 1 million cells in 50 µl 2/3 PBS were injected into the hindlimb skeletal muscle of frogs.

4.6.5.2 Clodronate Liposome-based Macrophage Depletion in *X. tropicalis* Frogs

Macrophage depletion was performed using clodronate liposomes from Liposoma Technology, with liposomes containing only PBS served as a control. In order to rule out the effect of injection as such frogs without any liposome's injection were also used as a control group. 400 µl liposomes was injected directly into the dorsal lymphatic sac. The subsequent two doses of liposomes with the same volume, were administered at 48-hour intervals following the initial injection. Cardiac surgery (apical resection) was conducted on the day after the third liposome administration. To evaluate the distribution range of liposomes, fluorescent DiI liposomes (Liposoma Technology) were administered following the same protocol.

4.6.5.3 Heart Apex Resection in *X. tropicalis*

The apical resection experiments were conducted following the protocol established by Liao et al. (Liao et al., 2017), as outlined in Fig. 28, panels A1-A6. Briefly, the heart apex resection was conducted under semi-sterile conditions, with all tools and surfaces regularly

disinfected using 70% ethanol. Frogs were anesthetized with 0.2% MS222 (Sigma-Aldrich) and 0.2% $NaHCO_3$ solution for approximately 8 minutes. Once the frogs ceased movement and lost hind leg grasp reflexes, they were transferred to a surgical table and secured to prevent movement. A V-shaped incision was made on the chest using surgical scissors. The sternum was then grasped with forceps, followed by an incision through the muscles. The heart was gently extruded with circular movements across the chest. The pericardium was carefully incised with scissors to fully expose the heart chamber. During diastole, forceps were used to grasp the apex of the heart, and approximately 5% of the cardiac chamber tissue was resected using surgical scissors. Hemostasis was achieved with sterile cotton wool. Finally, the cavity was closed, and the skin was sutured four to five times using multifilament surgical sutures (Ethicon). Only female frogs were included in further analysis due to the higher mortality rate observed in males following clodronate liposome treatment and subsequent heart surgery.

4.6.5.4 Immunofluorescence

The frogs were euthanized using 0.2% MS222 (Sigma-Aldrich) and 0.2% $NaHCO_3$ solution 7 days after apical resection. The hearts and livers were then removed and rinsed in cold 2/3 PBS. Heart regeneration morphology was observed under a Leica TL3000 Ergo stereo microscope. Subsequently, the hearts and livers were fixed in 4% paraformaldehyde overnight at 4°C. The following day, they were washed three times in 2/3 PBS for 10min each and then immersed in 10ml 20% sucrose solution in a 15ml Eppendorf tube overnight at 4°C. The organs were later embedded in O.C.T. medium (Tissue-Tek) and stored at -80°C.

For cryosectioning, the deep-frozen tissue was cut using a Leica cryostat at -20°C into 10 µm thick sections, which were then placed on SuperFrost Plus™ Adhesion slides (Epredia) and washed three times in 2/3 PBS for 5 minutes each.

The staining procedure commenced with the fixation of tissue sections in 4% paraformaldehyde for 5 minutes. Permeabilization was achieved using 1% SDS for 5 minutes, followed by blocking with 2% BSA for 1 hour at room temperature. Primary antibodies were applied, including CH1 (anti-tropomyosin, DSHB) and FN1 (anti-fibronectin, Sigma-Aldrich), and incubated for 60 minutes in a humid chamber at room temperature. Secondary antibodies (Alexa Fluor 488 anti-mouse and Alexa Fluor 594, Thermo Fisher Scientific) were subsequently applied and incubated for 45 minutes in a

humid chamber at room temperature. For isolectin B4 staining (Fluorescein, Vector Laboratories), a 1:200 dilution was used, omitting the step with secondary antibodies. Finally, the sections were mounted in Mowiol/DAPI, covered with a coverslip, and sealed with nail polish. Negative controls using secondary antibodies alone were included. Imaging of the stained samples was performed using a Leica DM6 FS fixed stage fluorescence microscope.

4.6.6 CRISPR-Cas9 Knock-In for Generating Transgenic Animals

4.6.6.1 Vector Construction

4.6.6.1.1 Pax7 CRISPR/Cas9 Knock-In Vector Construction Strategy

The vector backbone is pBluescript SK (+) from addgene (https://www.addgene.org/vector-database/1951/).

TurboFP gene from pTurboFP635-C vector was firstly cloned to pBluescript SK (+) backbone. This was achieved by performing several steps: 1) Recover XbaI site by transforming pTurboFP635-C vector into dam- host (Methyltransferase deficient E. coli) and make fresh DNA. 2) Remove multiple cloning site (MCS) of pTurboFP635-C by cutting at XhoI, XbaI site. 3) Blunt. 4) Ligate. 5) PCR of the ligated plasmid for TurboFP gene (TurboFP635_Forward primer: CGGGATCCTCCGCTAGCGCTACCGGTCG , TurboFP635_Reverse primer: TCCCCCGGGTGAGTTTGGACAAACCACAAC). 6) The pBluescript SK (+) vector was cut at BamHI and SmaI site and ligate with TurboFP PCR products generated above.

Next, γ-crystallin (γCry) promoter was inserted. 1) Distrupt HindIII sites in pγCry1GFP3 vector by cutting at HindIII site, blunt and ligate. 2) Cut the plasmid generated in the above step at XbaI and BamHI site and insert to TurboFP-pBluescript SK (+) vector at XbaI and BamHI restriction sites.

Next, GFP gene was insert to γ-crystallin (γCry)-TurboFP-pBluescript SK (+) vector. GFP sequence is from pLenti-C-mGFP-P2A-Puro Lentiviral Gene Expression Vector (https://www.origene.com/catalog/vectors/lentiviral-gene-expression-vectors/ps100093/plenti-c-mgfp-p2a-puro-lentiviral-gene-expression-vector).

Main steps include: 1) PCR of GFP gene (GFP_Forward primer_EcoRI: GGAATTCATGAGCGGGGGCGAGGAGCTGTTCG, GFP_Reverse primer_PstI: AACTGCAGTCAAACTCTGAGTCCGGACCT). 2) Cut γ-crystallin (γCry)-TurboFP-pBluescript SK (+) vector at PstI, EcoRI restriction sites. 3) Ligate.

Next, add T2A sequence to GFP-γ-crystallin (γCry)-TurboFP-pBluescript SK (+) vector. T2Asequence (ATCGAGGGCAGAGGAAGTCTGCTAACATGCGGTGACGTCGAGGAGAATCCTGGCCCAGAATTCC) was produced from LDT company with extra 5' EcoRV and 3' EcoRI recognition sequences. The GFP-γ-crystallin (γCry)-TurboFP-pBluescript SK (+) vector was cut at EcoRV, EcoRI restriction site. Finally T2A and the open vector were ligated together.

Next, Pax7 bait (GFP side) sequence was cloned to T2A-GFP-γ-crystallin (γCry)-TurboFP-pBluescript SK (+) vector. The steps include: 1) PCR of Pax7 bait (GFP side) (Forward primer: CCCAAGCTTTCACCTGGGAGTTCCATGAC, Reverse primer: ATCGTAGGCCTGGCCGGTCTCCA) which in the meantime introduced extra HindIII, EcoRV recognition site at Pax7 bait (GFP side) sequence's two sides, with template from *X. tropicalis* genome DNA. 2) Cut T2A-GFP-γ-crystallin (γCry)-TurboFP-pBluescript SK (+) vector at HindIII, EcoRV restriction sites. 3) Ligate.

Next, Pax7 bait (RFP side) was cloned to Pax7 bait (GFP side)-T2A-GFP-γ-crystallin (γCry)-TurboFP-pBluescript SK (+) vector. The steps are as follows: 1) PCR of Pax7 bait (RFP side) (Forward primer: ATAAGAATGCGGCCGCACCCACACTGACAGGACACA, Reverse primer: TGCTCTAGAGTAGGCCTGGCCGGTCTCCA) which in the meantime introduced extra recognition site at Pax7 bait (RFP side) sequence's two sides, with template from *X. tropicalis* genome DNA. 2) Cut Pax7 bait (GFP side)-T2A-GFP-γ-crystallin (γCry)-TurboFP-pBluescript SK (+) vector at NotI, XbaI restriction sites. 3) Ligate.

Finally, Pax7 3'UTR sequence was cloned to Pax7 bait (RFP side)-Pax7 bait (GFP side)-T2A-GFP-γ-crystallin (γCry)-TurboFP-pBluescript SK (+) vector. The steps are as follows: 1) PCR of Pax7 3'UTR (Forward primer: GGGAGCCAAGGGAATCCTCTGCC, Reverse primer: GGGTGCAGGTTAGAATTTCATCTTCTT) which in the meantime introduced

extra SmaI at Pax7 3'UTR sequence two sides, with template from *X. tropicalis* genome DNA. 2) Cut Pax7 bait (RFP side)-Pax7 bait (GFP side)-T2A-GFP-γ-crystallin (γCry)-TurboFP-pBluescript SK (+) vector at SmaI restriction site. 3) Ligate

4.6.6.1.2 MMP7 CRISPR/Cas9 Knock-In Vector Construction Strategy

The vector backbone is pBluescript SK (+) from addgene (https://www.addgene.org/vector-database/1951/).

The first few steps are the same as Pax7 knock-in vector cloning: TurboFP gene cloning, γ-crystallin (γCry) promoter cloning, GFP gene cloning, T2A sequence cloning.

Then, MMP7 bait (GFP side) cloning to T2A-GFP-γ-crystallin (γCry)-TurboFP-pBluescript SK (+) vector. The steps include: 1) PCR of MMP7 bait (GFP side) (Forward primer:CCCAAGCTTCAGCTTTTAACTGGGGCAAC, Reverse primer : ATCTTGCC TTCTTCCATATATTGACTG) which in the meantime introduced extra HindIII, EcoRV restriction sites at MMP7 bait (GFP side) two sides, with template from *X. tropicalis* genome DNA. 2) Cut T2A-GFP-γ-crystallin (γCry)-TurboFP-pBluescript SK (+) vector at HindIII, EcoRV restriction sites. 3) Ligate.

Next, MMP7 bait (RFP side) was cloned to MMP7 bait (GFP side)-T2A-GFP-γ-crystallin (γCry)-TurboFP-pBluescript SK (+) vector. The steps are as follows: 1) PCR of MMP7 bait (RFP side) (Forward primer: ATAAGAATGCGGCCGCCAGCTTTTAA CTGGGGCAAC, Reverse primer: GCTCTAGATTGCCTTCTTCCATATATTGACTG) which in the meantime introduced NotI, XbaI at MMP7 bait (RFP side) two sides. 2) Cut MMP7 bait (GFP side)-T2A-GFP-γ-crystallin (γCry)-TurboFP-pBluescript SK (+) vector at NotI, XbaI restriction sites. 3) Ligate.

Finally, MMP7 3'UTR was cloned to MMP7 bait (RFP side)-MMP7 bait (GFP side)-T2A-GFP-γ-crystallin (γCry)-TurboFP-pBluescript SK (+) vector. The steps are as follows: 1) PCR of MMP7 3'UTR (Forward primer: GGGGTGCAAAGTCACATGCTTTAG, Reverse primer: GGGAGGCACATGTAAGCTTTTAATC) which in the meantime introduced extra SmaI at MMP7 3'UTR sequence two sides, with template from *X. tropicalis* genome DNA. 2) Cut MMP7 bait (RFP side)-MMP7 bait (GFP side)-T2A-GFP-γ-crystallin (γCry)-TurboFP-pBluescript SK (+) vector at SmaI restriction site. 3) Ligate.

4.6.6.2 Gene Cloning Protocols

4.6.6.2.1 High-Fidelity PCR

Component 50 μL

H2O： ul

5x PhusionTM HF Buffer: 10 μL

10 mM dNTPs: 1 μL

Forward and Reverse primer: 2ul

Template DNA 250ng: ul

PhusionTM High–Fidelity DNA Polymerase 0.5 μL (last component to add)

PCR program (2-step method with annealing temperature: 72°C):

Cycles	Temperature	Time
1	98°C	30 s
30	98°C 72°C	10 s 45 s
1	72°C	10 min
1	4°C	Hold

4.6.6.2.2 DNA Electrophoresis

Around 5ul PCR products are loaded to 0.8%-1.5% agrose gel (based on fragment length) and then the gel was runned in TBE buffer, with the running voltage set to 110-120V.

To examine the PCR product, ethidium bromide was used as loading dye. To recycle the PCR product, crystal violet (0.8ul/ml gel; Or 24ul/30ml gel;) was used.

4.6.6.2.3 Restriction Enzyme Digest

Normal Volume for PCR product examination

Plasmid Vector: 1ug

Enzyme: 1ul

10x Buffer Orange: 2ul

dd H2O: ul

Total: 20ul

Mix and then incubate via water bath. Mix and briefly centrifuge after a while.

Large Volume for PCR product recycling

Plasmid Vector: 4ug

Enzyme: 6ul

10x Buffer Orange: 8ul

dd H2O: ul

Total: 80ul

Total 80ul separate to 4 tubes, each with 20ul.

Mix and then incubate via water bath. Mix and briefly centrifuge after a while.

Take 4ul for control experiment.

The restriction enzymes used are listed in Table 1 below:

Enzyme	Brand	Temperature	Time

* EcoRI	Thermo Scientific™,FD0274	37°C	30min
BglII	Thermo Scientific™,ER0082	37°C	1hour
PstI	Thermo Scientific™, ER0611	37°C	1hour
*BamHI	NEB, BamHI-HF®, R3136S	37°C	1hour
* BamHI	Thermo Scientific™,FD0054	37°C	1hour
* SmaI	Thermo Scientific™, ER0662	37°C	1hour
SmaI	Thermo Scientific™, ER0661	37°C	1hour
*XbaI	Thermo Scientific™, ER0682	37°C	1hour
*AflII	Thermo Scientific™, ER0831	37°C	1hour
*SacII:	Thermo Scientific™, ER0201	37°C	1hour
*EcoRV	Thermo Scientific™,FD0304	37°C	1hour
EcoRV	Thermo Scientific™, ER0301	37°C	1hour
*AatII	Thermo Scientific™, ER0991	37°C	1hour
NotI	Thermo Scientific™, ER0591	37°C	1hour

* Fast digest enzyme

Table 1. Restriction Enzymes used for cloning experiment.

There are more enzymes listed in the above table than which were described in Pax7 and MMP7 vector cloning strategy. The reason is that some restriction enzymes are used for validation of the vector construct in order to check the fragment length.

4.6.6.2.4 Recycling of PCR Products

PCR products were purified using E.Z.N.A Cycle pure kit from Omega. The maxi load of one column is ~10ug DNA. Use 30ul elution buffer to dissolve, and then measure DNA using Nanodrop.

4.6.6.2.5 Blunting

Linear DNA: 1ug

dNTP Mix, 1 mM each: 2µL (0.1 mM final concentration)

T4 DNA Polymerase:0.2 µL (1 U)

5x Reaction Buffer: 4µL

dd H2O: ul

Total: 20ul

* T4 DNA polymerase (Fermentas/Thermo fisher #EP0061)

Mix thoroughly, spin briefly and incubate at room temperature for 30 min.

Stop the reaction by heating at 75 °C for 10 min.

4.6.6.2.6 Ligation
Self Ligation:

DNA: 50ng

Enzyme: 1ul

5x Buffer: 4ul

dd H2O: ul

Total: 20ul

*Rapid DNA Ligation Kit, Roche, 11635379001, 5 U/µl

Incubate at 16 °C overnight.

Ligation of DNA Fragment to Open Vector

Normally, initial trial to set the moler ratio of open vector: DNA insert=1:10

Negative control for plasmid self-ligation

Open Vector: (the same amount for ligation experiment)

Ligase: 0.25ul

5x Buffer: 1ul

dd H2O: ul

Total: 5ul

Experiment setting

Open Vector: ul

DNA Insert: ul

Ligase: 0.5ul

5x Buffer: 2.5ul

dd H2O: ul

Total: 10ul

*Rapid DNA Ligation Kit, Roche, 11635379001, 5 U/µl

Incubate the reaction at 16 °C overnight.

4.6.6.2.7 Transformation to DH5α/dam- host Competent Cells

1) Take out the competent cells from the -80°C freezer and immediately put them on ice. Let it thaw on ice.

2) Add 100ul DH5α/dam- competent cells to the 5ul ligation product. Mix by gently tapping. There are two experiments: one for negative control and the other for experiment group.

3) Incubate the mixture on ice for 30 minutes.

4) Heat shock in 42°C water bath 60s.

5) Put on ice for 5 min.

6) Add 250 ul of SOC medium, shaking at 500 rpm at 37°C for 40min-1h.

7) Plant on two agar plates (amp+/kan+): one plate with 50ul, the other plate with all the remaining.

For negative control group, put all mixted solution to one agar plate. Grow at 37°C overnight.

8) The next day, pick up 6-8 colonies in experiment group and grow at 37°C overnight in 3ml LB medium**.** The negative control plate theoretically has no colony on the plate.

4.6.6.2.8 Plasmid DNA Extraction (Alkaline Lysis) and Validation

Plasmid DNA Extraction

1) Centrifuge 3ml bacterial cells at top speed for 5minute. Aspirate supernatant.

2) Resuspend cell pellet in 100ul of Solution I.

3) Add 200ul of lysis Solution II. Gently invert tube up and down 6-8 times.

Solution II should be made fresh just before use.

Solution II:

Per 1ml

125ul 8%SDS

200ul 1M NaOH

675ul ddH_2O

4) Immediately add 150ul Solution III. Gently invert tube up and down 6-8 times.

5) Centrifuge at top speed 10min.

6) Transfer supernatant to a new tube. Do not pick up any white flakes.

7) Precipitate using 950ul 99% ethanol. Put the tube at -20° for at least 10min.

8) Centrifuge at top speed 10min.

9) Aspirate off all the ethanol supernatant and wash the pellet by 950ul 70% ethanol.

10) Aspirate off all the supernatant and dry the pellet for 5-10min.

11) Dissolve DNA in 80ul TE buffer or ddH_2O.

12) Nanodrop measurement.

Plasmid DNA Validation

Validation is firstly through enzyme digest of the extracted vector to check the fragment length.

1)Restriction Enzyme Digest

Plasmid Vector: 1ug

Enzyme: 1ul

10x Buffer Orange: 2ul

dd H2O: ul

Total: 20ul

Mix and then incubate via water bath. Mix and briefly centrifuge after a while.

2)Choose one colony with positive enzyme digest fragment, and re-grow in 3ml LB medium at 37°.

3)Purify using E.Z.N.A Cycle pure kit from Omega.

4)Use 60ul elution buffer to dissolve, and Nanodrop measurement.

5)Sanger sequencing.

4.6.6.2.9 Primer Design

Primers used for the cloning was designed using Primer 3 online software (https://bioinfo.ut.ee/primer3-0.4.0/). The template is from *X. tropicalis* v10genome (https://www.ncbi.nlm.nih.gov/nuccore/NC_030683.2?report=fasta&from=130403835&to=130507883&strand=true) .

4.6.6.3 gRNA Design

4.6.3.3.1 Pax7 gRNA design

gRNA was designed using Crispr scan (https://www.crisprscan.org/).

gRNA is in the last intron of Pax7 gene. The Design sequence used as below:

TCACCTGGGAGTTCCATGACCTGTATAAAAGCCCTTGGCCTTCAGCCTCGTCCCTGGAATG
GCCTTAAAGGGGCGGTTCACCTTTTCGTCAACTTTTAGTATGTTATAGAATGGCCAATTCTA
AGCAGCTTTTTAAATGGTCTTCATTATTTATTTTTTTATAGTTTTTAAACTATTTGACTTCTG
CCTCTTTCCAGCTTTCAAATGGGGGTCACTGACCCCGGCAGCCAAACCCTATTGCTCTGTGA
GGCTCCAGTTTTATTGTTACTGTTACTTTTTATTCCTTATCTTTCTATTCAGCCCCTCTCCTAT
TCATATACCAGCCTCTCATTCAAACCACTCCCTGGTTACTAAGGTAATTTGGACCCTAGCAA

CCAGAAAGCTGCTAAAACTCCAAACTGCAGAGCTGCTGAACAAAAAAGTGAAATAACAAA
AAAAAAACCAAATAATAAAAAATGAAGACCAATTGCAAGTTGTCTCAGAATATCACTCTC
TACATCATACTAAAAGCTAACTCATCTCTAAATATAAGCAGCTTTGCAGTTGGTCCTCTGTC
TCATTTCTGATGTAAATGATAAGTGTTGGGTTGGGGGATAACAGCTAGTAATGTAATAAGC
ACAATAATAATCTAAAAATTCATTTTTTTGTTCCTGTTTTGCAG

Parameters: Frog-*Xenopus tropicalis*, 4 mismatches, T7 or Sp6 promoter.

gRNA was evaluated based on their score and was further double checked via CHOPCHOP (https://chopchop.cbu.uib.no/).

The gRNA sequence chosen for microinjection experiments:

gRNA1: GGATGTAAATGATAAGTGTT

gRNA2: GGCCCTGGAATGGCCTTAAA

4.6.3.3.2 MMP7 gRNA design

gRNA was designed using Crispr scan (https://www.crisprscan.org/).

gRNA is in the last intron of MMP7gene. The Design sequence used as below:

CAGCTTTTAACTGGGGCAACACTGAGTATATTTTGGTGCAACATACAAATGTTTCCCTGTAC
ATATTGGCTGGTTTTGCATATAAGACTCCCTTAAGTCATAAACTTTTACAGGTTTAATATGC
AACAGAGAATAGCAAGGCTGTTAGTTACAGTTGCACAGAGCTGGTATTCATACAGCAGGT
CATTCTGACTGCAGCTAATCATTTGAATGAATGACATATACTATAGATCAGTGATCCCCAG
CCAGTGGCTCTGGGGCAACATGTTGCTCCCCAACACCTTGGATGTTGCTCTCAGTGGCCTC
AAAGTAGGTGCTTGTTTTTGAATTCCTGGCTTGGAGGCAAGTGCTGATTGCATAAAACCCA
GTGTGAAGCCTAACTGAACCTTCTATAGGCTGCCACTCCACATAGGGGCCAATAACCAATT
ATAGCTCTTATTTGCACCCCAGGAACTTTTTTCCCTGCTTGTGTTGCTCCTCAACACATTTTT
CATTTGAATGTGGCTCACGGGTATAAAAGGTTGGGGATCCCTGCTATAGACTGTATATATG
CAGCCATACATATCCCTGATGGTCCTTTCTTTTGGCAG

Parameters: Frog-*Xenopus tropicalis*, 4 mismatches, T7 or Sp6 promoter.

gRNA was evaluated based on their score and was further double checked via CHOPCHOP (https://chopchop.cbu.uib.no/).

The gRNA sequence chosen for microinjection experiments: GGAGCTGGTA TTCATACAGC

4.6.3.4 Delivery of CRIPSR-Cas9, gRNA, Knock-in Vector to X. tropicalis embryos

The injection mix was prepared as below:

Cas9 mRNA: 0.4ul

gRNA: 0.46ul

Nuclease Free Water: ul

Mix gently, incubate at 37°C for 2min-5min.

Plasmid (QIAGEN Plasmid Midi Kit purified): 250ng

Total: 5ul

2nl injection mix was injected per embryo. Injection was performed in 6% ficoll solution.

The injection was performed in 1-cell stage *X. tropicalis* embryos. The embryos were generated via IVF protocol mentioned above, except that the sperm incubation time shortened from 20min to 10min.

The injection plates should be washed with 1%BSA solution, to make the bottom not stickiness. While injection should be performed in Ficoll solution. And after injection, the embryos should still be kept in Ficoll solution until 4-cell stage. Then transfer to normal 0.05x MMR+Gentamycin solution for embryo development. The next day, pick out bad embryos. On the 3rd day and 4th day, red or green fluorescent can be detected under the microscope.

sgRNA preparation

Stock Solution

Upon receipt, resuspend TrueGuide™ Synthetic gRNA in 1× TE buffer to prepare a 100 µM (100 pmol/µL) stock solution. Store the resuspended gRNA at –20°C until use. To prevent RNA degradation, always handle the gRNA using RNase-free reagents, tubes, and pipette tips.

Working Solution

The preparing of working solution of TrueGuide™ Synthetic gRNA is strictly following protocol manual as below:

1) Before opening, centrifuge each TrueGuide™ Synthetic gRNA tube at low speed (maximum RCF 4,000 × g) to collect the contents at the bottom of the tube, then remove the cap from the tube carefully.

2) Using a pipette and sterile tips, add the required volume of 1x TE buffer to prepare 100 µM (100 pmol/µl) stock solutions.

3) Vortex the tube to resuspend the oligos, briefly centrifuge to collect the contents at the bottom of the tube, then incubate at room temperature for 15–30 minutes to allow the gRNA oligos to dissolve.

4) Vortex the tube again to ensure that all the contents of the tube is resuspended, then briefly centrifuge to collect the contents at the bottom of the tube.

5) Optional: Check the concentration of the resuspended oligos using the NanoDrop™ Sprectrophotometer (or equivalent) or a UV-base plate reader. Optional: Aliquot the

working stock into one or more tubes for storage.

6)Use working stocks immediately or freeze at –20°C until use.

4.6.3.5 Genotyping of F0 tadpoles
Based on the diagram showed below

(Fig. 11), F0 tadpoles genome DNA was extracted (ENZO Kit, Omega) and primers for Pax7 construct and MMP7 construct were designed. PCR was performed to validate the PCR bands sizes.

The primers for Pax7 construct genotyping:

1: Pax7 Intergenic: TGTGCTGCAGTCTGCTCCATAT

2: Pax7_Forward: TCTGTCACATGACTCAGTAAAGC

3: Pax7-GFP_Reverse: CACGTTGGTCTGGTAGTGGTC

4: Pax7-RFP_Reverse: CCACACTGAGGGGATGCTAT

Annealing temperature for all primer pairs is 62 ℃.

PCR System

14.6	µl	H_2O	
2	µl	TAQ pufr + KCl	(10x)
1.2	µl	$MgCl_2$	(25 mM)
0.4	µl	primer F+R	(10 µM)
0.4	ul	dNTP	
1	µl	RT- or cDNA	
0.4	µl	TAQ Polymerase	(1 U/ul)
20	µl	Total	

Figure 11. Genotyping analysis of targeted integration in positive founder tadpoles Diagrammatic representation of RT-PCR primer designs for forward targeted integration of the exogenous cassette induced by the 2-bait Cas strategies. F1/R1 primer pair was used to amplify the 5' junction between the genome and exogenous DNA. F3/R3 primer pair was used to amplify the 3' junction for the 2-bait Cas strategy (Mao et al., 2018).

Although no positive genotyping results were obtained from the selected F0 tadpoles, we deemed it worthwhile to raise them to sexual maturity. These F0 frogs were then bred to generate F1 offspring, allowing further screening for potential germline transmission of the transgene by assessing the presence of RFP and GFP fluorescence signals in the F1 tadpoles.

5 RESULTS

5.1 Function of XtiSCs in *X. tropicalis* Tadpole Tail Regeneration

5.1.1 XtiSCs Could Survive in *X. tropicalis* Tadpoles for More Than One Month after Injection

One major consideration for cell transplantation research is tissue compatibility. MSC cells had very poor cell viability and cell compatibility in previous reports (Chang et al., 2013). In our experiments, XtiSCs have excellent cell viability when injected into tadpole tail tissue. The majority of tadpoles survive well after 7 days of XtiSCs injection, and when raised the tadpoles for longer period more than one month, the XtiSCs signal can still be detected as shown in Fig. 12. Moreover, the XtiSCs went through obvious cell growth in the tadpole body. This finding resonates with prior research indicating Sertoli cells' longevity in host organisms (Trivedi et al., 2006; Dufour et al., 2008).

Interestingly, when inject the XtiSCs to tadpole heart vein, XtiSCs can successfully stay in heart vein area but the majority of them could only survive for 3 days. This suggested that tissue transplantation is more efficient way for XtiSCs survivial compared with heart vein injection.

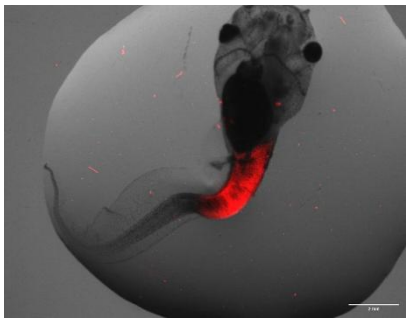

Figure 12. Long-Term Persistence of XtiSCs at Injection Sites in *X. tropicalis*.
RFP-labeled XtiSCs were injected into the upper tail region of tadpoles. XtiSCs remained detectable at the injection site for over one month. Red: XtiSCs. Scale bar: 2 mm.

5.1.2 XtiSCs Exhibit Injury-Directed Movement Following Tail Amputation in Tadpoles

To investigate the ability of XtiSCs to migrate toward injury sites, we utilized XtiSCs labeled with Katushka RFP, which allowed for clear visualization and tracking following transplantation (Shcherbo et al., 2007; Tlapakova et al., 2016). Our results demonstrate that these cells not only survive efficiently within tadpole tissues but are also capable of relocating to the regenerating tail region. This migration was observed at multiple time points: immediately after injection, and at 1, 3, 5, and 7 days following tail amputation.

Notably, XtiSCs showed a strong tendency to accumulate at the injury site, with significantly higher cell presence in amputated tadpoles compared to uninjured controls. This suggests that XtiSCs respond to regenerative cues released upon injury. Overall, these observations underscore the potential of XtiSCs in tissue regeneration and provide insights into their migratory behavior in a regenerative context (Fig. 13).

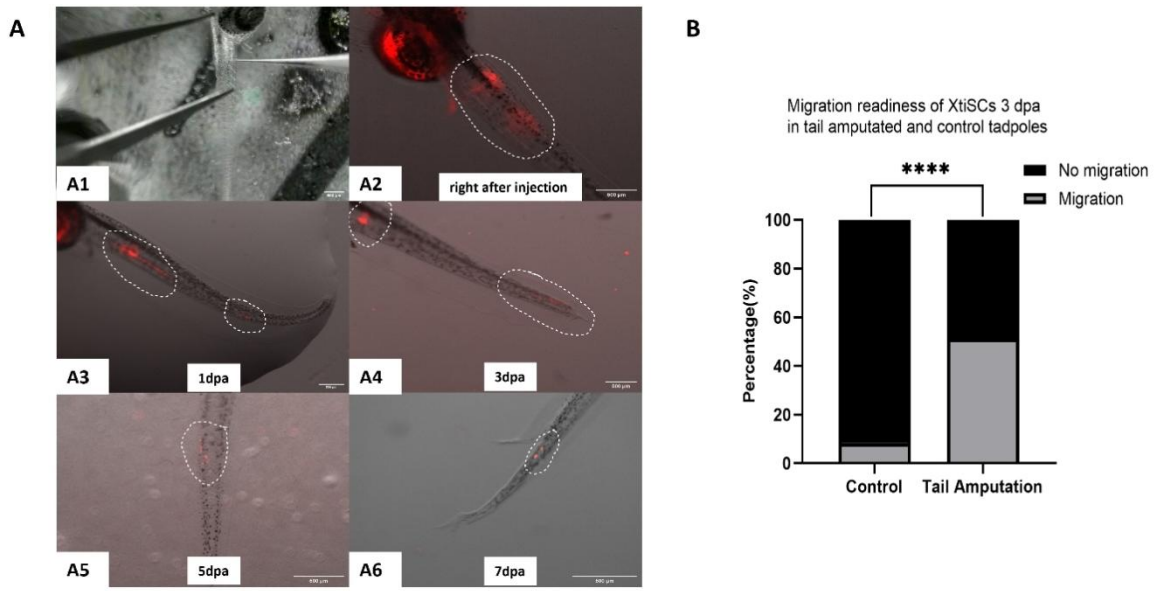

Figure 13. XtiSCs migrate to the site of tail regeneration following amputation.
(A) XtiSCs were microinjected into the upper tail region of *Xenopus tropicalis* tadpoles. Panels A2–A6 illustrate representative fluorescence images capturing XtiSC behavior over time: **A2** shows distribution immediately after injection; **A3–A6** display localization at 1, 3, 5, and 7 days post-amputation (dpa), respectively. Katushka RFP labeling marks the XtiSCs in red. Scale bar: 500 µm. **(B)** Tail amputation markedly enhanced the directed movement of XtiSCs toward the injury site compared to intact controls, as determined by Fisher's exact test (****P < 0.0001). Data were obtained from three independent experiments: Control group (n = 71); Amputated group (n = 135).

5.1.3 XtiSCs Injection Didn't Alter The Macrophage Numbers in Tadpole Tail

The immunoregulatory functions of Sertoli cells in allo- and xenogeneic transplantation contexts are well-established (Fallarino et al., 2009; Bistoni et al., 2012; Jhao et al., 2019; Kaur et al., 2020). Notably, Vegrichtova et al. (2022) demonstrated that *Xenopus tropicalis* immature Sertoli cells (XtiSCs) can modulate immune activity even in phylogenetically distant hosts. Building on these findings, we investigated whether XtiSCs exhibit similar immunomodulatory effects when transplanted into *X. tropicalis* tadpoles.

To assess macrophage dynamics, we injected XtiSCs into tadpoles (without liposomes) and quantified macrophage populations using fluorescein-conjugated isolectin B4, which specifically labels α-d-galactose residues on macrophage membranes (Sorokin and Hoyt,

1992; Godwin et al., 2017). Control tadpoles received 2/3× PBS injections. Macrophage density was calculated as the number of isolectin B4+ cells per unit area.

Comparative analysis revealed no statistically significant differences in macrophage density between XtiSC-transplanted and control tadpoles at any examined time point (1–7 days post-amputation, dpa). This consistency was observed both in the entire tail and the tail trunk region (Fig. 14).

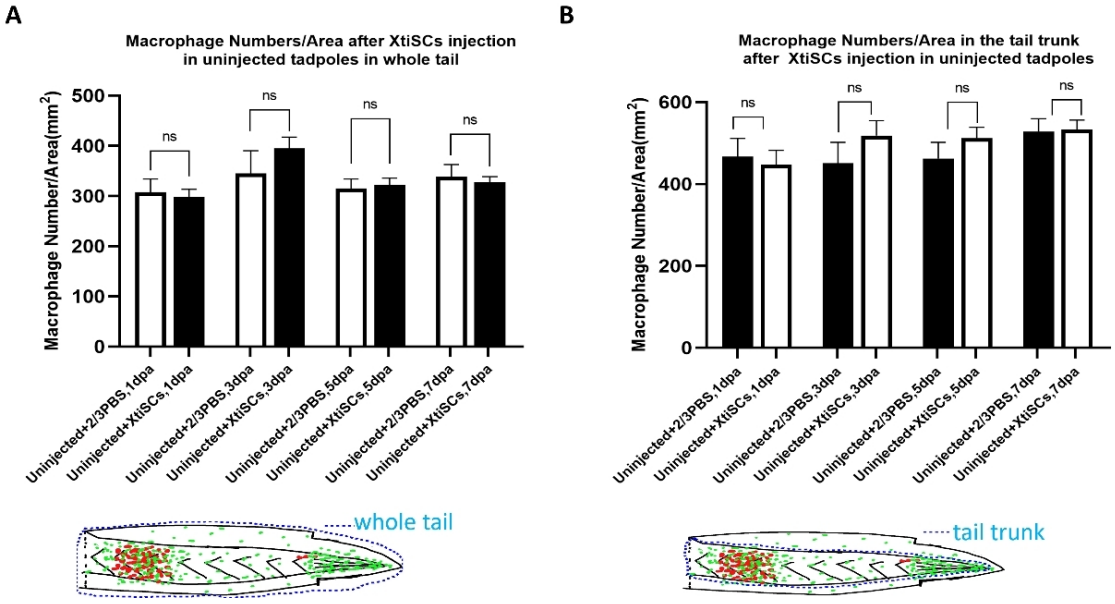

Figure 14. Injection of XtiSCs into uninjected (no liposome-injected) tadpoles does not significantly affect macrophage counts.
The macrophage numbers per area in the whole tail and tail trunk were calculated and are presented separately in (A) and (B). Macrophages were stained using isolectin B4. Quantification of macrophage density in the tail trunk was performed with ImageJ, normalizing results to macrophage count per unit area. Statistical analyses were conducted using GraphPad Prism, applying Student's t-test to compare treatment groups within each category. Data represent results from at least 8 tadpoles per group, obtained from three independent biological replicates.

5.1.4 XtiSCs Is Negative for Isolectin B4 Staining

To exclude the possibility that isolectin B4 might non-specifically label XtiSCs in addition to macrophages, potentially confounding the quantification of macrophages, we performed isolectin B4 staining on cultured XtiSCs. The results demonstrated that XtiSCs did not exhibit any isolectin B4 labeling (Fig.15). This confirms that isolectin B4 selectively stains macrophages in our experimental context, ensuring the accuracy of macrophage quantification without interference from XtiSCs.

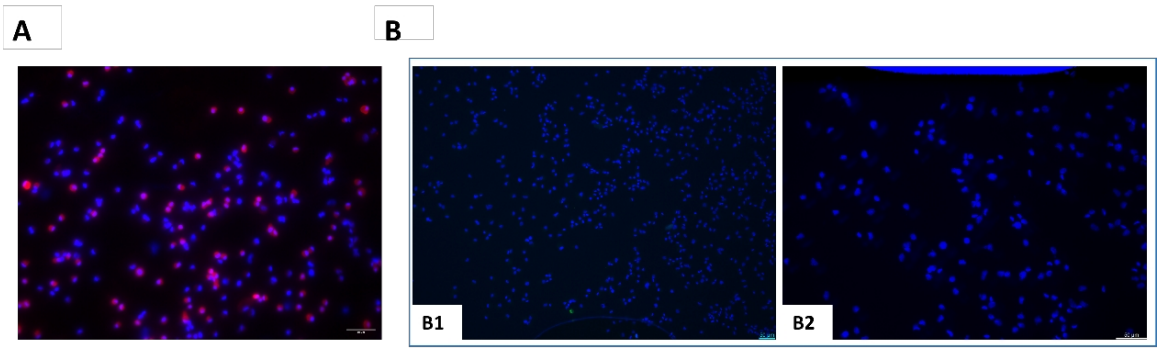

Figure 15. Isolectin B4 does not stain XtiSCs.
XtiSCs were subjected to immunostaining with isolectin B4 (fluorescein-conjugated, green). (A) As a positive control, RFP-XtiSCs were stained with an anti-RFP antibody, showing Katushka RFP-positive XtiSCs in red with DAPI-stained nuclei in blue. Scale bar: 50 μm. (B) shows the absence of isolectin B4 staining in XtiSCs, with B1 at 10× magnification and B2 at 20× magnification. Nuclei are stained with DAPI (blue), while isolectin B4 signal, which would appear green if present, is absent. Scale bar: 50 μm.

5.1.5 Clodronate Liposomes Administration for Macrophage Depletion

These findings prompted us to further investigate the role of XtiSCs in a macrophage-depleted environment. To this end, we utilized clodronate liposomes to achieve *in vivo* macrophage depletion in *X. tropicalis* tadpoles. Clodronate, a bisphosphonate compound, exhibits poor membrane permeability and rapid systemic clearance. Therefore, encapsulation within liposomes is critical for enabling its selective uptake by phagocytic cells, leading to intracellular accumulation, cytotoxicity, and targeted depletion of macrophages (Rooijen and Sanders, 1994; Danenberg et al., 2002).

Fig. 16A illustrates the experimental design, including the timeline of clodronate liposome administration, XtiSCs implantation, and sample collection. The experimental sequence involved initial macrophage depletion via liposome injection, followed by XtiSCs microinjection into the dorsal tail region. Tail amputation was then performed, and samples were collected on the same day post-amputation (0 dpa), as well as on days 1, 3, 5, and 7 post-amputation.

The results confirmed the efficacy of clodronate-mediated macrophage depletion, with a marked reduction in macrophage numbers as visualized and quantified (Fig. 16B, C).

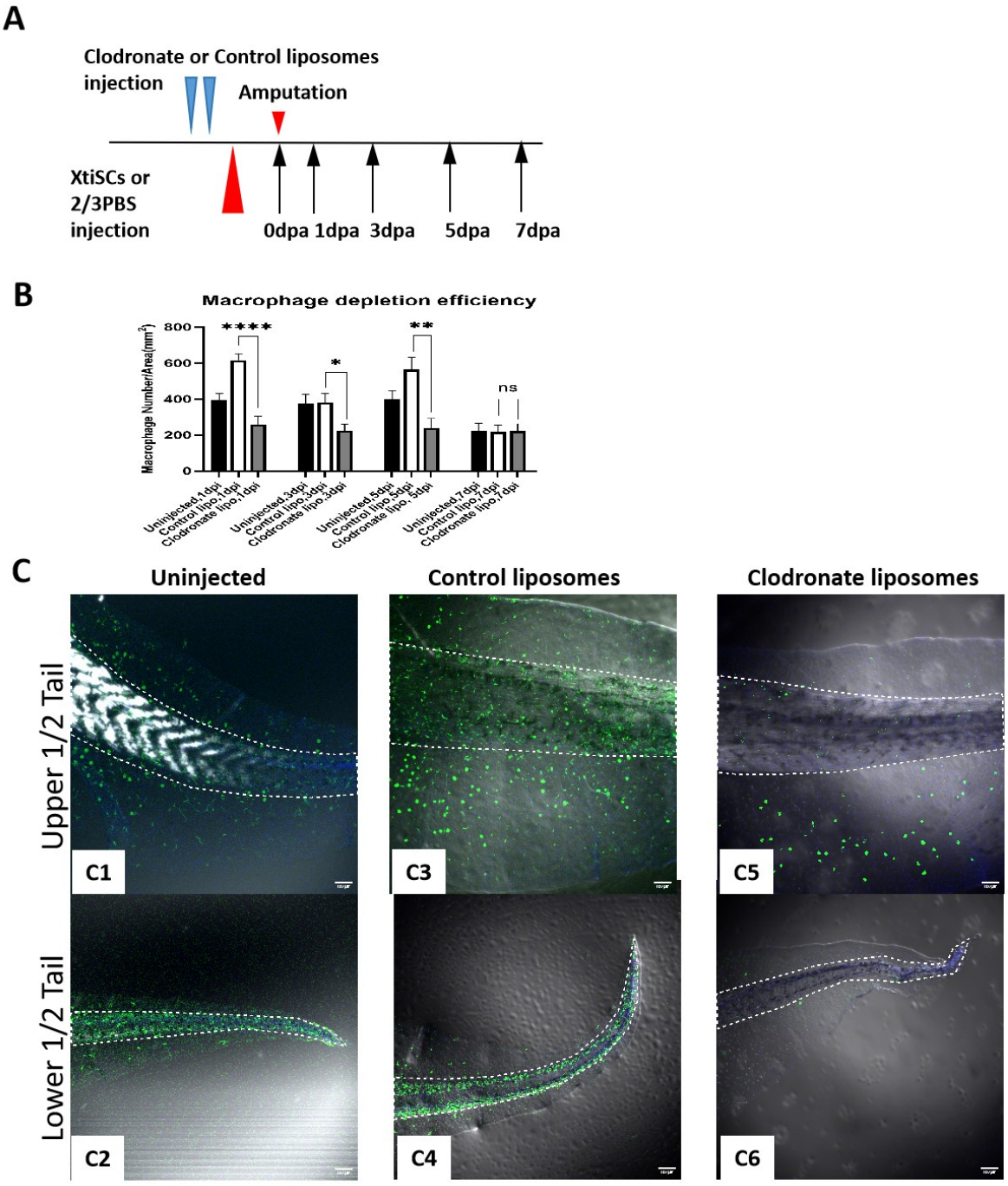

Figure 16. XtiSCs induce macrophage enrichment in the tail trunk of clodronate liposome–depleted tadpoles.

(A) Schematic overview of the experimental procedure used for macrophage depletion and XtiSC transplantation. Tadpoles received two sequential heart vein injections—administered on consecutive days—with either clodronate or control liposomes. One day after the second liposome treatment, XtiSCs or 2/3 PBS (as control) were delivered into the upper tail region. Tail amputation was performed one day following the XtiSC/PBS injection. Regenerative progress was assessed by collecting samples at multiple post-amputation time points: 1, 3, 5, and 7 days. **(B)** Treatment with

clodronate liposomes effectively diminished macrophage populations within the tail at 1, 3, and 5 days post-injection (dpi). Macrophage density in the tail trunk was calculated using ImageJ and normalized to total tail trunk area (refer to Materials and Methods). Statistical differences were analyzed using Student's *t*-test in GraphPad (*P < 0.05, **P < 0.01, ****P < 0.0001; n.s., not significant). Data reflect results from at least seven tadpoles per group in three independent experiments, with the exception of 7 dpi: uninjected (n = 4), control liposome group (n = 2), and clodronate liposome group (n = 4). **(C)** Representative images showing macrophages labeled by isolectin B4 (green) in tail sections from uninjected, control liposome–treated, and clodronate liposome–treated tadpoles at 5 dpi. Nuclei were stained with DAPI (blue). Panels C1–C2: uninjected group; C3–C4: control liposome group; C5–C6: clodronate liposome group. Scale bar: 100 µm.

5.1.6 Clodronate Injection Reduces Tadpole Tail Regeneration Capacity

Heart vein injection proved to be an effective method for delivering clodronate liposomes into the circulatory system of *X. tropicalis* tadpoles. This was demonstrated using fluorescent DiI-labeled liposomes, which enabled visualization of liposome distribution throughout the tadpole body. As shown in Fig. 17A, the DiI liposomes exhibited widespread systemic dissemination, particularly within the vasculature, thereby confirming the efficacy of the heart vein injection method and serving as a procedural control for subsequent experiments.

Tail regeneration in tadpoles was categorized into four distinct morphological outcomes: excellent, good, partial, and none, based on the extent and structure of regenerated tissue. In our experiments, macrophage depletion via clodronate liposome administration markedly impaired tail regeneration. As illustrated in Fig. 17B, a significant reduction in regenerative capacity was observed, underscoring the essential role of macrophages in supporting tissue repair and regeneration in *X. tropicalis*.

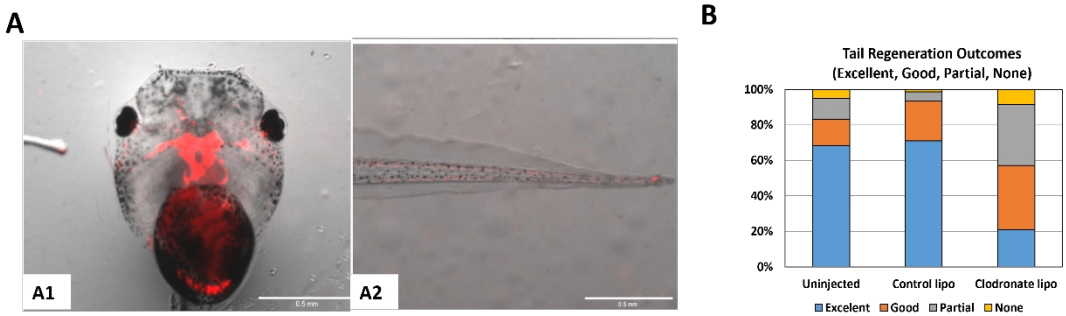

Figure 17. Clodronate liposome injection into the heart vein inhibits tail regeneration in tadpoles.
(A) Control fluorescent DiI liposomes were used to evaluate the distribution and penetration efficiency of liposomal injections (Clodronate or 2/3 PBS) in *X. tropicalis* tadpoles. DiI fluorescence

was detectable throughout the entire body for at least 7 days following the final injection (data not shown). Panels A1 and A2 show representative images of the tadpole head and tail, respectively. Scale bar: 0.5 mm. (B) Tail regeneration was categorized into four qualitative levels: *Excellent*—complete and morphologically perfect regeneration, comparable to an intact tail; *Good*—regenerated tail with similar length to an intact tail but with minor structural deficits, often in the fin; *Partial*—shorter regenerated tail with morphological abnormalities, such as curvature; and *None*—absence of visible regeneration. Sample sizes were as follows: Uninjected, $n = 60$; Control liposomes-injected (*Control lipo*), $n = 76$; Clodronate liposomes-injected (*Clodronate lipo*), $n = 105$. Data were collected from at least three independent biological replicates. Tadpoles treated with clodronate liposomes exhibited significantly impaired tail regeneration, likely due to macrophage depletion, consistent with previous reports (Aztekin et al., 2020).

5.1.7 XtiSCs Enhance Macrophage Accumulation in the Tail Trunk Post-Amputation

Notably, administration of XtiSCs led to a marked increase in macrophage density specifically within the tail trunk at 3 and 5 days post-amputation (dpa) in tadpoles treated with clodronate liposomes. This elevation was not evident when macrophages were quantified across the entire tail, including the fin region (Fig. 18A), implying a possible redistribution of macrophages from the fin to the trunk in response to injury. Conversely, in control tadpoles injected with non-depleting liposomes, XtiSC treatment did not significantly alter macrophage levels in either the trunk or the whole tail at corresponding time points (Fig. 18A, B).

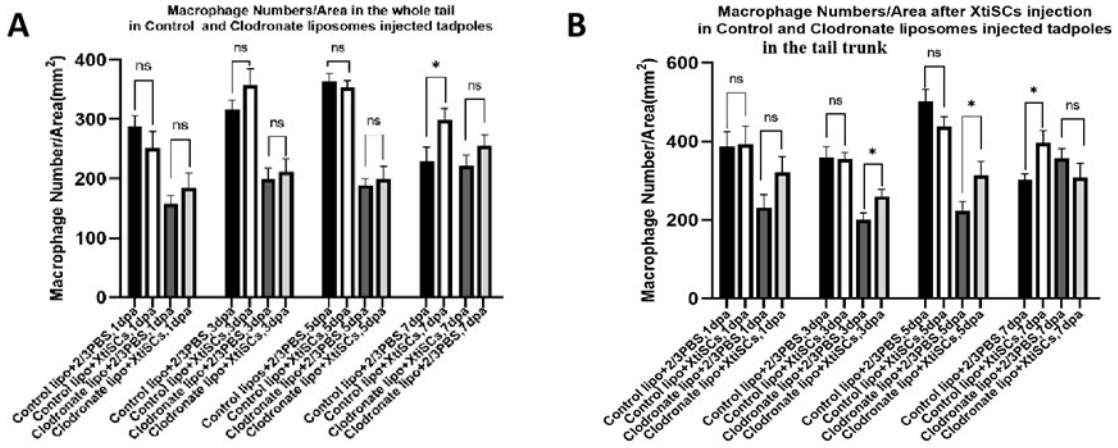

Figure 18. Injection of XtiSCs does not significantly affect overall macrophage count in the entire tail, but alleviated the macrophage numbers in the tail trunk.
(A) Macrophage distribution was assessed by calculating the number of macrophages per unit area across the various treatment conditions. Statistical analysis was carried out in GraphPad Prism using Student's t-test to determine intergroup differences. The label "ns" indicates results that were not statistically significant. Each treatment group consisted of at least nine tadpoles, pooled from three separate biological replicates. **(B)** Quantification of macrophage density specifically within the tail trunk region was performed after XtiSC injection in tadpoles pre-treated with either control or clodronate liposomes. Statistical comparisons were made using Student's t-test in GraphPad Prism. A

p-value < 0.05 was considered significant, while "ns" denoted non-significant differences. Each group included a minimum of six tadpoles from three independent replicates.

5.1.8 XtiSCs Promote Increased Macrophage Presence at Both the Injection Area and the Regenerating Tail

Upon analyzing the imaging data, we observed a clear accumulation of macrophage signals at both the injection site and the regenerated tail region. Subsequent statistical evaluation indicated a notable increase in macrophage density in these regions following tail amputation in *X. tropicalis* tadpoles that had undergone macrophage depletion through clodronate liposome treatment, followed by XtiSC transplantation, when compared with control tadpoles receiving 2/3 PBS under the same condition, at either 3 or 5 days post-amputation (dpa) (Fig. 19A and 19B). Furthermore, the control cohorts—including uninjected tadpoles and those injected with control liposomes—did not show any significant change in macrophage presence in the areas of interest. A notable exception occurred in the uninjected group at 3 dpa, where a significant increase in macrophage numbers was detected at the injection site in the XtiSC-treated subgroup when compared to PBS-injected controls (Fig. 19A, uninjected + XtiSCs vs. uninjected + 2/3 PBS).

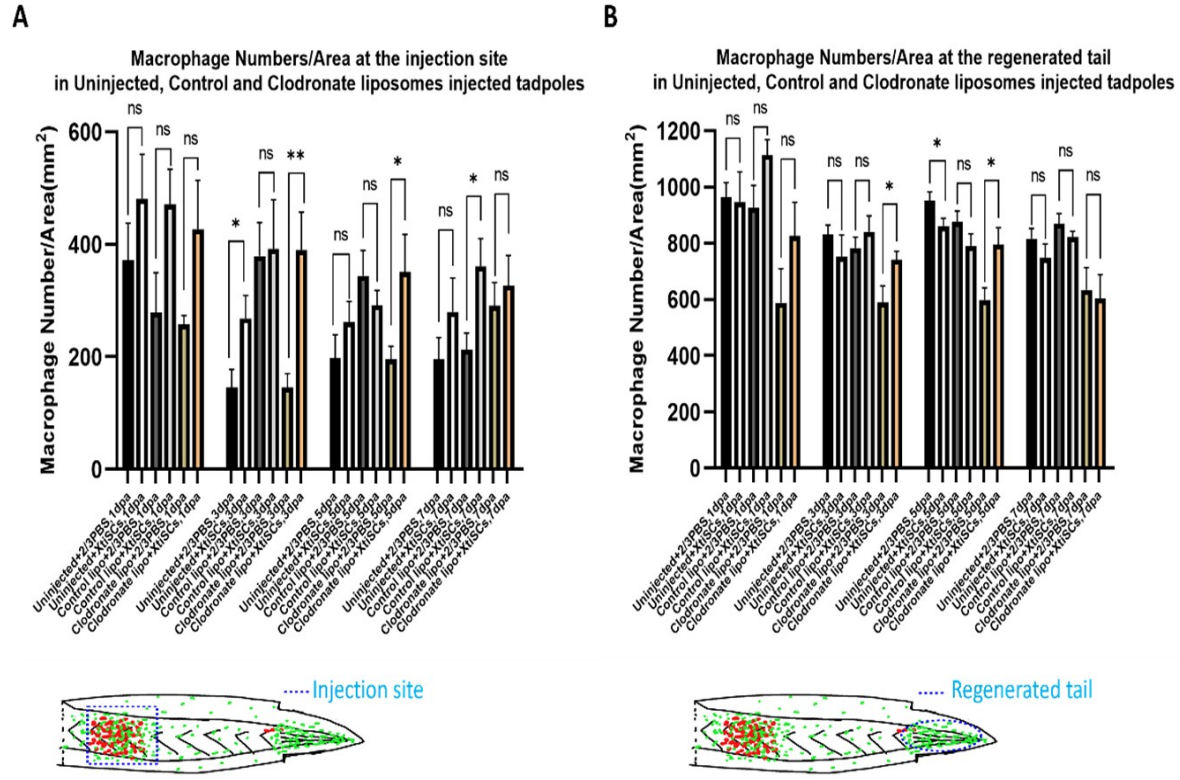

Figure 19. XtiSCs increase macrophage numbers at both the injection site and within the regenerated tail.

Macrophage density was measured at the XtiSC injection site (A) and within the regenerated tail region (B), expressed as the number of macrophages per unit area. Statistical comparisons between

groups were conducted using Student's *t*-test via GraphPad Prism. Significance thresholds were designated as follows: $P < 0.05$ (*), $P < 0.01$ (**), and non-significant differences as n.s. The dataset for panel (A) included at least 7 tadpoles per group, while that for panel (B) involved a minimum of 9 tadpoles per group. All experiments were replicated independently three times.

5.1.9 Macrophage Enrichment Is More Obvious in A Macrophage Depleted Environment

Interestingly, upon focusing on macrophage enrichment at both the XtiSCs injection site and the regenerating tail, we observed that this enrichment was markedly more pronounced in tadpoles subjected to macrophage depletion via clodronate liposome administration. Quantitative analysis (Fig. 20A, D) revealed that the relative macrophage densities in this cohort were significantly higher compared to both uninjected controls and those injected with control liposomes, particularly at 3 and 5 days post-amputation (dpa).

These data suggest that XtiSCs possess a remarkable capacity not only to recruit macrophages to sites of cellular disruption but also to promote their redistribution in a manner that supports regenerative processes. Collectively, these findings position XtiSCs as key modulators within the immunoregulatory landscape of tissue regeneration.

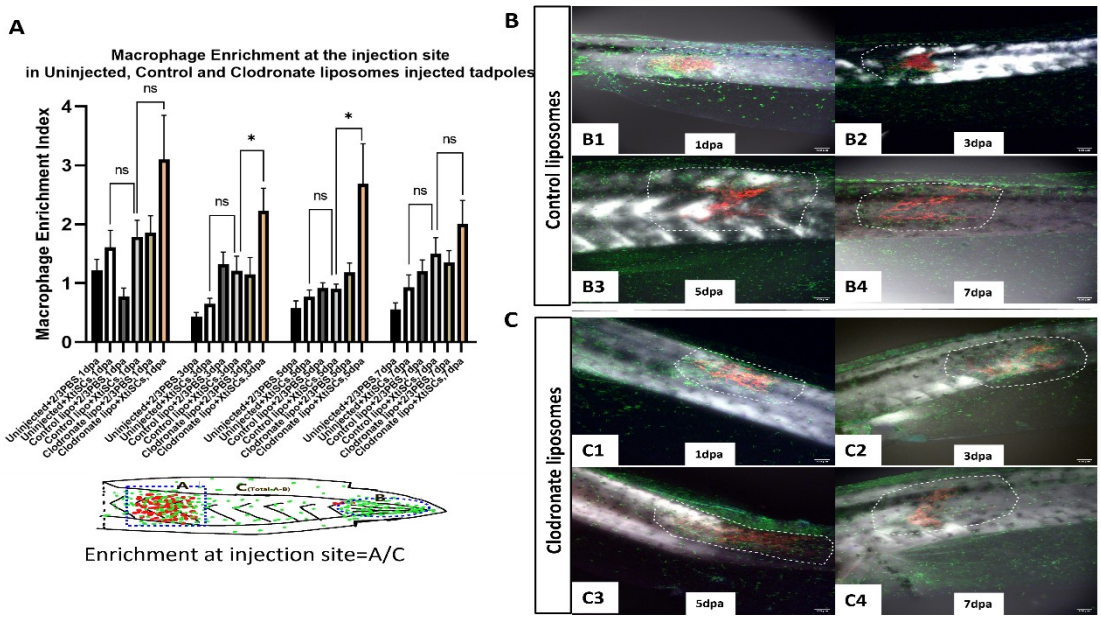

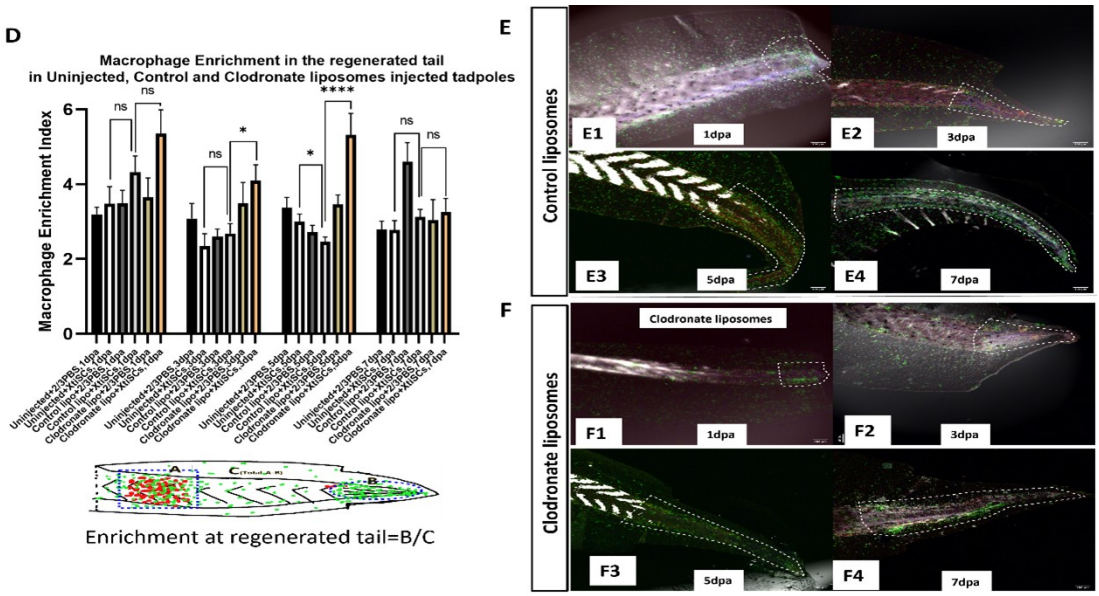

Figure 20. Macrophage enrichment induced by XtiSCs is more pronounced in a macrophage-depleted environment.
Macrophage enrichment was quantified using a macrophage enrichment index, calculated by dividing the total number of macrophages per mm² in the injection site or regenerated tail by the macrophage density in the remainder of the tail (excluding both the injection and regenerated regions). Statistical analysis was performed using GraphPad Prism, applying Student's t-test for comparisons between treatment groups within each condition. Significance is indicated as *P < 0.05, **P < 0.0001, and n.s. for non-significant differences. Data for panel (A) were obtained from at least 7 tadpoles per group, while panel (D) includes data from a minimum of 9 tadpoles per group, each collected across three independent biological replicates. Panels (B1–B4) and (C1–C4) display representative images of isolectin B4-stained macrophage enrichment at the injection site in control and clodronate liposome-treated tadpoles, respectively, from 1 to 7 days post-amputation (dpa). Similarly, panels (E1–E4) and (F1–F4) illustrate macrophage enrichment at the regenerated tail in the same treatment groups over the same time period. DAPI stains nuclei (blue), and isolectin B4 labels macrophages (green). Scale bar: 100 μm.

5.1.10 XtiSCs Promote Regenerated Tail Length in Uninjected Tadpoles at 3 days After Amputation

To determine how XtiSCs influence tail regeneration after amputation, we measured the length of the regrown tail tissue. As shown in Fig. 21, by 3 days post-amputation (3 dpa), tadpoles treated with XtiSCs demonstrated a markedly greater extent of tail regeneration when compared to those that received the control treatment with 2/3 PBS. However, this enhancement was not observed in tadpoles pretreated with either clodronate liposomes or control liposomes. These findings suggest that the pro-regenerative effect of XtiSCs is contingent upon an intact and functional immune environment, particularly the presence of macrophages.

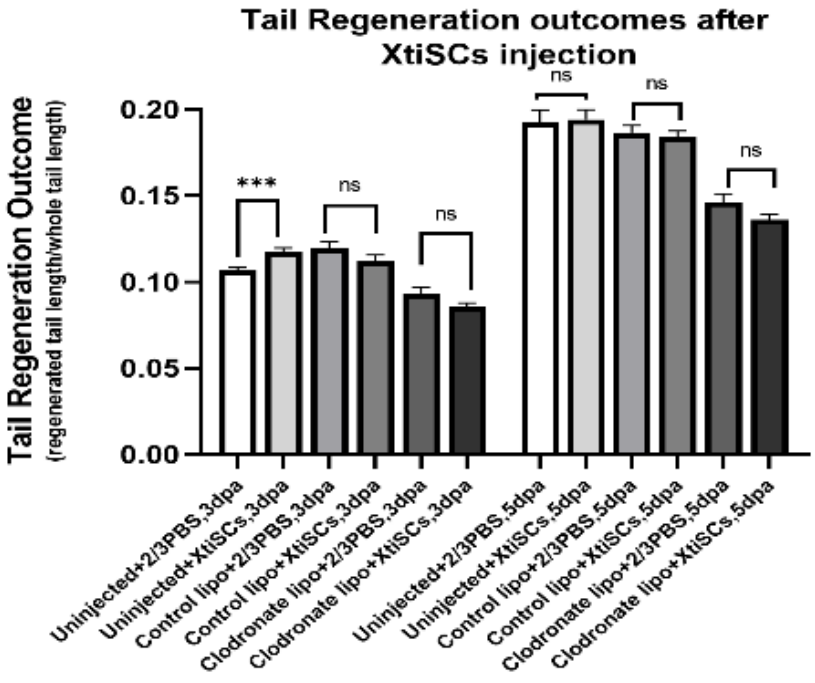

Figure 21. XtiSCs promote tail regeneration in uninjected tadpoles at 3 days post-amputation. Tail regeneration was evaluated by calculating a ratio between the length of the regenerated tail (from the amputation site to the tail tip along the trunk axis) and the full tail length (measured from the junction of the tail myotomes with the body wall to the tail tip). Statistical comparisons were conducted using the Student's t-test in GraphPad Prism. Results are reported as highly significant ($P < 0.001$) or not significant (n.s.). Data were collected from three separate biological experiments, each with at least 52 tadpoles per treatment group.

5.1.11 XtiSCs Stabilize Injured Muscle Fibers at 1 day Post Amputation in Tadpoles Following Tail Amputation

Next, we assessed the regeneration of striated muscle fibers. In Xenopus tadpoles, damaged myofibers typically appear near the amputation site by one day post-amputation (1 dpa), and their breakdown continues through 2 to 3 dpa (Rodrigues et al., 2012). Our results revealed that administration of XtiSCs led to a significant delay in muscle fiber degradation at 1 dpa compared to tadpoles treated with control liposomes, as shown in Fig. 22A. Notably, this trend was also seen in groups treated with clodronate liposomes, where no significant difference was found between tadpoles injected with XtiSCs or 2/3 PBS. One possible explanation is that XtiSCs may act as an anti-inflammatory modulator. In the control liposome-injected group, where liposomal delivery may induce local inflammation, XtiSCs might contribute to stabilizing the immune environment, thereby preserving more intact muscle fibers at the analyzed time point. Conversely, in clodronate liposome-injected groups, characterized by a macrophage-depleted microenvironment, XtiSCs may exert a similar modulatory effect. However, due to the already diminished macrophage population,

both the XtiSCs- and PBS-treated conditions could maintain comparable levels of undegraded muscle fibers. This suggests that in a macrophage-depleted context, the capacity of XtiSCs to further modulate muscle preservation may be limited by the already attenuated inflammatory response.

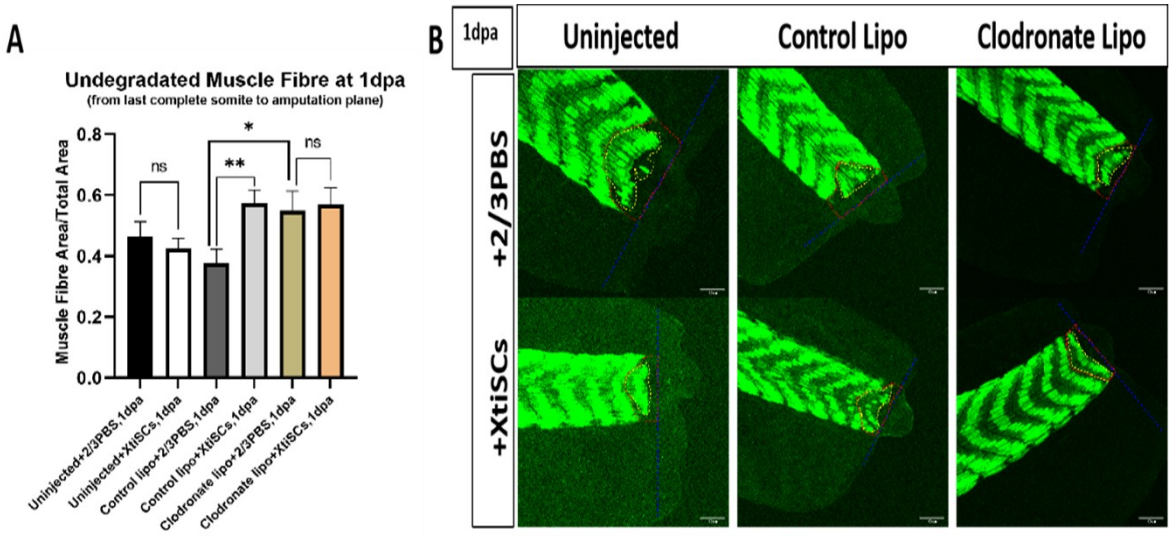

Figure 22. XtiSCs stabilize injured muscle fibers.
(A) At 1 day post-amputation (1 dpa), the area of undegraded muscle fibers was measured by calculating the ratio of the remaining muscle fiber area—originating from the last intact somite—to the total area between the last complete somite and the amputation plane. This analysis included data from a minimum of three biological replicates, with sample sizes of at least 14 tadpoles per group. **(B)** Representative images display preserved muscle fibers stained with the 12/101 antibody (DSHB) at 1 dpa in three groups: uninjected tadpoles, those injected with control liposomes, and those treated with clodronate liposomes. The amputation plane is indicated by blue dashed lines; yellow dashed lines outline the residual muscle fibers located between the last intact somite and the amputation site; red dashed lines define the overall area spanning from the last intact somite to the amputation plane. Scale bar represents 100 μm. Muscle fibers are shown in green.

5.1.12 Injection of XtiSCs Enhances Muscle Regeneration at 3 days Post Amputation in Tadpoles Following Tail Amputation

Starting at 3 days post-amputation (3 dpa), newly formed muscle fibers became clearly visible. Our results indicate that administration of XtiSCs significantly stimulated the growth of these emerging muscle fibers at 3 dpa in both the control and clodronate liposome-treated groups, as shown in Fig. 23A. This improvement in muscle regeneration might be linked to an increase in pro-regenerative M2 macrophages and/or the promotion of the shift from pro-inflammatory M1 macrophages to the anti-inflammatory M2 phenotype, both essential processes in effective tissue healing. However, by 5dpa, this effect was no longer observed, suggesting that the regenerative landscape, particularly the muscle fiber architecture, may

have already been established by this stage, rendering it less responsive to further modulation by XtiSCs.

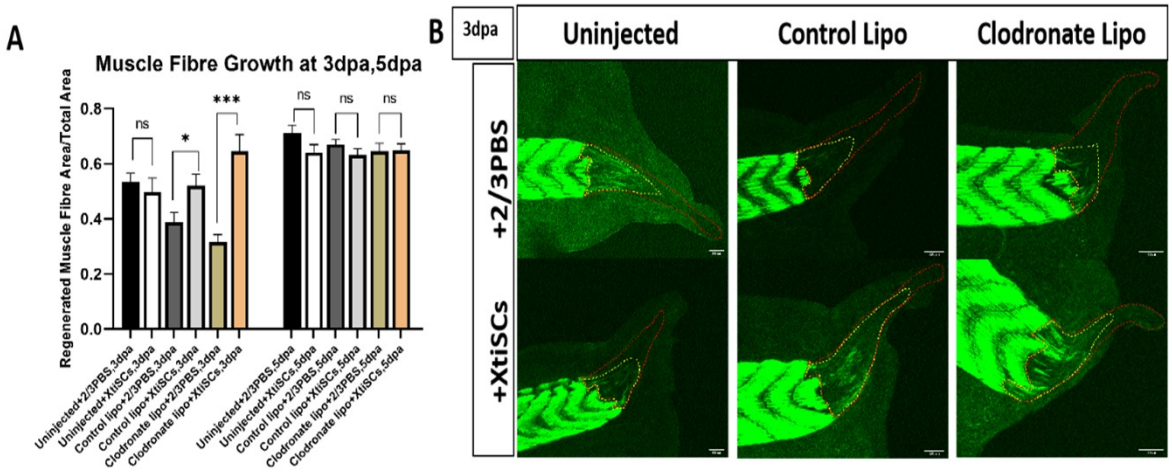

Figure 23. XtiSCs enhance muscle fiber growth.
(A) Muscle fiber growth was assessed at 3 and 5 days following amputation (3 dpa and 5 dpa). This was quantified by calculating the ratio of the area occupied by new muscle fibers to the total area extending from the amputation site to the farthest point of the notochord (excluding the fin region). Data were obtained from a minimum of three independent biological replicates, with at least 12 samples per group. (B) Representative images illustrating muscle fiber growth at 3 dpa stained with 12/101 (DSHB) are shown. The yellow dashed lines delineate the newly formed muscle fiber region, whereas the red dashed lines mark the entire regenerated area. Scale bar: 100 µm. Muscle fibers are shown in green. Statistical significance was evaluated using Student's t-test, with P values indicated as *P < 0.05, **P < 0.001, and n.s. for non-significant differences.

5.1.13 Direct Interactions Between XtiSCs and Macrophages

By employing confocal microscopy alongside whole-mount fluorescence imaging, we detected direct interactions between XtiSCs and macrophages in live *X. tropicalis* tadpoles. The overlapping signals of red fluorescence from XtiSCs and green fluorescence marking macrophages were distinctly observed, suggesting close physical proximity or possible cellular interaction (Fig. 24A–C). These findings visually support a spatial relationship between XtiSCs and macrophages during regeneration.

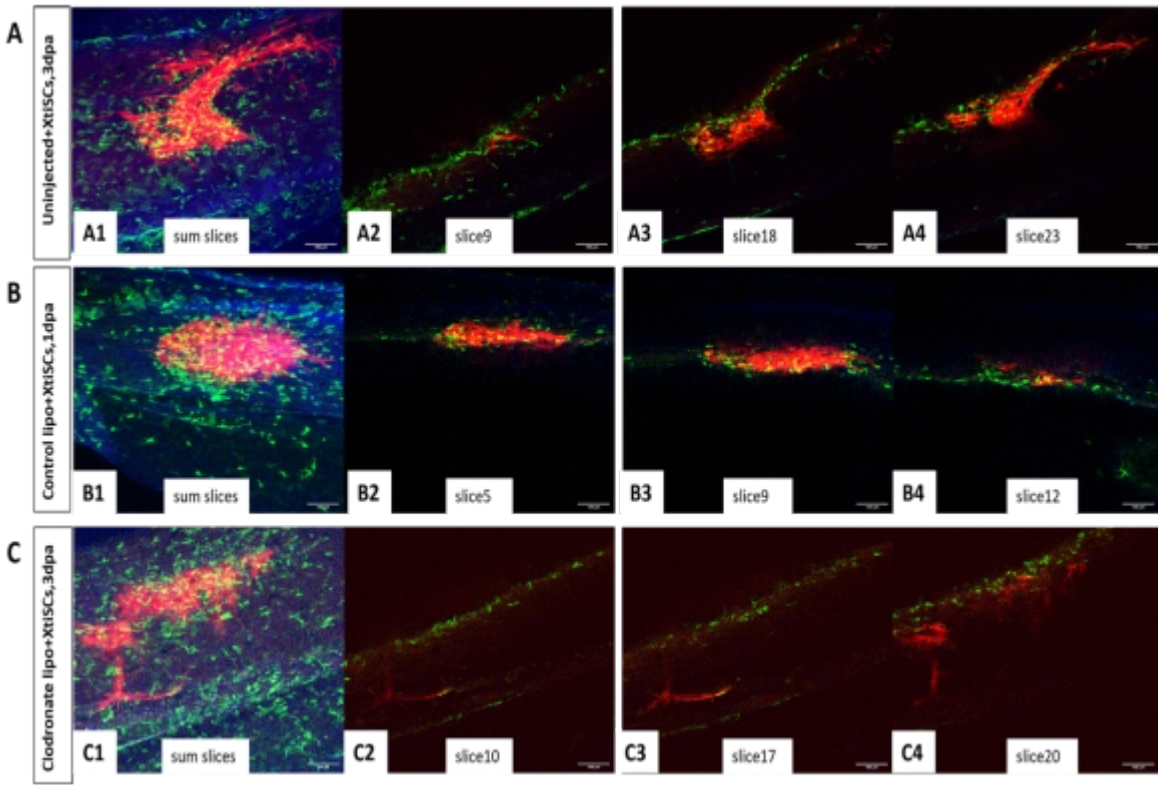

Figure 24. XtiSCs and XtiSCs' mitochondria directly interact with macrophages.
Co-localization of XtiSCs and macrophages at the injection site was observed, including mitochondrial signals from XtiSCs detected within macrophages close to both the regenerated tail and the injection region. (A–C) The overlap of Katushka RFP-labeled XtiSCs (red) and isolectin B4-labeled macrophages (green) was identified through whole-mount immunostaining and confocal microscopy using z-stack scanning. The images are displayed as maximum intensity projections (sum slices) alongside three selected individual z-stack slices. Cell nuclei are stained with DAPI (blue). Scale bar: 100 μm.
A1–A4: Uninjected tadpoles injected with XtiSCs at 3 days post-amputation (3 dpa). A1: sum slices; A2–A4: z-stack slices 9, 18, and 23.
B1–B4: Tadpoles injected with control liposomes followed by XtiSCs at 1 dpa. B1: sum slices; B2–B4: z-stack slices 5, 9, and 12.
C1–C4: Tadpoles treated with clodronate liposomes prior to XtiSC injection at 3 dpa. C1: sum slices; C2–C4: z-stack slices 10, 17, and 20.

5.1.14 MitoTracker Dye Can't Be Uptaken Specifically by Macrophages

To exclude the possibility that Mitotracker dye alone could be nonspecifically taken up by macrophages, we performed high-dose Mitotracker injections and subsequently assessed dye distribution at multiple time points (2 hours, 1 day, 2 days, and 3 days post-injection). No co-localization of unspecific red fluorescence with green macrophage signals was observed at any of these time points (Fig. 25). These results indicate that macrophages do not specifically uptake Mitotracker dye under the experimental conditions employed, confirming the specificity of our mitochondrial labeling strategy.

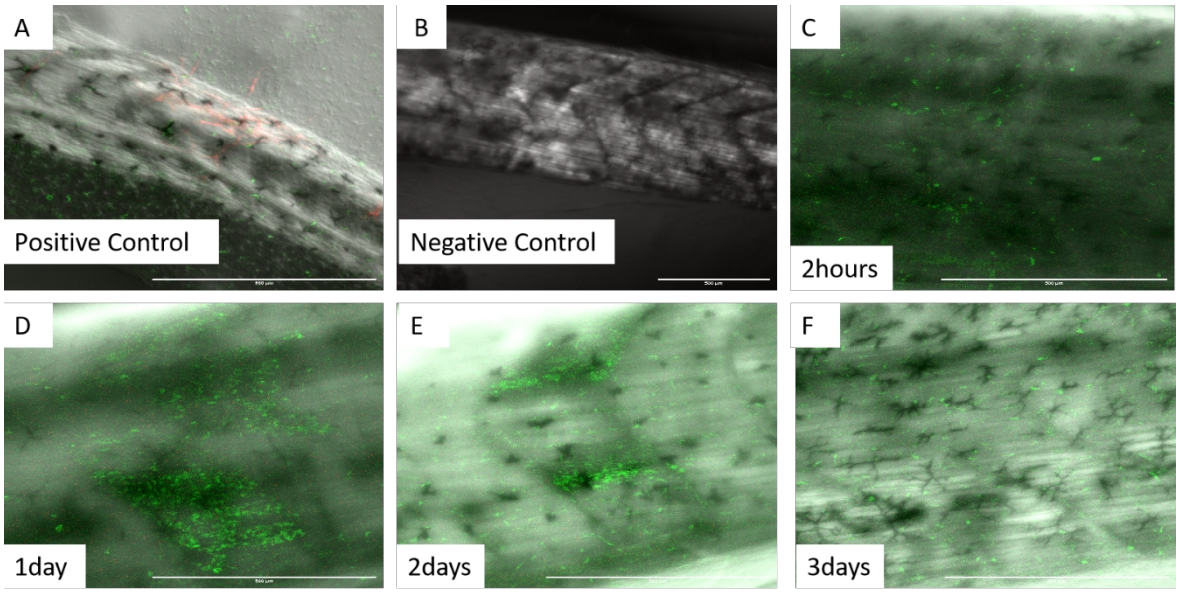

Figure 25. MitoTracker dye can't be uptaken specifically by macrophages.
50nl of 100 µM MitoTracker dye was injected into 4-week-old *X. tropicalis* tadpoles. Whole-mount immunostaining for isolectin B4 (green), a macrophage marker, was performed on tadpoles collected at 2 hours, 1 day, 2 days, and 3 days post-injection. **(A)** Positive control: tadpoles injected with RFP-labeled XtiSCs showing red signal representing XtiSCs. **(B)** Negative control: tadpoles injected only with MitoTracker dye without isolectin B4 staining. **(C–F)** Tadpoles collected at 2 hours (C), 1 day (D), 2 days (E), and 3 days (F) post MitoTracker injection. Green: isolectin B4-labeled macrophages. Scale bar: 500 µm.

5.1.15 Co-localization of XtiSCs' Mitochondria and Macrophages

Further analysis employing MitoTracker staining to label XtiSC-derived mitochondria revealed a clear overlap between the red mitochondrial signal and green fluorescence marking macrophages, indicating the presence of XtiSC-derived mitochondria within some macrophages in the tadpole (Fig. 26A). These findings provide compelling *in vivo* evidence for mitochondrial transfer from XtiSCs to macrophages. This intercellular organelle transfer may play a critical role in enhancing macrophage anti-inflammatory functions and shaping the immune environment conducive to regeneration.

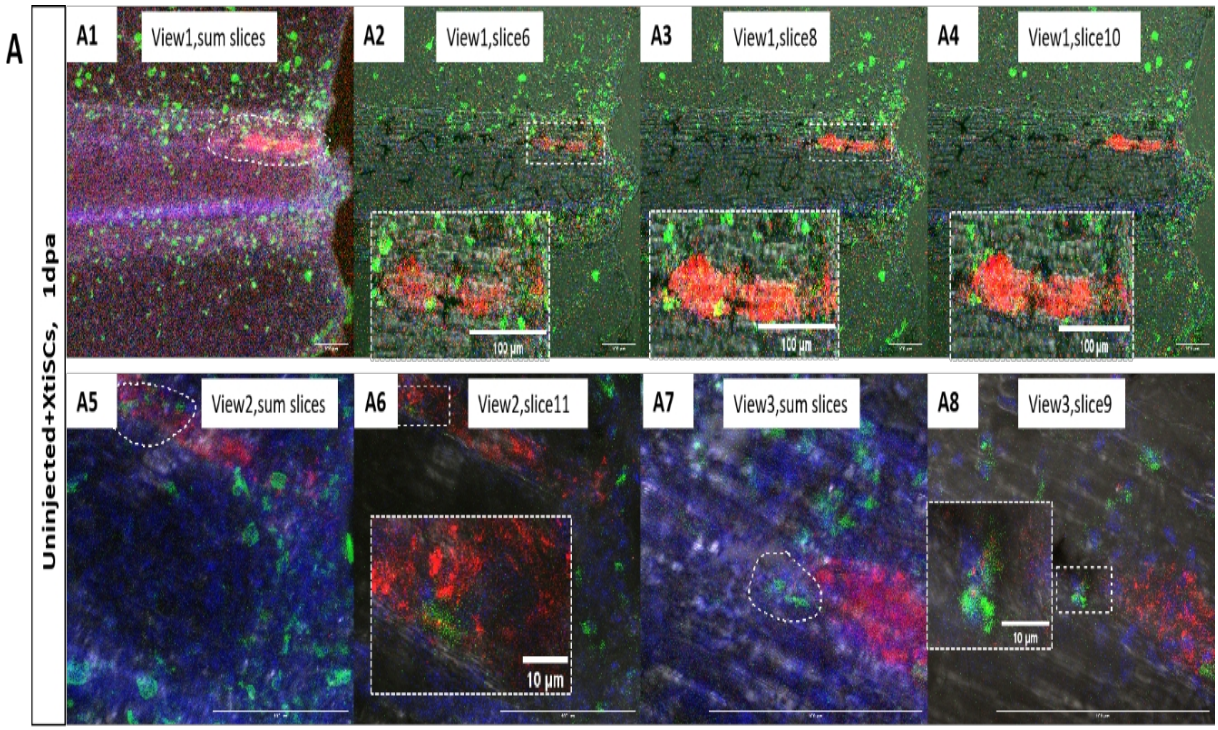

Figure 26. XtiSCs' mitochondria directly interact with macrophages.
Co-localization of XtiSC mitochondria and macrophages was observed near the regenerated tail and injection site at 1 day post-amputation (1 dpa). The overlapping area in a single z-slice was enlarged within a larger dashed box and displayed alongside the original image. Red indicates mitochondria of XtiSCs labeled with MitoTracker® Red; green marks macrophages stained with isolectin B4; blue represents DAPI-stained nuclei. Scale bars are 100 µm except for panels A6 and A8, which have a scale bar of 10 µm. Images labeled View 1, 2, and 3 correspond to different regions from the same tadpole: View 1 was captured at 10× magnification, while Views 2 and 3 used 63× magnification. Panels A1, A5, and A7 show maximum intensity projections (sum slices) from z-stack images, whereas A2–A4, A6, and A8 present single slices from the z-stack.

5.1.16 Evidence That XtiSCs May Transdifferentiate to Macrophages in Single Cell Level

Finally, we investigated whether XtiSCs possess the potential to transdifferentiate into other cell types, such as macrophages. To test this, we prepared single-cell suspensions from tadpoles injected with XtiSCs and performed isolectin B4 staining to label macrophages. Confocal microscopy revealed rare instances of cells co-expressing the red fluorescent protein Katushka RFP and the fluorescein-conjugated isolectin B4 signal (Fig. 27). Given our previous observation that XtiSCs alone are not labeled by isolectin B4 (Fig. 15), this co-expression strongly suggests the possibility of transdifferentiation of XtiSCs into macrophage-like cells *in vivo*.

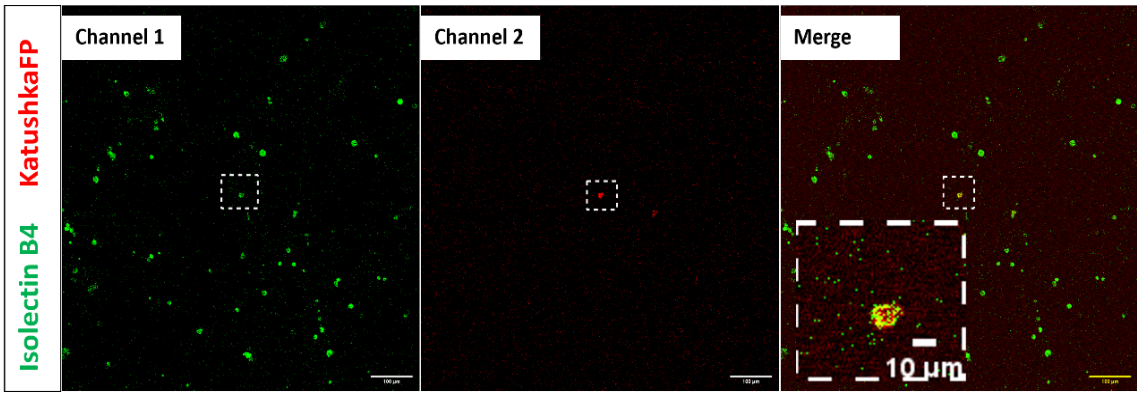

Figure 27. Co-expression of Katushka RFP-labeled XtiSCs and isolectin B4 (macrophage marker) was examined at the single-cell level.
A single-cell suspension was prepared from tadpole tails at 5 days post-amputation (5 dpa). Cells were stained with isolectin B4 to label macrophages (green fluorescence), while Katushka RFP-labeled XtiSCs displayed inherent red fluorescence without additional staining. Scale bar: 100 µm.

5.2 Function of XtiSCs in *X. tropicalis* Heart Regeneration Study

5.2.1 Apical Resection of *X. tropicalis* Heart

Among the commonly utilized models for studying cardiac regeneration mechanisms in zebrafish are apical resection, cryoinjury, and genetic ablation (Sanchez-Iranzo et al., 2013), as shown in Fig.28. While these models share similar initial injury responses, they differ notably in the degree of transient fibrotic tissue accumulation and the time required to achieve complete regeneration. Considering both procedural feasibility and consistency with prior literature (Liao et al., 2017; Lv et al., 2020; Lv et al., 2023), we selected the apical resection model to induce cardiac injury in adult *X. tropicalis*. The surgical procedure used for apical resection is illustrated in Fig. 29.

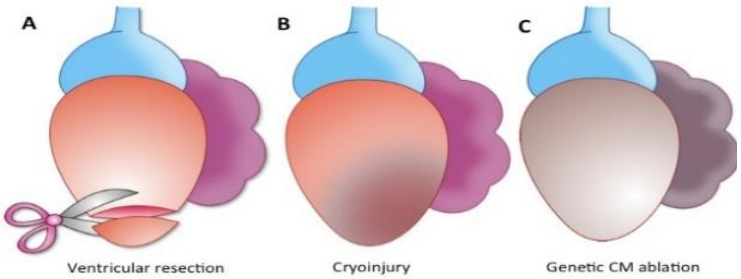

Figure 28: Current used models to study mechanisms of cardiac regeneration. (A) ventricular apex resection, (B) ventricular cryoinjury (C) cardiomyocytes genetic ablation.

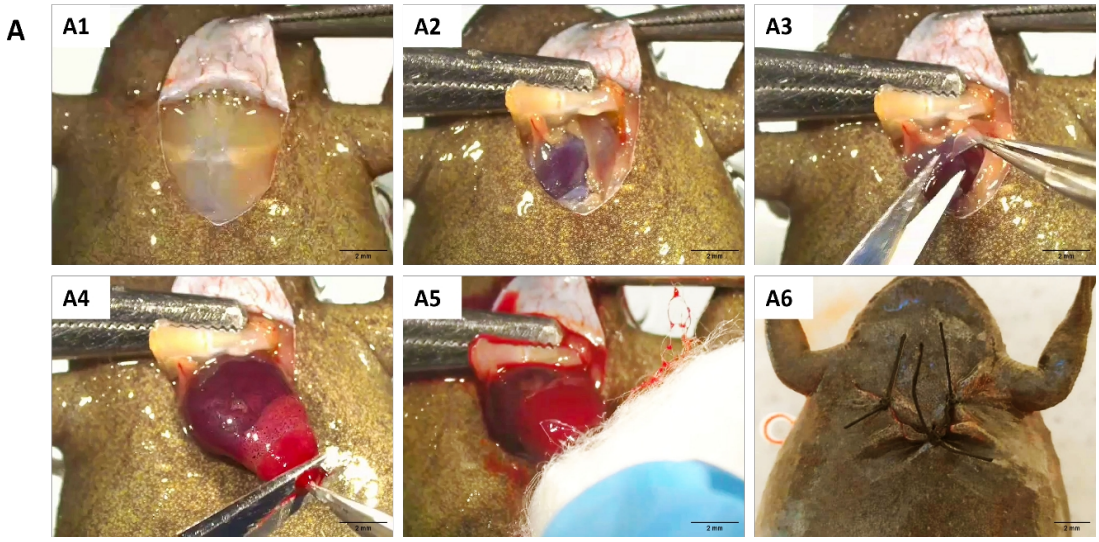

Figure 29. Apical resection of *X. tropicalis* heart
(A) The experiment procedure of heart apical resection in *X. tropicalis*. A1: V-shaped skin incision. A2: Incision of chest muscles. A3: Dissection of the pleura. A4: Dissection of the pericardium and resection of the heart apex with scissors. A5: Blood coagulation after heart apex resection with sterile cotton. A6: Skin incision closure with stitches. Scale bar:2mm.

5.2.2 Hind Limb Muscle Bed XtiSCs Injection Is More Effective in Heart Injury Healing

Assessment of fibrotic scar formation at 7 days post-apical resection revealed that tadpoles receiving XtiSC injections into the skeletal muscle bed three days prior to surgery showed significantly less scar tissue compared to both the 2/3 PBS control group and the group with XtiSCs implanted directly into the heart (Fig. 30). Thus, in this experiment, we utilized hind limb muscle bed injection as the delivery method for XtiSCs.

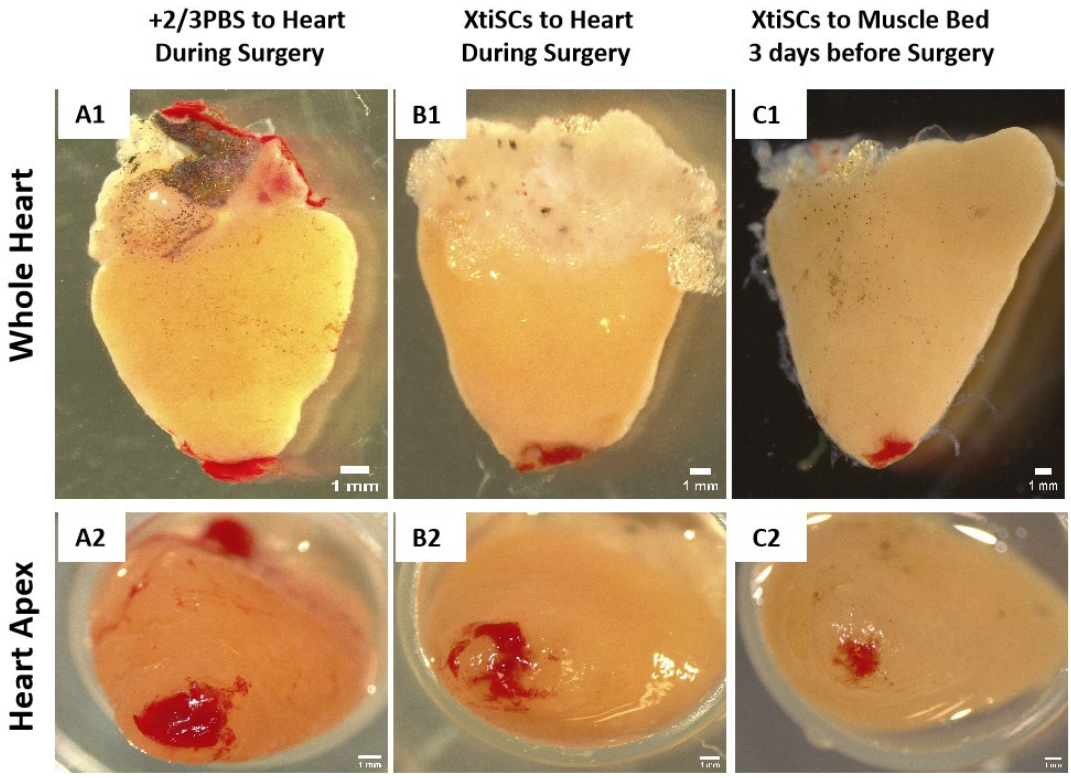

Figure 30. Comparison of Three XtiSCs Administration Methods

XtiSCs injection into the hind limb muscle bed three days prior to apical heart resection resulted in more efficient healing outcomes compared to direct administration of XtiSCs into the heart during surgery. Fibrotic tissue formation was evaluated 7 days post-resection among three experimental groups: (A1, A2) 2/3 PBS injected directly into the heart during surgery, (B1, B2) XtiSCs delivered into the heart at the time of resection, and (C1, C2) XtiSCs pre-injected into the hind limb muscle bed three days before the procedure. Panel A1 depicts the heart following PBS injection; A2 provides a magnified view of the apex. Panel B1 shows the heart after direct intramyocardial XtiSCs injection, with B2 highlighting the apex in greater detail. Panel C1 illustrates the heart from tadpoles that received XtiSCs into the hind limb muscle bed in advance of injury, and C2 offers a close-up of the apex area. Scale bar: 1 mm.

5.2.3 XtiSCs Survive in The Hind Limb Muscle Bed for Up to Three Weeks Post-injection

Initially, we attempted to inject XtiSCs directly into the heart or bloodstream; however, no surviving cells were detected in the heart tissue post-injection (data not shown). Subsequently, we administered XtiSCs into the hind limb skeletal muscle bed, where robust cell survival was observed for over three weeks post-transplantation (Fig. 31).

This outcome aligns with our prior findings in *X. tropicalis* tadpoles (Qing Zhao et al., 2024), which highlighted the high compatibility and viability of XtiSCs in transplantation settings. Notably, the red fluorescence signal from XtiSCs gradually diminished over time, with detectable signals at 10 days, 2 weeks, and 3 weeks post-injection.

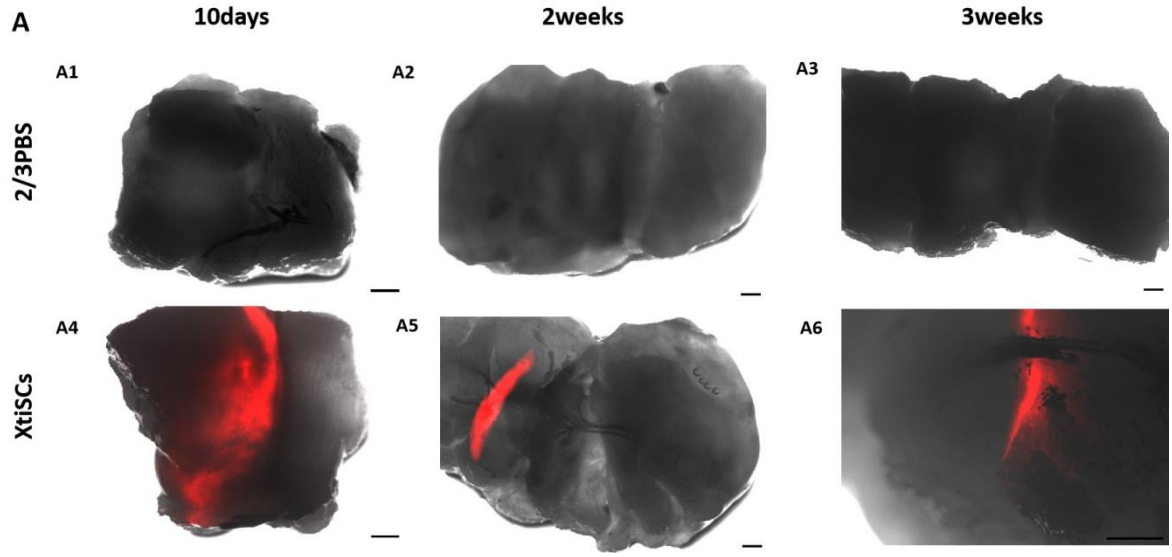

Figure 31. XtiSCs exhibit sustained viability in the hind limb skeletal muscle bed.
Survival of XtiSCs 10 days, 2weeks and 3weeks after injection into muscle bed. A1-A3: 2/3PBS injected control group at 10 days, 2weeks and 3weeks after injection, respectively. B2-B3: XtiSCs injected group at 10 days, 2weeks and 3weeks after injection, respectively. All images show merged views of brightfield and red fluorescence channels (Katushka RFP) captured under a fluorescence microscope. Scale bar: 1 mm.

5.2.4 Administration of Clodronate Liposomes Effectively Depletes Macrophages in Adult *X. tropicalis* Frogs

Macrophage depletion during the early post-injury phase has been shown to impair heart regeneration in salamanders (Godwin et al., 2017). However, whether macrophages play a similar role in *X. tropicalis* heart regeneration remains unclear. To investigate this, we depleted macrophages in adult *X.tropicalis* frogs by administering three doses of clodronate liposomes into the dorsal lymph sac every two days. Direct cardiac injection was attempted but proved lethal, with no survivors. We then assessed the impact of macrophage depletion on heart regeneration and whether co-administration of XtiSCs could mitigate any regeneration deficits.

Macrophage depletion was confirmed seven days after the final clodronate liposome injection, as evidenced by a marked reduction in macrophage markers in both the heart and liver tissues (Fig. 32C, D). In contrast, DiI-labeled control liposomes were found to be widely distributed throughout these tissues, demonstrating effective systemic delivery (Fig. 32A, B).

To evaluate the potential immunomodulatory and regenerative benefits of XtiSCs, we devised an experimental strategy (Fig. 32E) in which XtiSCs were implanted into the hind limb muscle bed of macrophage-depleted frogs. This was followed by surgical apical

resection of the heart. Cardiac regeneration was assessed seven days post-injury, a critical time point characterized by maximal fibrotic tissue formation and robust cardiomyocyte proliferation (Liao et al., 2017).

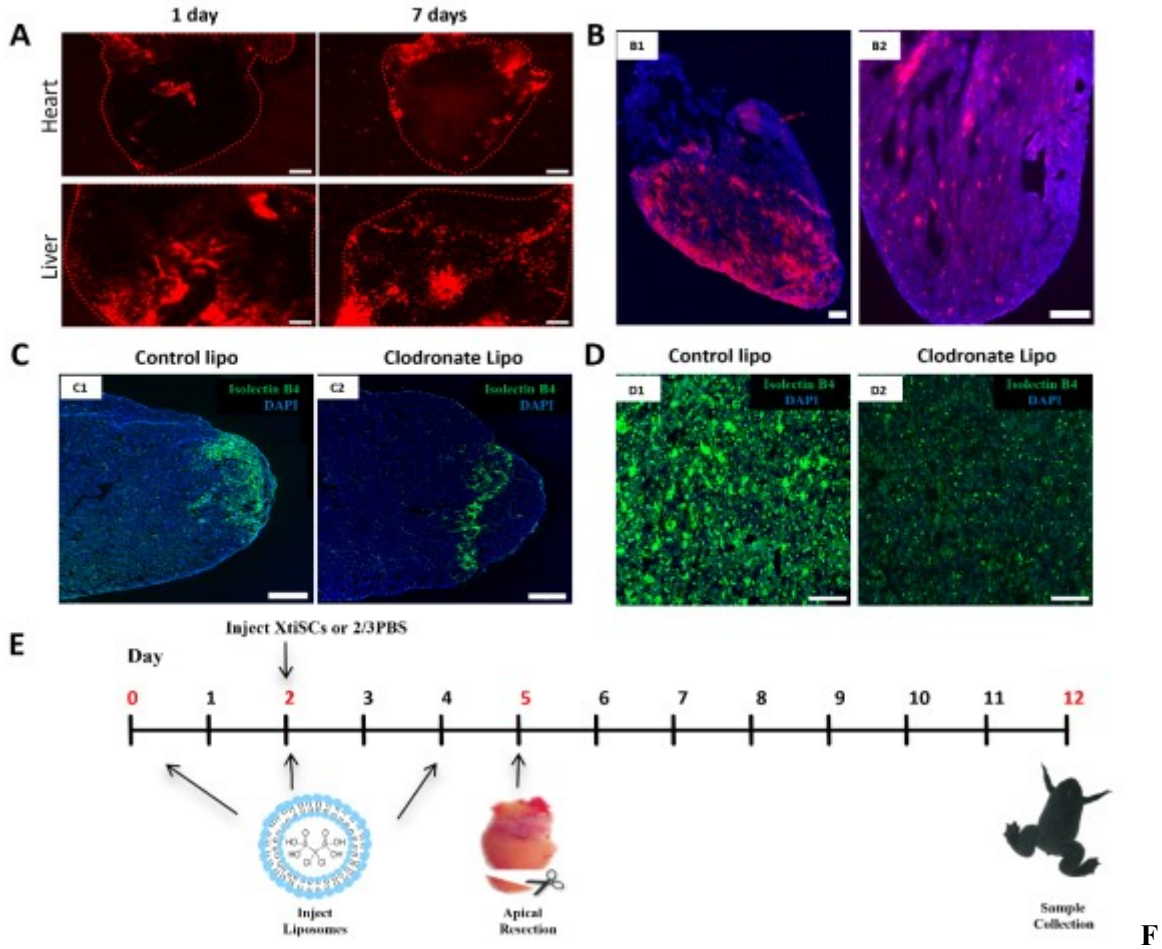

Figure 32. Macrophage depletion in adult *X. tropicalis*.

Injection of clodronate liposomes into the dorsal lymph sac three times, every two days successfully depleted macrophages *in vivo* in adult *X. tropicalis* frogs. (A) Fluorescent DiI liposomes distribution in heart and liver at 1day and 7 days after the last dose of fluorescent liposomes, as detected under stereo fluorescent microscope. Red dashed lines delineate the border of the tissues. Red: Fluorescent DiI liposomes. Scale bar: 1 mm. (B) Heart section at 8 days after the last dose of fluorescent DiI (7 days after heart surgery) showed that liposomes were filled in the heart tissue. Scale bar: 400 µm. (C) Isolectin B4 (macrophage marker) staining on heart sections at 8 days after the last dose of liposomes (7 days after heart surgery) in control liposomes (C1) treated and clodronate liposomes (C2) treated groups. Scale bar: 400 µm. 3 frogs were checked for clodronate liposomes depletion efficiency. (D) Isolectin B4 (macrophage marker) staining on liver sections at 8 days after the last dose of liposomes (7 days after heart surgery) in control liposomes (D1) treated and clodronate liposomes (D2) treated groups. Scale bar: 200 µm. 3 frogs were checked for clodronate liposomes depletion efficiency. (E) Experimental setting for macrophage depletion, XtiSCs injection and heart apex resection experiment. Briefly, three dosages of clodronate liposomes or control liposomes were injected into dorsal lymphatic sac and the XtiSCs or 2/3PBS (control) were administered into hind limb muscle bed the same day with 2nd dose injection. One day after last injection, heart injury was performed. Frogs were sacrificed and samples were imaged and collected at 7 days post-surgery.

5.2.5 XtiSCs Promote Restoration of Original Heart Apex Morphology After Resection

The morphological assessment of regenerated *X. tropicalis* hearts was conducted 7 days post-surgical injury using stereomicroscopy (Fig. 33). In all samples, fibrotic tissue formation was evident at the site of apical resection. Notably, the most severe fibrotic phenotypes were observed in the macrophage-depleted groups treated with clodronate liposomes (Fig. 33E1, E2, F1, F2), suggesting impaired regenerative capacity in the absence of macrophages. Remarkably, in all experimental groups that received XtiSCs injections into the hind limb muscle bed, fibrotic tissue deposition was markedly reduced compared to their respective 2/3 PBS control groups. These observations support a protective and pro-regenerative role of XtiSCs, particularly in limiting fibrotic remodeling following cardiac injury.

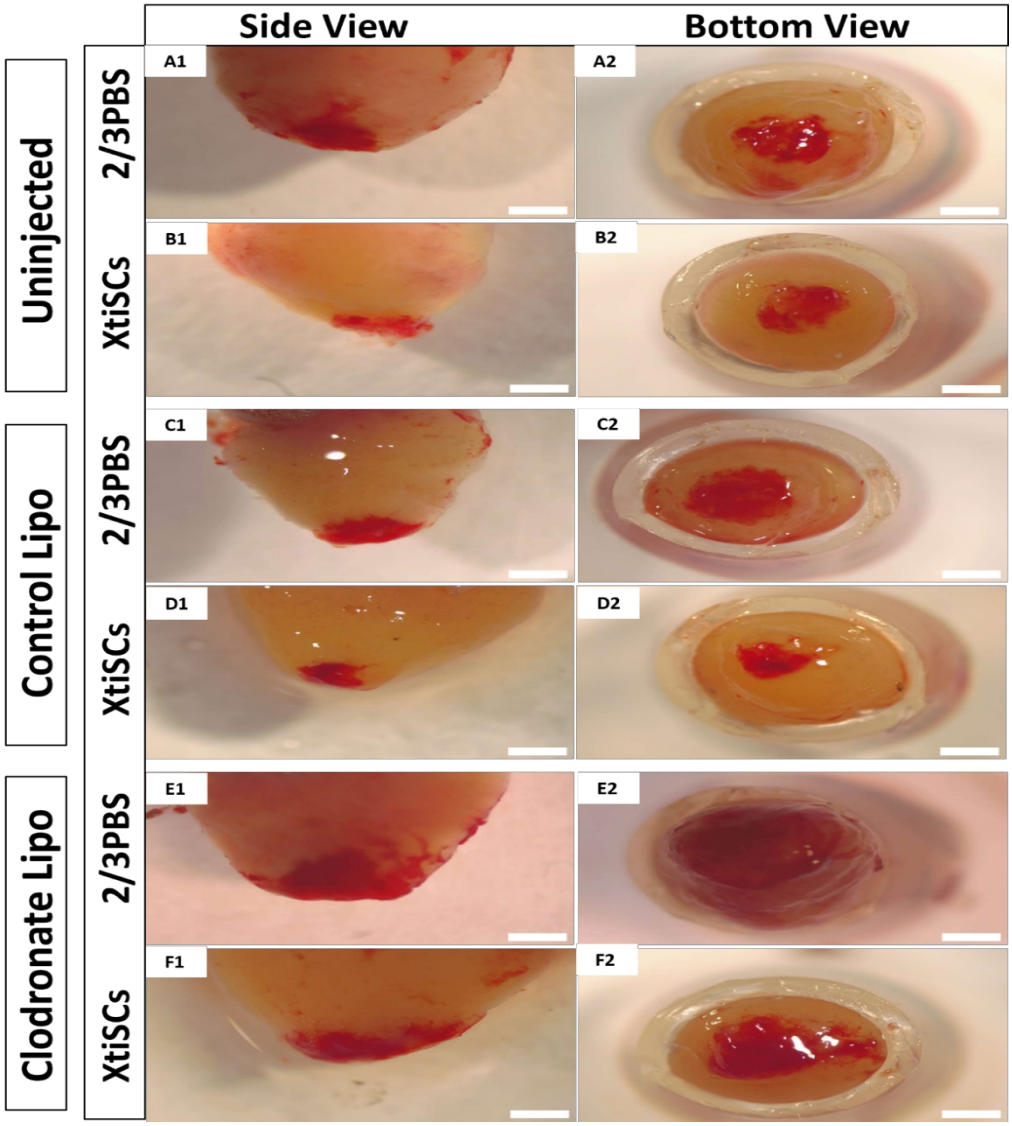

Figure 33. XtiSCs enhance normal morphology of regenerated heart apex after resection. Representative images of regenerated heart morphology in the six experimental groups at 7 days post-heart surgery were displayed. A1, A2: Frog without liposomes treatment and injected with 2/3 PBS. B1, B2: Frog without liposomes treatment and injected with XtiSCs. C1, C2: Frog with control liposomes treatment and injected with 2/3 PBS. D1, D2: Frog with control liposomes treatment and injected with XtiSCs. E1, E2: Frog with clodronate liposomes treatment and injected with 2/3 PBS. F1, F2: Frog with clodronate liposomes treatment and injected with XtiSCs. A1-F1: Side view of the heart apex, A2-F2: Bottom view of the heart apex. Scale bar: 1mm. Three frogs were inspected for each group respectively.

5.2.6 XtiSCs Improve Cardiac Muscle Regeneration and Reduce Scar Formation in The Frog Apical Resection Model

As demonstrated by Liao et al. (Liao et al., 2017), endogenous cardiomyocyte proliferation is essential for heart regeneration in adult *X. tropicalis*, with the injured myocardium capable of regenerating mature cardiomyocytes within approximately 30 days. Fibronectin, a major extracellular matrix (ECM) component, serves as a key marker of fibrotic tissue accumulation (Godwin et al., 2017). In our study, immunostaining for tropomyosin (a cardiomyocyte marker) and fibronectin (a fibrosis marker) revealed that injection of XtiSCs into the hind limb muscle bed significantly enhanced myocardial regeneration at 7 days post-injury across all experimental groups (uninjected, control liposomes, and clodronate liposomes), compared to their respective 2/3 PBS controls. Correspondingly, fibrotic scar formation was markedly reduced following XtiSCs administration.

Importantly, our results provide the first evidence that macrophage depletion via clodronate liposomes in adult *X. tropicalis* frogs leads to impaired cardiac regeneration (Fig. 34), underscoring the essential role of macrophages in this process. Previous studies have indicated that inflammatory cell infiltration and fibrotic tissue production peak within the first 7 days post-injury (Liao et al., 2017). Within this critical window, we observed a substantial increase in cardiomyocyte regeneration and a decrease in fibrosis in XtiSC-treated, macrophage-depleted animals, suggesting that XtiSCs may act through modulation of the immune environment to promote regenerative outcomes in the heart.

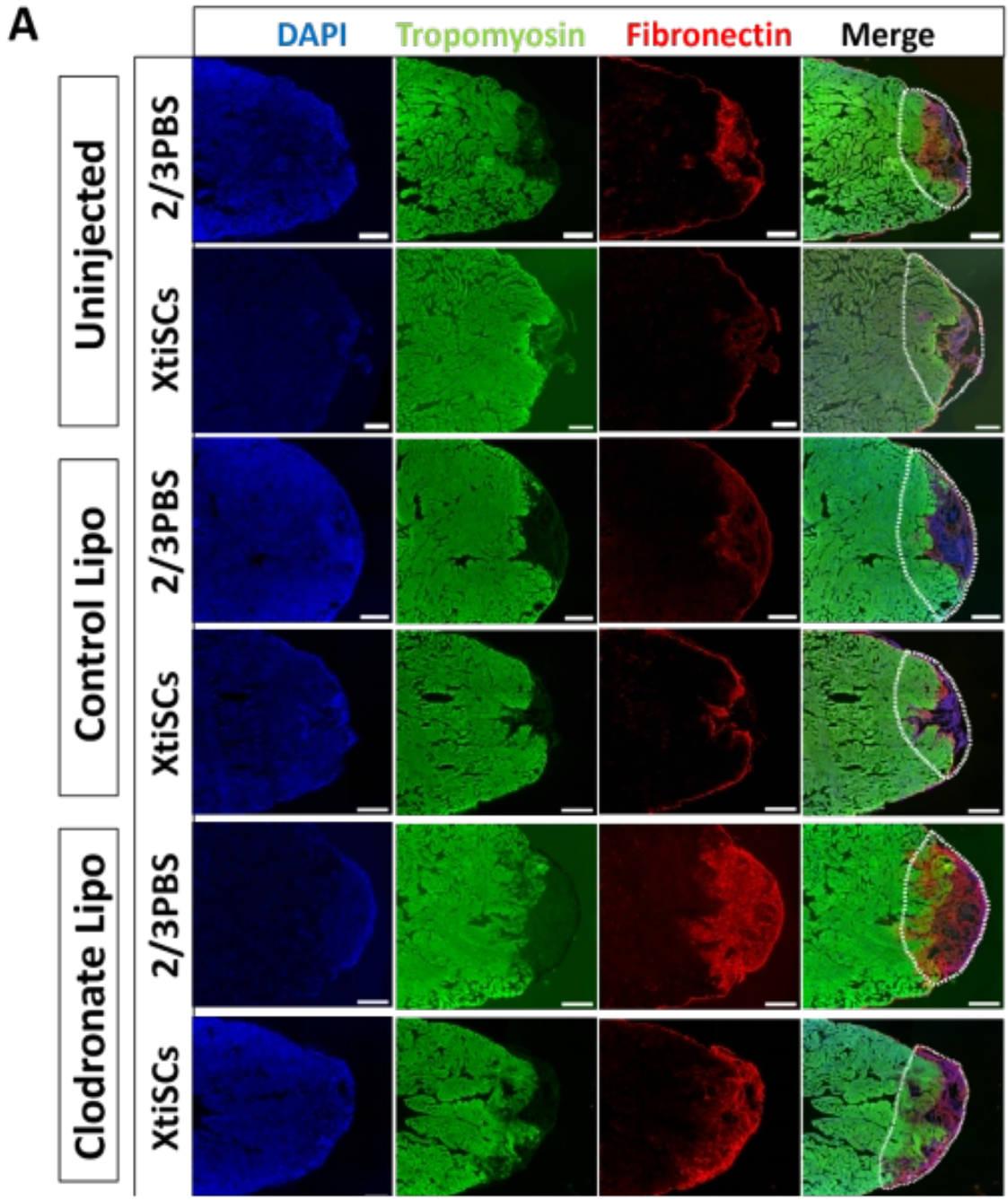

Figure 34. XtiSCs implantation increase heart muscle regeneration and decrease scar formation.

Heart regeneration and scar formation were visualized by immunostaining frog heart sections for tropomyosin signal (as a cardiomyocyte marker (Wieczorek, 2018)) and for fibronectin (a component of the extracellular matrix (ECM) used here as a marker of fibrotic scar). Figure.34A shows representative pictures of tropomyosin and fibronectin staining in heart sections in 6 experimental groups, Scale bar: 400 μm.

5.2.7 XtiSCs Increase Macrophage Infiltration in The Regenerated Heart of Adult *X. tropicalis*

The immunomodulatory properties of Sertoli cells in transplantation contexts are well-established, and recent studies have demonstrated the ability of *Xenopus tropicalis* immature Sertoli cells (XtiSCs) to modulate immune responses both in murine models (Vegrichtova et al., 2022) and in the *X. tropicalis* tadpole tail regeneration model (Qing Zhao et al., 2024). To further explore this immunomodulatory potential in adult frogs, we assessed macrophage distribution following XtiSCs administration in macrophage-depleted animals using isolectin B4, a validated marker for macrophages (Sorokin and Hoyt, 1992; Godwin et al., 2017).

Comparative analysis revealed that XtiSCs treatment significantly increased macrophage density in the liver of clodronate liposome-injected frogs relative to the 2/3 PBS control group (Fig. 35A). In the heart, XtiSCs did not merely increase macrophage presence but also modulated their spatial distribution, promoting infiltration into the regenerating myocardium rather than confinement to the injury margin, as observed in the 2/3 PBS control group (Fig. 35B). These findings suggest that XtiSCs not only enhance systemic macrophage presence in macrophage-depleted environments but also redirect macrophages toward regenerative zones, supporting their role as key immunoregulatory agents in heart regeneration.

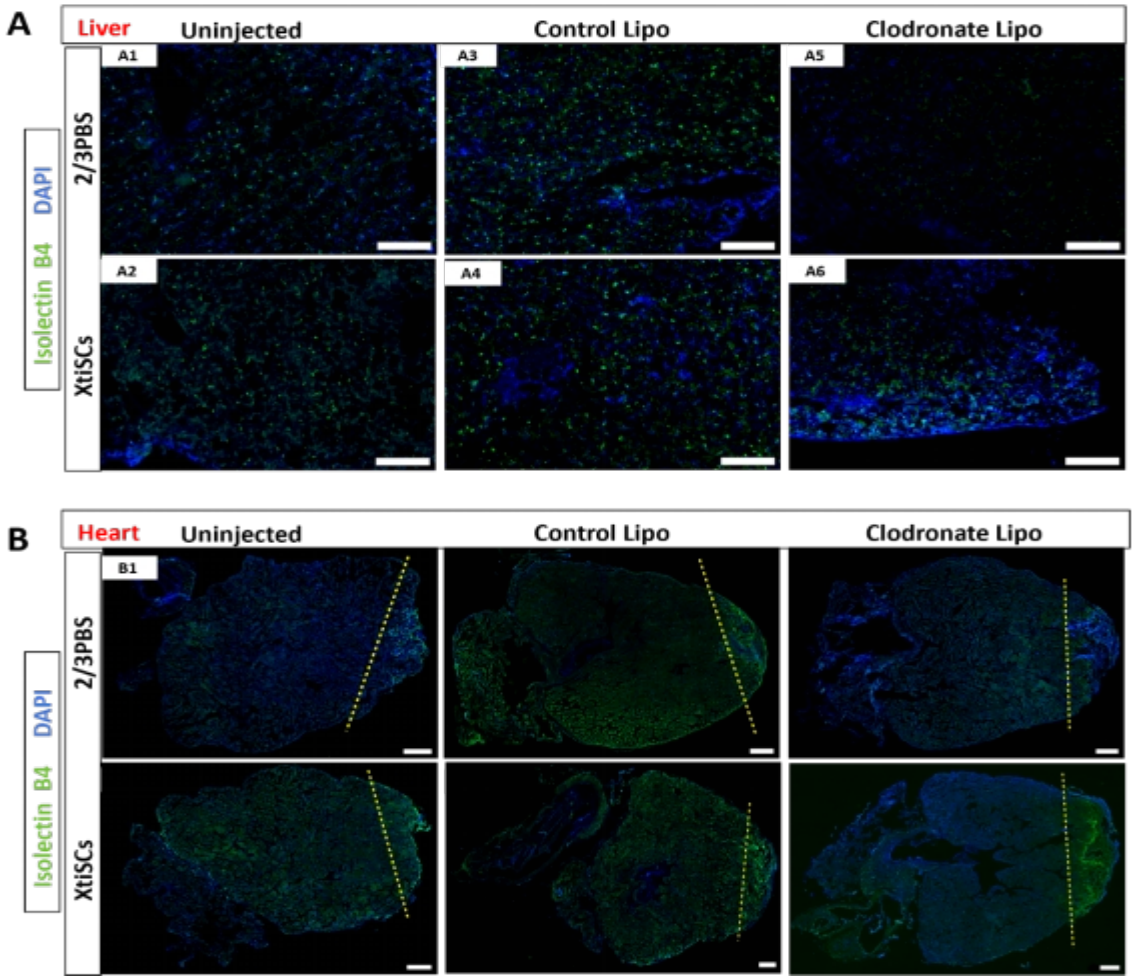

Figure 35. XtiSCs implantation increases macrophage infiltration at the regeneration area. Macrophage numbers and their distribution were assessed in the heart and liver 7 days post-heart apex injury. Macrophages were labeled with Isolectin B4 coupled with fluorescein, shown in green, while blue signal (DAPI) represents cell nuclei. A: Macrophages in liver tissue in groups of A1, A2: 2/3PBS control and XtiSCs under non-injection group; A3, A4: 2/3PBS control and XtiSCs under control liposomes injected group; A5, A6: 2/3PBS control and XtiSCs under clodronate liposomes injected group. Scale bar: 200um. B: Macrophages in heart tissue in groups of B1, B2: 2/3PBS control and XtiSCs under non-injection group; B3, B4: 2/3PBS control and XtiSCs under control liposomes injected group; B5, B6: 2/3PBS control and XtiSCs under clodronate liposomes injected group. Dashed line delineates presumable cutting line. Scale bar: 400um.

5.2.8 XtiSCs Increase Survival Following Heart Apical Resection Surgery

Beyond their established roles in improving heart regeneration morphology, enhancing cardiomyocyte proliferation, and reducing fibrotic scar formation, XtiSCs also contributed to improved survival outcomes following cardiac injury. We conducted a statistical analysis of frog survival rates post-surgery across three experimental groups: no liposome injection, control liposome injection, and clodronate liposome injection. Notably, XtiSCs

administration significantly increased survival in both the control and clodronate liposome groups, with the increase reaching statistical significance in the control liposome group (Fig. 36). These findings suggest that XtiSCs confer systemic benefits that may be associated with immune stabilization, particularly under the immune-perturbing conditions induced by liposome treatments.

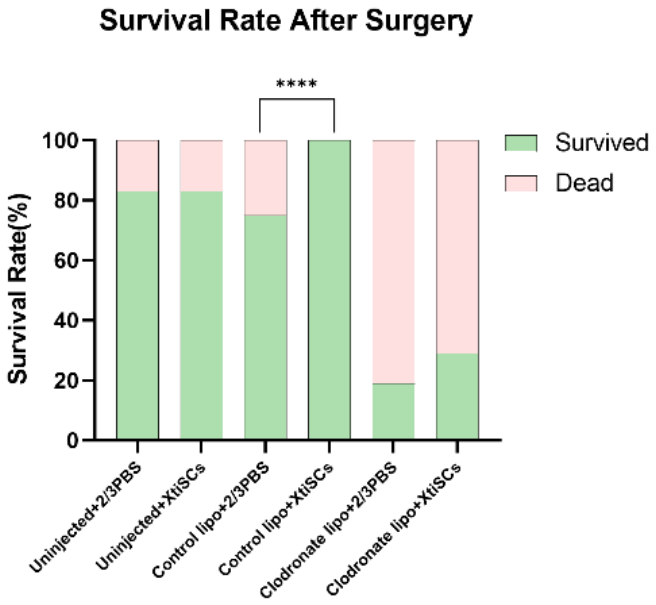

Figure36. XtiSCs increased the frog survival rate after heart apex surgery.
Survival rates were assessed post-surgery across different treatment groups. Tadpoles treated with clodronate liposomes—whether receiving 2/3 PBS or XtiSCs—exhibited markedly elevated mortality. Statistical significance was determined using a two-way ANOVA, with p-values indicating levels of significance as follows: *$p \leq 0.05$; **$p \leq 0.001$. Additionally, Fisher's exact test revealed highly significant differences (****$P < 0.0001$). Data were compiled from a minimum of three independent experiments with at least four tadpoles per group ($n \geq 4$).

5.3 Generation of CRISPR-Cas9 Transgenic *X. tropicalis* Animals

5.3.1 Construction CRISPR-Cas9 Knock-In Plasmid

5.3.1.1 Construction of Pax7 Knock-In Plasmid

We successfully constructed a *Pax7* knock-in plasmid designed for CRISPR/Cas9-mediated genome editing in *X. tropicalis* (Fig. 37). The donor plasmid was engineered to include two homologous "bait" sequences flanking a GFP reporter cassette under the control of the endogenous *Pax7* regulatory context. These baits were placed such that the CRISPR/Cas9 guide RNA (gRNA) target site is located between them, promoting precise cleavage at the *Pax7* locus.

Each gene insertion during plasmid assembly was validated through Sanger sequencing. Importantly, the donor construct also included a gamma-crystallin promoter driving a

TurboFP reporter, which functions as a transgenesis marker. The TurboFP reporter is expressed upon successful genomic integration regardless of the cassette's orientation, providing a reliable readout of insertion events.

Targeted integration of the GFP cassette into the *Pax7* locus in the correct (forward) orientation is facilitated via the non-homologous end joining (NHEJ) pathway. The use of a conventional transcription terminator ensures proper cleavage and polyadenylation of the inserted sequences.

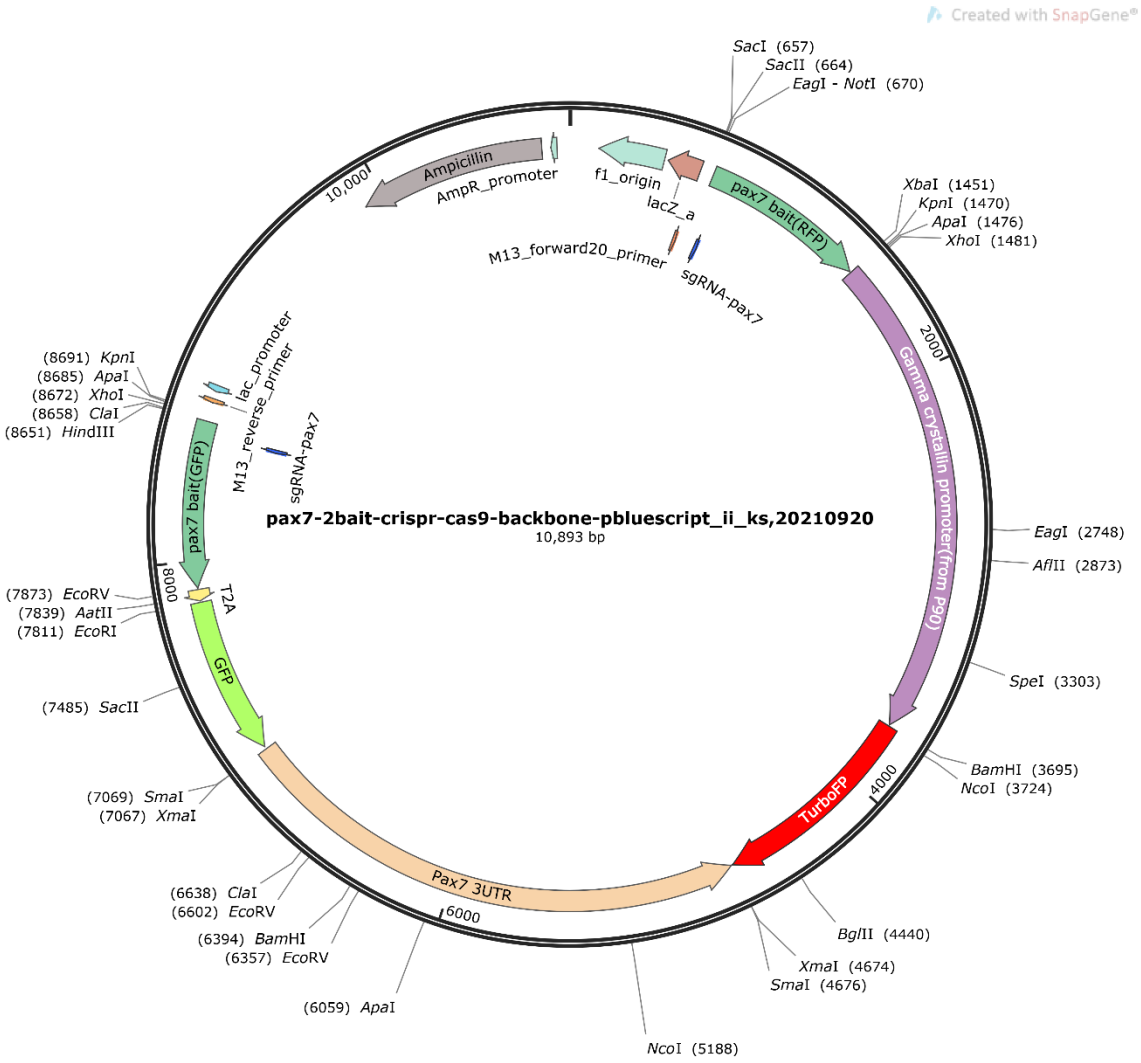

Figure 37. Plasmid map of 2 Bait Cas9 Strategy for *Pax7* Knock-in Plasmid.
Created with SnapGene.This plasmid has a full sequence of 10893bp and contains components: gamma crystallin (γCry) promoter, TurboFP, GFP, T2A, Pax7 bait (GFP side), Pax7 bait (RFP side).

5.3.1.2 Construction of MMP7 Knock-In Plasmid

We successfully constructed the *MMP7* knock-in plasmid using a donor plasmid designed to induce concurrent cleavages at the target genomic locus and two bait sites within the plasmid

(Fig. 38). The guide RNA (gRNA) target sequence is embedded within the two MMP7 bait sequences flanking the insertion cassette. This setup facilitates precise double-strand breaks at both the endogenous *MMP7* locus and within the donor plasmid.

Each gene insertion during the cloning process was rigorously validated by sequencing to ensure accuracy. Integration of the GFP reporter cassette into the *MMP7* locus in the forward orientation is driven by the non-homologous end joining (NHEJ) repair pathway. Simultaneously, the gamma crystallin promoter-driven TurboFP cassette is expressed independent of the orientation of integration, serving as an insertion marker.

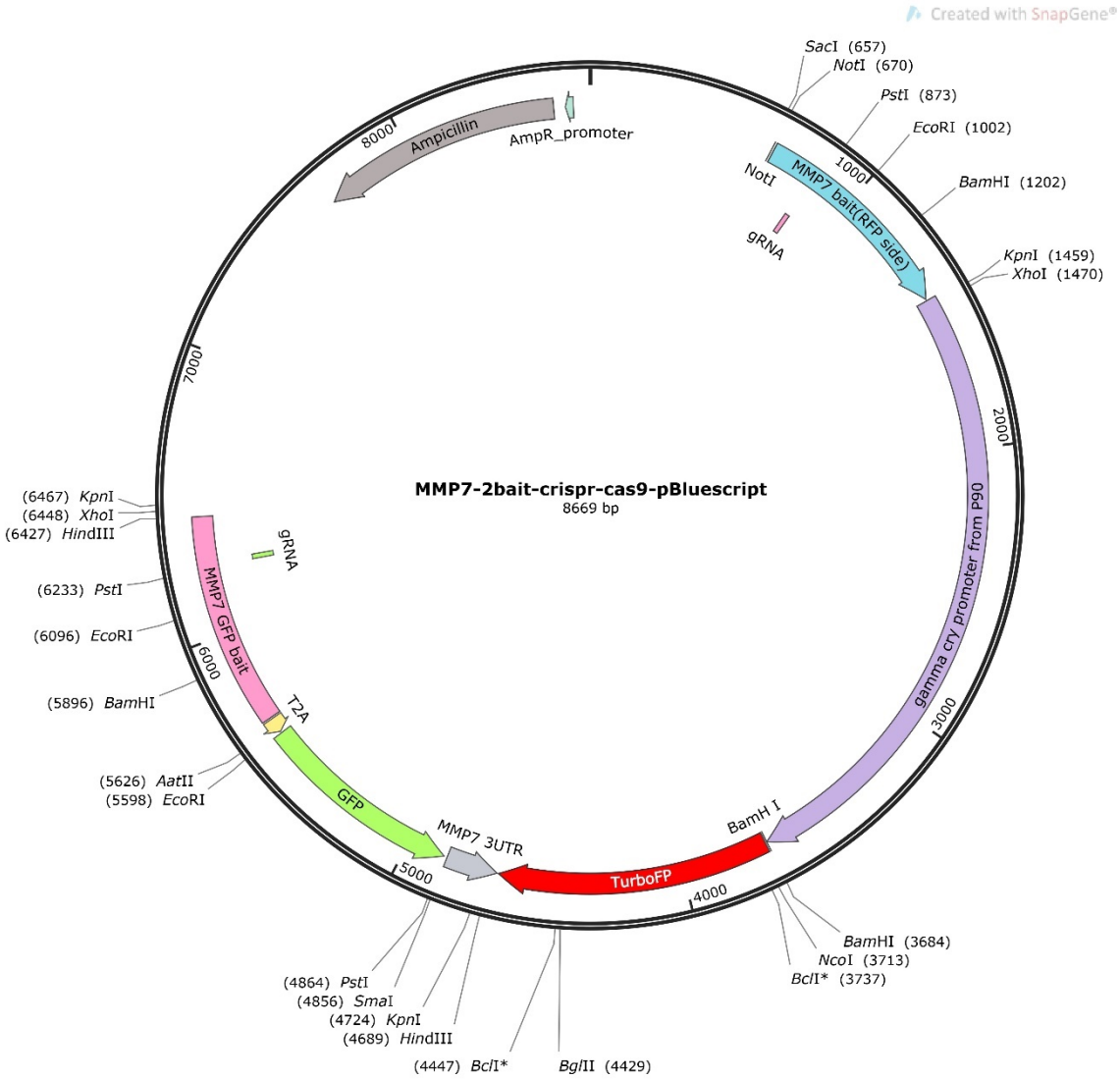

Figure 38. Plasmid map of 2 Bait Cas9 Strategy for MMP7 Knock-in Plasmid.
Created with SnapGene.This plasmid has a full sequence of 10893bp and contains components: gamma crystallin (γCry) promoter, TurboFP, GFP, T2A, MMP7 bait (GFP side), MMP7 bait (RFP side).

5.3.2 Statistics of Survival Rate and Positive Signal Rate

5.3.2.1 Survival Rate of F0 Tadpoles

For both *Pax7* and *MMP7* knock-in experiments, injected tadpoles were categorized into four groups (shown below). Across all categories, the average survival rate of injected tadpoles was generally below 60%. This relatively low survival rate reflects the impact of the injection procedure and genome editing on tadpole viability.

5.3.2.2 Statistical Analysis of F0 Tadpoles Signal for Pax7 Knock-in System

We performed multiple rounds of microinjections using the *Pax7* knock-in system and analyzed the resulting F0 tadpoles at 3 dpf for fluorescence expression.

GFP^+ RFP^+: 79%

GFP^+ RFP^-: 7%

GFP^- RFP^+: 6%

GFP^- RFP^-: 8%

*The RFP signal can be in both eyes or only in one eye.

Theoretically, the F0 tadpoles after microinjection of the *Pax7* or *MMP7* knock-in plasmid can be categorized into three groups based on fluorescence signals:

1)GFP^+ RFP^+ ---Tadpoles expressing both GFP and RFP.

2)GFP^- RFP^+ ---Tadpoles expressing RFP only.

3)GFP^- RFP^- ---Tadpoles expressing neither fluorescent protein.

Theoretically, because the GFP cassette insertion into the target locus can occur in either forward or reverse orientation with equal probability via the NHEJ pathway, the ratio of GFP^+ RFP^+ to GFP^- RFP^+ tadpoles is expected to be approximately 1:1. The RFP signal originates from the gamma crystallin promoter-driven TurboFP cassette, which is expected to express regardless of insertion direction, while GFP expression depends on correct orientation at the target locus.

Surprisingly, our experimental data show a significantly higher proportion of GFP^+ RFP^+ double-positive F0 tadpoles compared to the GFP^- RFP^+ group. Importantly, none of the GFP^+ RFP^+ F0 tadpoles transmitted the transgene to F1 progeny.

This strongly suggests that the majority of GFP^+ RFP^+ signals in F0 tadpoles derive from transient expression of the plasmid backbone rather than stable, targeted genomic integration. The plasmid backbone likely remains episomal or is randomly integrated in non-target loci, producing fluorescence without functional knock-in.

Therefore, while fluorescence in F0 is useful for screening, these data highlight the importance of verifying germline transmission to confirm successful knock-in events.

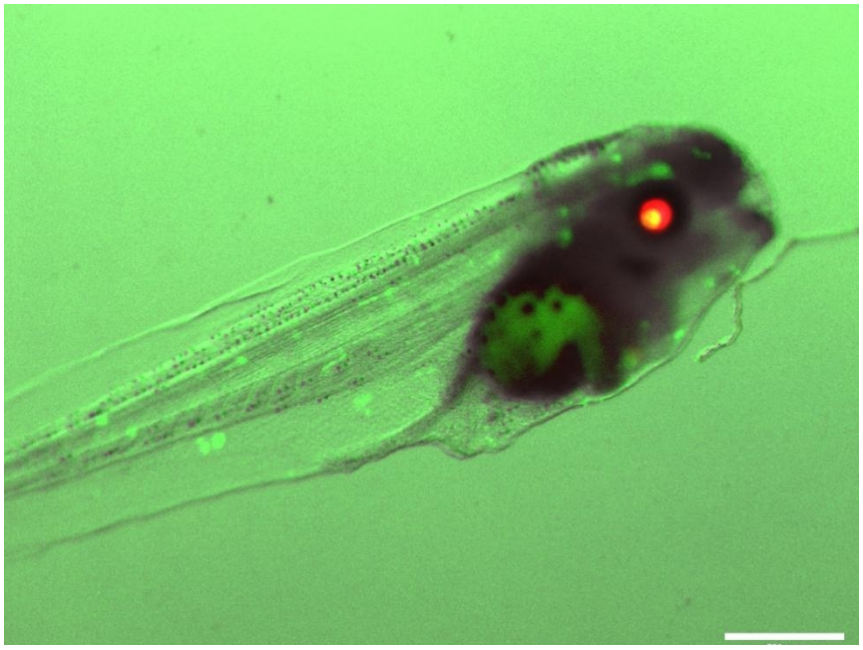

Figure 39. Representative images of F0 tadpoles under *Pax7* knock-in system at 3 days post-fertilization (3dpf) were captured and analyzed.
Green channel: GFP signal, which theoretically indicates expression in muscle stem cells and brain regions. Red channel: TurboFP signal driven by the gamma crystallin promoter, specifically expressed in the eyes. Scale bar: 500um.

5.3.2.3 Statistical Analysis of F0 Tadpoles Signal for MMP7 Knock-in System

We performed multiple rounds of microinjections using the *MMP7* knock-in system and analyzed the resulting F0 tadpoles at 3 dpf for fluorescence expression.

GFP^+ RFP^+ :86.9%

GFP^-, RFP^+/RFP^-: 13, 10%

Similarly, the *MMP7* knock-in F0 tadpoles also exhibited a disproportionately high rate of GFP^+/RFP^+ double-positive individuals. However, no true transgenic F0 frogs were obtained, suggesting that, as with the *Pax7* system, the majority of double-positive signals may result from transient backbone plasmid expression rather than successful targeted genomic integration.

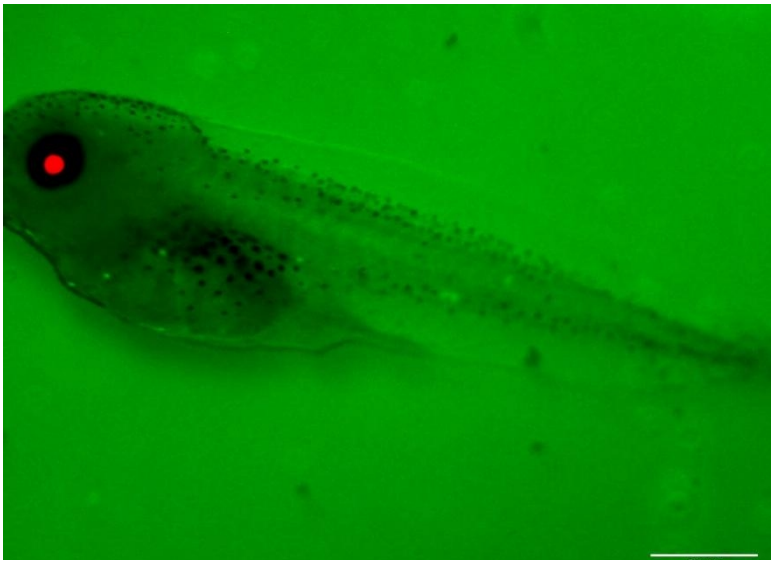

Figure 40. Representative images of F0 tadpoles under *MMP7* knock-in system at 3 days post-fertilization (3dpf) were captured and analyzed.
Green channel: GFP signal, which theoretically indicates expression in macrophages. Red channel: TurboFP signal driven by the gamma crystallin promoter, specifically expressed in the eyes. Scale bar: 500um.

5.3.3 F1 progeny from Transgene Frog Genotyping

Despite generating a high number of GFP^+ RFP^+ F0 tadpoles for both the *Pax7* and *MMP7* knock-in systems (over 400 for each construct) following multiple rounds of microinjection, none of the resulting F0 frogs produced transgenic offspring when crossed with wild-type frogs. Screening of the F1 progeny revealed no fluorescent signals, indicating that no true germline transmission occurred, and that the GFP^+ RFP^+ signals observed in F0 were likely due to episomal plasmid expression or non-specific integration events.

In parallel, genotyping efforts for both *Pax7* and *MMP7* F0 tadpoles were unsuccessful. Attempts to validate targeted integration by PCR amplification of intergenic regions flanking the knock-in cassette consistently failed, likely due to technical challenges associated with amplifying across large or complex genomic regions, or due to mosaicism and low abundance of correctly integrated sequences. Additionally, false-negative results may have occurred in GFP^+RFP^+ tadpoles, as fluorescence alone proved insufficient to confirm true genomic integration. These issues further support the hypothesis that most fluorescent F0 individuals were the result of transient plasmid expression rather than precise, heritable knock-in events.

Interestingly, the F0 frogs exhibited markedly delayed sexual maturation, often requiring over one year to reach fertility, in contrast to the typical six-month timeline observed in wild-

type *X. tropicalis*. This delay suggests that either the microinjection process or the presence of the CRISPR/Cas9 and donor plasmids had a developmental impact on the embryos, potentially affecting germline development or overall physiological stability.

6 DISCUSSION

6.1 Effect of XtiSCs in *X. tropicalis* Tadpole Tail Regeneration

In our study of tail regeneration in *X. tropicalis* tadpoles using an allotransplantation model, we identified several distinctive properties of immature Sertoli cells (XtiSCs) that differentiate them from conventional mesenchymal stem cells (MSCs). We found that XtiSCs predominantly remained at the injection site in the upper tail region, maintaining viability over extended periods and, in some instances, actively migrating toward the site of injury after tail amputation. This behavior reflects a higher degree of cellular retention and injury-directed movement than is typically reported for MSCs, which often exhibit lower persistence and non-specific distribution (Trounson and McDonald, 2015). Additionally, we observed a marked decline in XtiSC viability following direct injection into the bloodstream, indicating that localized tissue delivery may be a more effective method for harnessing Sertoli cells' regenerative potential in therapeutic applications.

Consistent evidence supports the pivotal role of Sertoli cells in enhancing muscle morphology and function in vivo. Notably, they have been shown to promote myoblast proliferation and facilitate the terminal differentiation of dystrophic myoblasts, as reported in studies by Chiappalupi et al. (2015, 2016, 2021) and Salvadori et al. (2021). Our findings align with these reports, demonstrating that XtiSCs effectively mitigate muscle fiber degradation at one day post-amputation and significantly promote muscle fiber growth by three days post-amputation. These observations not only underscore the therapeutic potential of XtiSCs in muscle regeneration but also suggest their broader applicability in enhancing the regenerative capacity of Xenopus tadpoles.

Addressing the pivotal role of the immune system in regeneration, our study focuses on the inflammatory response following muscle injury, which involves the sequential recruitment of neutrophils and the subsequent polarization of macrophages into pro-inflammatory M1 and anti-inflammatory M2 subtypes, as described by Fielding et al. (1993), Lu et al. (2011), and Mantovani et al. (2004). Given the immunomodulatory capacity of XtiSCs—particularly their ability to induce an immunosuppressive phenotype—we examined their impact on macrophage dynamics within the regenerative environment. Our findings reveal that XtiSCs significantly enhance macrophage accumulation both at the injection site and within the regenerating tail. This effect is especially pronounced in macrophage-depleted conditions, such as those induced by clodronate liposome treatment.

Interestingly, only a subset of tadpoles exhibited XtiSCs within the regenerated tail, suggesting that their influence on macrophage recruitment may extend beyond direct cell-cell interactions at the site of injury. It is plausible that XtiSCs mediate this effect through endocrine and paracrine signaling. Specifically, they may secrete immunomodulatory and chemotactic factors such as transforming growth factor-beta (TGF-β), chemokine (C-C motif) ligand 2 (CCL2), and C-X-C motif chemokine ligand 12 (CXCL12), thereby promoting a pro-regenerative immune environment (Papa et al., 2018; Lynch et al., 2020). This capacity to modulate macrophage behavior reinforces the notion that XtiSCs serve as key orchestrators of the immune response during tissue repair and regeneration.

Reflecting on the remarkable regenerative capabilities of Xenopus tadpoles—which include the restoration of complex tissues such as the spinal cord, muscle, and vasculature until metamorphosis, as reported by Beck et al. (2003), Filoni and Bosco (1981), Gaete et al. (2012b), and Love et al. (2011)—our study extends this paradigm by highlighting the regenerative enhancements following XtiSC transplantation. Notably, the transition from pro-inflammatory M1 to anti-inflammatory M2 macrophages, a critical step in progressing from the proliferative to the differentiation phase of myogenesis, appears to be supported by the presence of XtiSCs. This observation aligns with previous findings by Rigamonti et al. (2013) and Villalta et al. (2011), and is echoed in our own data, which show macrophage population shifts following XtiSC injection.

These findings underscore a compelling link between immune modulation and regenerative success. To further elucidate the mechanisms by which XtiSCs influence macrophage behavior and tissue repair, future work should aim to characterize M1 and M2 macrophage subtypes during the regeneration timeline post-XtiSC transplantation. Additionally, defining the molecular pathways involved—including specific cytokines and chemokines—will be essential for understanding how XtiSCs orchestrate immune responses to foster a pro-regenerative environment.

Our study is among the first to elucidate the interactive dynamics between XtiSCs and macrophages, emphasizing both direct cell-cell contact and the potential transfer of mitochondria as key mechanisms underlying enhanced macrophage function. This hypothesis is supported by previous findings from Morrison et al. (2017) and Porubska et al. (2021), which describe similar intercellular interactions contributing to immune modulation. Another intriguing aspect concerns the potential transdifferentiation of XtiSCs into macrophage-like cells. Colocalization evidence supports the hypothesis that XtiSCs may

adopt macrophage-like phenotypes, thereby revealing a novel dimension of Sertoli cell plasticity and functional versatility in regenerative environments. This idea is consistent with previous findings where various cell types, such as bone marrow B-cell precursors, vascular smooth muscle cells, and regulatory T cells (Tregs), have been shown to undergo transdifferentiation into macrophage-like cells, as demonstrated in multiple studies by Feil et al. (Feil et al., 2014), Wang et al. (Wang et al., 2021b)and Chen et al. (Chen et al., 2022). Given that Sertoli cells not only exhibit phagocytic activity but also express markers commonly associated with macrophages (Turek et al., 1996), it is plausible that XtiSCs may undergo transdifferentiation into macrophage-like cells. Supporting this hypothesis, we observed co-localization of red XtiSC signals and green macrophage markers within individual cells (Fig. 27), based on single-cell suspensions obtained from in vivo tadpoles following XtiSC injection. These findings provide preliminary evidence for the potential transdifferentiation of XtiSCs. However, to rigorously test this hypothesis, further studies are warranted. These should include fluorescence-activated cell sorting (FACS) to isolate cells double-positive for Katushka RFP (XtiSCs) and fluorescein (macrophage marker), followed by detailed gene expression profiling of the sorted populations to confirm lineage identity and functional characteristics.

6.2 Effect of XtiSCs in *X. tropicalis* Heart Regeneration Study

The immunomodulatory function of Sertoli cells has been extensively documented in various studies (Washburn et al., 2022). In testicles, Sertoli cells protect germ cells through the formation of the blood-testis barrier (BTB) and their innate immunomodulatory capabilities (O'Bryan et al., 2005; Kaur et al., 2014). Studies have shown that Sertoli cells inhibit the activation and maturation of dendritic cells in the presence of lipopolysaccharides (Lee et al., 2008). In addition, microencapsulated porcine Sertoli cells have demonstrated immunomodulatory potential in treating metastatic spread of Lewis lung carcinoma (LLC) cells in primary tumors (Chiappalupi et al., 2024).

In this study, when injected into the frog hind limb muscle bed, XtiSCs survived for more than three weeks and positively influenced heart regeneration, likely through autocrine signaling. Consistent with observations from tadpole injections, direct administration of XtiSCs into the heart or bloodstream resulted in significantly reduced cell survival and signal detection. These results strongly support local tissue implantation of XtiSCs as the preferred approach for Sertoli cell therapy to optimize clinical outcomes. Notably, XtiSCs injection

into the skeletal muscle bed three days prior to surgery resulted in markedly reduced scar deposition compared to both the control group (2/3PBS injection) and the heart implantation group (Fig. 30). Conversely, XtiSCs injection into the skeletal muscle bed during the surgery was associated with zero survival, and thus was excluded from further comparisons. This outcome suggests a rapid inflammatory response following apical resection or cardiac injury and underscores the necessity of pre-surgical XtiSC implantation to effectively evaluate their therapeutic role in cardiac injury response which echoes the findings reported by De Lemos et al. and Han et al. (De Lemos et al., 2003; Han et al., 2015).

This study is the first investigation of clodronate liposomes based method for systemic macrophage depletion in adult frogs. Macrophages are pivotal to the immune system, and their depletion can lead to various diseases (Wynn et al., 2013; Zaman and Epelman, 2022; Yang et al., 2023). In our experiment, the survival rate in the macrophage-depleted group (clodronate liposome-injected) following heart apex surgery was notably low (Fig. 37). Interestingly, statistical analysis revealed that XtiSCs injection significantly improved survival rates in the groups injected with control liposomes. Macrophages play a crucial role in heart regeneration following injury. While macrophage depletion does not impair the activation of cardiomyocyte proliferation, it leads to the formation of a permanent, highly cross-linked extracellular matrix scar (Godwin et al., 2017). In our study, we observed that treatment with XtiSCs obviously enhanced cardiac regeneration and reduced fibrotic scar formation at 7 days post-surgery in a frog heart apex resection model. The morphology of the heart apex also showed improved recovery in all XtiSCs treatment groups compared to the 2/3PBS control. Collectively, these findings underscore the capability of XtiSCs to promote regeneration, potentially through modulation of macrophage distribution or phenotype transition.

Given the excellent performance of XtiSCs in facilitating heart regeneration even in a macrophage-depleted environment, we examined the distribution of macrophages after XtiSCs implantation under these conditions in both the liver and heart. We observed a significant increase in macrophage density in the liver and a noticeable alteration in macrophage profiles within the injury area of the heart. These findings suggest that the beneficial effects of XtiSCs on heart regeneration may be mediated through modulation of macrophage populations, consistent with our earlier findings in *X. tropicalis* tadpole tail regeneration (Qing Zhao et al., 2024).

Many questions remain unanswered regarding the mechanisms by which XtiSCs facilitate heart regeneration. The observation that muscle bed injection effectively promotes heart repair suggests that XtiSCs may act primarily through endocrine signaling rather than direct cell-to-cell contact, likely via specific secreted factors that influence the regeneration site, a mechanism that has been reported in many studies (Amram et al., 2021; Easterling et al., 2019; Graham and Huang, 2021; Love et al., 2013; Sachs and Buchholz, 2019). Investigating these factors and their regulatory pathways—such as Nitric Oxide (NO), which we have detected as produced by XtiSCs and previously implicated in *X. tropicalis* tail regeneration (data not shown), could provide valuable insights into their role in cardiac repair.

6.3 Generation of CRISPR-Cas9 Transgenic *X. tropicalis* Animals

Limited availability of antibodies for Xenopus has restricted many avenues of research that require antibody-based methods. To study the function of specific genes or proteins, generating transgenic animals is often an effective strategy. With the increasing application of CRISPR-Cas9 technology in biological research, numerous attempts have been made to utilize this method in Xenopus (Shi et al., 2015; Naert and Vleminckx, 2018b; Shi et al., 2019; Naert et al., 2020; Shi et al., 2022; Mochii et al., 2024). For example, Miao et al. successfully used a CRISPR-Cas9 complex together with a 2-bait (targeting the gene of interest) GFP plasmid backbone to knock in GFP downstream of target genes (at the 3' UTR) without disrupting gene structure (Mao et al., 2018).

Inspired by this approach, we constructed two backbone plasmids targeting the muscle satellite gene *Pax7* and the macrophage marker *MMP7*, then microinjected the CRISPR-Cas9–backbone plasmid complex into one-cell stage embryos. We obtained F0 tadpoles expressing GFP (at the knock-in gene site) and RFP (reporter line), and raised them to sexual maturity. However, for both *Pax7* and *MMP7* transgene lines, we did not observe any positive F1 frogs (no GFP or RFP signals), indicating that no true germline transmission occurred.

Interestingly, at 3 dpf, a surprisingly high percentage of F0 tadpoles showed $GFP^{+}RFP^{+}$ signals. Combined with the failure to detect positive F1 offspring, we suspect that this early signal likely originates from expression of uncut or episomal plasmid rather than true genomic integration.

Based on this experience, future trials should include screening at multiple developmental stages, such as 7 days, 2 weeks, 1 month post-fertilization, and pre-metamorphosis, tracking

individuals with persistent positive signals throughout. This would avoid the resource-intensive process of raising many candidates to sexual maturity without prior validation.

For the *Pax7* transgene trial, we attempted PCR validation of the presumed integration locus. This was unsuccessful, likely due to (1) insufficient genomic DNA input since we primarily used dead tadpoles to preserve living F0s, limiting available DNA; (2) the inherent difficulty in designing PCR primers targeting these complex transgene integration sites. Therefore, further optimization of PCR validation strategies is needed before advancing F0 signal-positive tadpoles to mature frogs. Identifying simpler, more reliable PCR targets would improve genotyping success.

Additionally, we must consider that some true transgenic F0 frogs may have been lost during rearing due to the low survival rate from tadpole to adult stages. Improving survival or earlier selection of candidates could enhance recovery of germline-transmitting founders.

7 CONCLUSIONS

This study presents a comprehensive investigation into the role of XtiSCs in tail regeneration, encompassing their viability, tissue retention, migratory capacity, and immunomodulatory functions. Our results confirm that XtiSCs significantly enhance regenerative outcomes, not only by promoting tissue repair but also by modulating the immune microenvironment. These findings underscore the need for further research to characterize specific macrophage subtypes and to unravel the molecular mechanisms underlying XtiSC-macrophage interactions. Advancing our understanding in these areas will be critical for realizing the full therapeutic potential of XtiSCs in regenerative medicine and may pave the way for innovative clinical applications.

Our research explored the role of XtiSCs in *X. tropicalis* heart regeneration. We found that XtiSCs significantly enhance cardiac regeneration and reduce fibrotic scar formation in both normally injured frogs and in frogs with macrophage depletion induced by clodronate liposomes. Furthermore, XtiSCs improved apex morphology consistently across all experimental groups, including uninjected controls, control liposome-injected, and clodronate liposome-injected frogs. Importantly, XtiSCs also increased macrophage numbers in the liver and altered macrophage infiltration patterns within the regenerating heart tissue. Collectively, these findings suggest that XtiSCs promote frog heart regeneration primarily through modulation of macrophage populations.

Our study presents a comprehensive analysis of the regenerative potential of XtiSCs, highlighting their robust survival, targeted homing capacity, and potent immunomodulatory effects. Together, these attributes underscore the multifaceted role of XtiSCs in promoting tissue regeneration. While our findings substantiate the regenerative efficacy of XtiSCs, they also point to the need for deeper investigation into the specific macrophage subtypes involved and the molecular pathways governing XtiSC–macrophage interactions. Elucidating these mechanisms will be essential for unlocking the full therapeutic potential of XtiSCs in regenerative medicine and may inform the development of innovative, cell-based treatments for tissue repair and immune modulation.

Regarding transgenic approaches, generating transgenic frogs provides an effective method to study gene and protein functions, especially given the limited availability of antibodies for Xenopus. Utilizing CRISPR-Cas9 knock-in technology, we successfully constructed two backbone plasmids targeting *Pax7* and *MMP7*, each containing dual gRNA

target sites flanking the region to guide precise GFP knock-in at the 3’ UTR of the respective genes. Despite obtaining numerous GFP-positive F0 tadpoles after multiple microinjections, we did not recover any GFP-positive F0 frogs. Future efforts will focus on implementing stringent selection controls at earlier developmental stages to identify and raise true positive tadpoles to adulthood, thereby optimizing resource use and increasing the likelihood of establishing stable transgenic lines.

8 REFERENCES

Ali, S. R., Hippenmeyer, S., Saadat, L. V., Luo, L., Weissman, I. L. and Ardehali, R. (2014). Existing cardiomyocytes generate cardiomyocytes at a low rate after birth in mice. *Proc Natl Acad Sci U S A* **111**, 8850–8855.

Amram, A. V., Cutie, S. and Huang, G. N. (2021). Hormonal control of cardiac regenerative potential. *Endocrine Connections* **10**,.

Arnold, L., Henry, A., Poron, F., Baba-Amer, Y., Van Rooijen, N., Plonquet, A., Gherardi, R. K. and Chazaud, B. (2007). Inflammatory monocytes recruited after skeletal muscle injury switch into antiinflammatory macrophages to support myogenesis. *The Journal of Experimental Medicine* **204**, 1057–1069.

Aslan, Y., Tadjuidje, E., Zorn, A. M. and Cha, S. W. (2017). High-efficiency non-mosaic CRISPR-mediated knock-in and indel mutation in F0 Xenopus. *Development (Cambridge)* **144**,.

Aurora, A. B., Porrello, E. R., Tan, W., Mahmoud, A. I., Hill, J. A., Bassel-Duby, R., Sadek, H. A. and Olson, E. N. (2014). Macrophages are required for neonatal heart regeneration. *Journal of Clinical Investigation* **124**,.

Aztekin, C., Hiscock, T. W., Marioni, J. C., Gurdon, J. B., Simons, B. D. and Jullien, J. (2019). Identification of a regeneration-organizing cell in the Xenopus tail. *Science* **364**, 653–658.

Aztekin, C., Hiscock, T. W., Butler, R., De Jesús Andino, F., Robert, J., Gurdon, J. B. and Jullien, J. (2020). The myeloid lineage is required for the emergence of a regeneration-permissive environment following Xenopus tail amputation. *Development* **147**, dev185496.

Bak, R. O., Gomez-Ospina, N. and Porteus, M. H. (2018). Gene Editing on Center Stage. *Trends in Genetics* **34**,.

Barrangou, R. (2015). The roles of CRISPR-Cas systems in adaptive immunity and beyond. *Current Opinion in Immunology* **32**,.

Beck, C. W., Christen, B. and Slack, J. M. W. (2003). Molecular Pathways Needed for Regeneration of Spinal Cord and Muscle in a Vertebrate. *Developmental Cell* **5**, 429–439.

Becker, R. O., Chapin, S. and Sherry, R. (1974). Regeneration of the ventricular myocardium in amphibians. *Nature* **248**, 145–147.

Belcastro, A. N., Arthur, G. D., Albisser, T. A. and Raj, D. A. (1996). Heart, liver, and skeletal muscle myeloperoxidase activity during exercise. *Journal of Applied Physiology* **80**,.

Bergmann, O., Bhardwaj, R. D., Bernard, S., Zdunek, S., Barnabé-Heider, F., Walsh, S., Zupicich, J., Alkass, K., Buchholz, B. A., Druid, H., et al. (2009b). Evidence for cardiomyocyte renewal in humans. *Science* **324**, 98–102.

Bergmann, O., Zdunek, S., Felker, A., Salehpour, M., Alkass, K., Bernard, S., Sjostrom, S. L., Szewczykowska, M., Jackowska, T., Dos Remedios, C., et al. (2015). Dynamics of Cell Generation and Turnover in the Human Heart. *Cell* **161**,.

Bistoni, G., Calvitti, M., Mancuso, F., Arato, I., Falabella, G., Cucchia, R., Fallarino, F., Becchetti, A., Baroni, T., Mazzitelli, S., et al. (2012). Prolongation of skin allograft survival in rats by the transplantation of microencapsulated xenogeneic neonatal porcine Sertoli cells. *Biomaterials* **33**, 5333–5340.

Blitz, I. L. (2012). Navigating the Xenopus tropicalis genome. *Methods in Molecular Biology* **917**,.

Bogdanove, A. J. and Voytas, D. F. (2011). TAL effectors: Customizable proteins for DNA targeting. *Science* **333**,.

Bolotin, A., Quinquis, B., Sorokin, A. and Dusko Ehrlich, S. (2005). Clustered regularly interspaced short palindrome repeats (CRISPRs) have spacers of extrachromosomal origin. *Microbiology* **151**,.

Bujak, M., Kweon, H. J., Chatila, K., Li, N., Taffet, G. and Frangogiannis, N. G. (2008). Aging-Related Defects Are Associated With Adverse Cardiac Remodeling in a Mouse Model of Reperfused Myocardial Infarction. *J Am Coll Cardiol* **51**, 1384–1392.

Chang, W., Song, B. W., Moon, J. Y., Cha, M. J., Ham, O., Lee, S. Y., Choi, E., Choi, E. and Hwang, K. C. (2013). Anti-death strategies against oxidative stress in grafted mesenchymal stem cells. *Histology and Histopathology* **28**,.

Chargé, S. B. P. and Rudnicki, M. A. (2004). Cellular and Molecular Regulation of Muscle Regeneration. *Physiological Reviews* **84**,.

Chen, Y., Zajac, J. D. and MacLean, H. E. (2005). Androgen regulation of satellite cell function. *Journal of Endocrinology* **186**,.

Chen, Y., Lin, G. and Slack, J. M. W. (2006). Control of muscle regeneration in the Xenopus tadpole tail by Pax7. *Development* **133**, 2303–2313.

Chen, C., Park, B., Ragonnaud, E., Bodogai, M., Wang, X., Zong, L., Lee, J.-M., Beerman, I. and Biragyn, A. (2022). Cancer co-opts differentiation of B-cell precursors into macrophage-like cells. *Nat Commun* **13**, 5376.

Chiappalupi, S., Luca, G., Mancuso, F., Madaro, L., Fallarino, F., Nicoletti, C., Calvitti, M., Arato, I., Falabella, G., Salvadori, L., et al. (2015). Effects of intraperitoneal injection of microencapsulated Sertoli cells on chronic and presymptomatic dystrophic mice. *Data in Brief* **5**,.

Chiappalupi, S., Luca, G., Mancuso, F., Madaro, L., Fallarino, F., Nicoletti, C., Calvitti, M., Arato, I., Falabella, G., Salvadori, L., et al. (2016). Intraperitoneal injection of microencapsulated Sertoli cells restores muscle morphology and performance in dystrophic mice. *Biomaterials* **75**,.

Chiappalupi, S., Salvadori, L., Mancuso, F., Arato, I., Calvitti, M., Riuzzi, F., Calafiore, R., Luca, G. and Sorci, G. (2021). Microencapsulated Sertoli cells sustain myoblast proliferation without affecting the myogenic potential. In vitro data. *Data Brief* **40**, 107744.

Chiappalupi, S., Salvadori, L., Borghi, M., Mancuso, F., Pariano, M., Riuzzi, F., Luca, G., Romani, L., Arato, I. and Sorci, G. (2024). Grafted Sertoli Cells Exert Immunomodulatory Non-Immunosuppressive Effects in Preclinical Models of Infection and Cancer. *Cells* **13**, 544.

Christian, M., Cermak, T., Doyle, E. L., Schmidt, C., Zhang, F., Hummel, A., Bogdanove, A. J. and Voytas, D. F. (2010). Targeting DNA double-strand breaks with TAL effector nucleases. *Genetics* **186**,.

Collins, C. A., Olsen, I., Zammit, P. S., Heslop, L., Petrie, A., Partridge, T. A. and Morgan, J. E. (2005). Stem cell function, self-renewal, and behavioral heterogeneity of cells from the adult muscle satellite cell niche. *Cell* **122**,.

Cong, L., Ran, F. A., Cox, D., Lin, S., Barretto, R., Habib, N., Hsu, P. D., Wu, X., Jiang, W., Marraffini, L. A., et al. (2013). Multiplex genome engineering using CRISPR/Cas systems. *Science* **339**,.

Contreras, E. G., Gaete, M., Sánchez, N., Carrasco, H. and Larraín, J. (2009). Early requirement of Hyaluronan for tail regeneration in Xenopus tadpoles. *Development* **136**,.

Cordani, N., Pisa, V., Pozzi, L., Sciorati, C. and Clementi, E. (2014). Nitric oxide controls fat deposition in dystrophic skeletal muscle by regulating fibro-adipogenic precursor differentiation. *Stem Cells* **32**,.

Danenberg, H. D., Fishbein, I., Gao, J., Mönkkönen, J., Reich, R., Gati, I., Moerman, E. and Golomb, G. (2002). Macrophage Depletion by Clodronate-Containing Liposomes Reduces Neointimal Formation After Balloon Injury in Rats and Rabbits. *Circulation* **106**, 599–605.

De Lemos, J. A., Morrow, D. A., Sabatine, M. S., Murphy, S. A., Gibson, C. M., Antman, E. M., McCabe, C. H., Cannon, C. P. and Braunwald, E. (2003). Association between plasma levels of monocyte chemoattractant protein-1 and long-term clinical outcomes in patients with acute coronary syndromes. *Circulation* **107**,.

Deuchar, E. M. (1975). Regeneration of the tail bud in Xenopus embryos. *Journal of Experimental Zoology* **192**,.

Dufour, J. M., Rajotte, R. V., Korbutt, G. S. and Emerich, D. F. (2003). Harnessing the immunomodulatory properties of Sertoli cells to enable xenotransplantation in type I diabetes. *Immunol Invest* **32**, 275–297.

Dufour, J. M., Dass, B., Halley, K. R., Korbutt, G. S., Dixon, D. E. and Rajotte, R. V. (2008). Sertoli cell line lacks the immunoprotective properties associated with primary Sertoli cells. *Cell Transplant* **17**, 525–534.

Easterling, M. R., Engbrecht, K. M. and Crespi, E. J. (2019). Endocrine Regulation of Epimorphic Regeneration. *Endocrinology* **160**,.

Fallarino, F., Luca, G., Calvitti, M., Mancuso, F., Nastruzzi, C., Fioretti, M. C., Grohmann, U., Becchetti, E., Burgevin, A., Kratzer, R., et al. (2009). Therapy of experimental type 1 diabetes by isolated Sertoli cell xenografts alone. *Journal of Experimental Medicine* **206**, 2511–2526.

Feil, S., Fehrenbacher, B., Lukowski, R., Essmann, F., Schulze-Osthoff, K., Schaller, M. and Feil, R. (2014). Transdifferentiation of vascular smooth muscle cells to macrophage-like cells during atherogenesis. *Circ Res* **115**, 662–667.

Fielding, R. A., Manfredi, T. J., Ding, W., Fiatarone, M. A., Evans, W. J. and Cannon, J. G. (1993). Acute phase response in exercise. III. Neutrophil and IL-1 beta accumulation in skeletal muscle. *Am J Physiol* **265**, R166-172.

Fijak, M. and Meinhardt, A. (2006). The testis in immune privilege. *Immunological Reviews* **213**,.

Filoni, S. and Bosco, L. (1981). Comparative analysis of the regenerative capacity of caudal spinal cord in larvae of serveral Anuran amphibian species. *Acta Embryol Morphol Exp (Halocynthia Assoc)* **2**, 199–226.

Fisher, M., James-Zorn, C., Ponferrada, V., Bell, A. J., Sundararaj, N., Segerdell, E., Chaturvedi, P., Bayyari, N., Chu, S., Pells, T., et al. (2023). Xenbase: Key features and resources of the Xenopus model organism knowledgebase. *Genetics* **224**,.

Flink, I. L. (2002). Cell cycle reentry of ventricular and atrial cardiomyocytes and cells within the epicardium following amputation of the ventricular apex in the axolotl, Amblystoma mexicanum: confocal microscopic immunofluorescent image analysis of bromodeoxyuridine-labeled nuclei. *Anat Embryol* **205**, 235–244.

França, L. R., Hess, R. A., Dufour, J. M., Hofmann, M. C. and Griswold, M. D. (2016). The Sertoli cell: One hundred fifty years of beauty and plasticity. *Andrology* **4**,.

Fratz, S., Hager, A., Schreiber, C., Schwaiger, M., Hess, J. and Stern, H. C. (2011). Long-term myocardial scarring after operation for anomalous left coronary artery from the pulmonary artery. *Annals of Thoracic Surgery* **92**,.

Gaete, M., Muñoz, R., Sánchez, N., Tampe, R., Moreno, M., Contreras, E. G., Lee-Liu, D. and Larraín, J. (2012b). Spinal cord regeneration in Xenopus tadpoles proceeds through activation of Sox2-positive cells. *Neural Development* **7**, 13.

Gaj, T., Guo, J., Kato, Y., Sirk, S. J. and Barbas, C. F. (2012). Targeted gene knockout by direct delivery of zinc-finger nuclease proteins. *Nature Methods* **9**,.

Gamba, L., Harrison, M. and Lien, C.-L. (2014). Cardiac Regeneration in Model Organisms. *Current Treatment Options in Cardiovascular Medicine* **16**,.

Gayraud-Morel, B., Chrétien, F. and Tajbakhsh, S. (2009). Skeletal muscle as a paradigm for regenerative biology and medicine. *Regenerative Medicine* **4**,.

Geach, T. J. and Zimmerman, L. B. (2011). Developmental Genetics in Xenopus tropicalis. In *Vertebrate Embryogenesis: Embryological, Cellular, and Genetic Methods* (ed. Pelegri, F. J.), pp. 77–117. Totowa, NJ: Humana Press.

Godwin, J. W. and Rosenthal, N. (2014). Scar-free wound healing and regeneration in amphibians: Immunological influences on regenerative success. *Differentiation* **87**,.

Godwin, J. W., Debuque, R., Salimova, E. and Rosenthal, N. A. (2017). Heart regeneration in the salamander relies on macrophage-mediated control of fibroblast activation and the extracellular landscape. *NPJ Regen Med* **2**, 22.

Gores, P. F., Field, M. J., Korbutt, G., Rajotte, R. V. and Hayes, D. H. (1999). Long-Term Survival of Intra-Testicular Xenogeneic Islets Without Immunosuppression in a Large Animal Model. *Transplantation* **67**,.

Graham, N. and Huang, G. N. (2021). Endocrine Influence on Cardiac Metabolism in Development and Regeneration. *Endocrinology (United States)* **162**,.

Haas, A. and Das, I. (2011). Describing east malaysian tadpole diversity: Status and recommendations for standards and procedures associated with larval amphibian description and documentation. *Bonner Zoologische Monographien* **57**, 29–46.

Halberstadt, C., Emerich, D. F. and Gores, P. (2004). Use of Sertoli cell transplants to provide local immunoprotection for tissue grafts. *Expert Opinion on Biological Therapy* **4**,.

Halevy, O., Piestun, Y., Allouh, M. Z., Rosser, B. W. C., Rinkevich, Y., Reshef, R., Rozenboim, I., Wleklinski-Lee, M. and Yablonka-Reuveni, Z. (2004). Pattern of Pax7 expression during myogenesis in the posthatch chicken establishes a model for satellite cell differentiation and renewal. *Developmental Dynamics* **231**,.

Hamilton, A. M., Balashova, O. A. and Borodinsky, L. N. (2021). Non-canonical Hedgehog signaling regulates spinal cord and muscle regeneration in Xenopus laevis larvae. *eLife*.

Hammond, C. L., Hinits, Y., Osborn, D. P. S., Minchin, J. E. N., Tettamanti, G. and Hughes, S. M. (2007). Signals and myogenic regulatory factors restrict pax3 and pax7 expression to dermomyotome-like tissue in zebrafish. *Developmental Biology* **302**,.

Han, C., Nie, Y., Lian, H., Liu, R., He, F., Huang, H. and Hu, S. (2015). Acute inflammation stimulates a regenerative response in the neonatal mouse heart. *Cell Research* **25**,.

Haubner, B. J., Schneider, J., Schweigmann, U., Schuetz, T., Dichtl, W., Velik-Salchner, C., Stein, J. I. and Penninger, J. M. (2016). Functional Recovery of a Human Neonatal Heart after Severe Myocardial Infarction. *Circulation Research* **118**,.

Hawke, T. J. and Garry, D. J. (2001). Myogenic satellite cells: Physiology to molecular biology. *Journal of Applied Physiology* **91**,.

Hellsten, U., Harland, R. M., Gilchrist, M. J., Hendrix, D., Jurka, J., Kapitonov, V., Ovcharenko, I., Putnam, N. H., Shu, S., Taher, L., et al. (2010). The genome of the western clawed frog xenopus tropicalis. *Science* **328**,.

Hille, F., Richter, H., Wong, S. P., Bratovič, M., Ressel, S. and Charpentier, E. (2018). The Biology of CRISPR-Cas: Backward and Forward. *Cell* **172**,.

Ho, D. M. and Whitman, M. (2008). TGF-β signaling is required for multiple processes during Xenopus tail regeneration. *Developmental Biology* **315**,.

Iismaa, S. E., Kaidonis, X., Nicks, A. M., Bogush, N., Kikuchi, K., Naqvi, N., Harvey, R. P., Husain, A. and Graham, R. M. (2018). Comparative regenerative mechanisms across different mammalian tissues. *npj Regenerative Medicine* **3**,.

Ishibashi, S., Cliffe, R. and Amaya, E. (2012). Highly efficient bi-allelic mutation rates using TALENs in Xenopus tropicalis. *Biology Open* **1**,.

Ito, K., Morioka, M., Kimura, S., Tasaki, M., Inohaya, K. and Kudo, A. (2014). Differential reparative phenotypes between zebrafish and medaka after cardiac injury. *Developmental Dynamics* **243**,.

J. Gordon Betts, Kelly A. Young, James A. Wise, Eddie Johnson, Brandon Poe, Dean H. Kruse, Oksana Korol, Jody E. Johnson, Mark Womble, and Peter DeSaix (2022). *Anatomy & Physiology*. 2nd Edition. XanEdu Publishing Inc.

Jhao, Y.-T., Chiu, C.-H., Chen, C.-F. F., Chou, T.-K., Lin, Y.-W., Ju, Y.-T., Wu, S.-C., Yan, R.-F., Shiue, C.-Y., Chueh, S.-H., et al. (2019). The Effect of Sertoli Cells on Xenotransplantation and Allotransplantation of Ventral Mesencephalic Tissue in a Rat Model of Parkinson's Disease. *Cells* **8**, 1420.

Jinek, M., Chylinski, K., Fonfara, I., Hauer, M., Doudna, J. A. and Charpentier, E. (2012). A programmable dual-RNA-guided DNA endonuclease in adaptive bacterial immunity. *Science* **337**,.

Jobin, P. G., Solis, N., Machado, Y., Bell, P. A., Kwon, N. H., Kim, S., Overall, C. M. and Butler, G. S. (2019). Matrix metalloproteinases inactivate the proinflammatory functions of secreted moonlighting tryptophanyl-tRNA synthetase. *Journal of Biological Chemistry* **294**,.

Jopling, C., Sleep, E., Raya, M., Martí, M., Raya, A. and Belmonte, J. C. I. (2010). Zebrafish heart regeneration occurs by cardiomyocyte dedifferentiation and proliferation. *Nature* **464**,.

Kabbesh, H., Riaz, M. A., Jensen, A. D., Scheiner-Bobis, G. and Konrad, L. (2023). Transmigration of macrophages through primary adult rat Sertoli cells. *Tissue Barriers* **11**,.

Kashiwagi, K., Kashiwagi, A., Kurabayashi, A., Hanada, H., Nakajima, K., Okada, M., Takase, M. and Yaoita, Y. (2010). Xenopus tropicalis: an ideal experimental animal in amphibia. *Exp Anim* **59**, 395–405.

Kaur, G., Thompson, L. A. and Dufour, J. M. (2014). Sertoli cells – Immunological sentinels of spermatogenesis. *Seminars in Cell & Developmental Biology* **30**, 36–44.

Kaur, G., Wright, K., Mital, P., Hibler, T., Miranda, J. M., Thompson, L. A., Halley, K. and Dufour, J. M. (2020). Neonatal Pig Sertoli Cells Survive Xenotransplantation by Creating an Immune Modulatory Environment Involving CD4 and CD8 Regulatory T Cells. *Cell Transplantation* **29**,.

Kyritsis, N., Kizil, C., Zocher, S., Kroehne, V., Kaslin, J., Freudenreich, D., Iltzsche, A. and Brand, M. (2012). Acute inflammation initiates the regenerative response in the adult zebrafish brain. *Science* **338**,.

Lavine, K. J., Epelman, S., Uchida, K., Weber, K. J., Nichols, C. G., Schilling, J. D., Ornitz, D. M., Randolph, G. J. and Mann, D. L. (2014). Distinct macrophage lineages contribute to disparate patterns of cardiac recovery and remodeling in the neonatal and adult heart. *Proceedings of the National Academy of Sciences of the United States of America* **111**,.

Lee, H.-M., Oh, B. C., Lim, D.-P., Lee, D.-S., Lim, H.-G., Park, C. S. and Lee, J. R. (2008). Mechanism of Humoral and Cellular Immune Modulation Provided by Porcine Sertoli Cells. *J Korean Med Sci* **23**, 514.

Lei, Y., Guo, X., Liu, Y., Cao, Y., Deng, Y., Chen, X., Cheng, C. H. K., Dawid, I. B., Chen, Y. and Zhao, H. (2012). Efficient targeted gene disruption in Xenopus embryos using engineered transcription activator-like effector nucleases (TALENs). *Proceedings of the National Academy of Sciences of the United States of America* **109**,.

Lepilina, A., Coon, A. N., Kikuchi, K., Holdway, J. E., Roberts, R. W., Burns, C. G. and Poss, K. D. (2006). A Dynamic Epicardial Injury Response Supports Progenitor Cell Activity during Zebrafish Heart Regeneration. *Cell* **127**, 607–619.

Levin, J. B. and Borodinsky, L. N. (2022). Injury-induced Erk1/2 signaling tissue-specifically interacts with Ca2+ activity and is necessary for regeneration of spinal cord and skeletal muscle. *Cell Calcium* **102**, 102540.

Li, T., Huang, S., Jiang, W. Z., Wright, D., Spalding, M. H., Weeks, D. P. and Yang, B. (2011). TAL nucleases (TALNs): Hybrid proteins composed of TAL effectors and FokI DNA-cleavage domain. *Nucleic Acids Research* **39**,.

Liao, S., Dong, W., Lv, L., Guo, H., Yang, J., Zhao, H., Huang, R., Yuan, Z., Chen, Y., Feng, S., et al. (2017). Heart regeneration in adult Xenopus tropicalis after apical resection. *Cell Biosci* **7**, 70.

Liao, S., Dong, W., Zhao, H., Huang, R., Qi, X. and Cai, D. (2018). Cardiac regeneration in Xenopus tropicalis and Xenopus laevis: discrepancies and problems. *Cell & Bioscience* **8**, 32.

Lin, G. and Slack, J. M. W. (2008). Requirement for Wnt and FGF signaling in Xenopus tadpole tail regeneration. *Developmental Biology* **316**,.

Lin, G., Chen, Y. and Slack, J. M. W. (2012). Transgenic Analysis of Signaling Pathways Required for Xenopus Tadpole Spinal Cord and Muscle Regeneration. *Anatomical Record* **295**,.

Love, N. R., Chen, Y., Bonev, B., Gilchrist, M. J., Fairclough, L., Lea, R., Mohun, T. J., Paredes, R., Zeef, L. A. and Amaya, E. (2011). Genome-wide analysis of gene expression during Xenopus tropicalis tadpole tail regeneration. *BMC Developmental Biology* **11**, 70.

Love, N. R., Chen, Y., Ishibashi, S., Kritsiligkou, P., Lea, R., Koh, Y., Gallop, J. L., Dorey, K. and Amaya, E. (2013). Amputation-induced reactive oxygen species are required for successful Xenopus tadpole tail regeneration. *Nature Cell Biology* **15**,.

Lu, H., Huang, D., Ransohoff, R. M. and Zhou, L. (2011). Acute skeletal muscle injury: CCL2 expression by both monocytes and injured muscle is required for repair. *FASEB J* **25**, 3344–3355.

Luca, G., Fallarino, F., Calvitti, M., Mancuso, F., Nastruzzi, C., Arato, I., Falabella, G., Grohmann, U., Becchetti, E., Puccetti, P., et al. (2010). Xenograft of microencapsulated sertoli cells reverses T1DM in NOD mice by inducing neogenesis of beta-cells. *Transplantation* **90**,.

Luca, G., Arato, I., Mancuso, F., Calvitti, M., Falabella, G., Murdolo, G., Basta, G., Cameron, D. F., Hansen, B. C., Fallarino, F., et al. (2016). Xenograft of microencapsulated Sertoli cells restores glucose homeostasis in db/db mice with spontaneous diabetes mellitus. *Xenotransplantation* **23**, 429–439.

Lv, L., Liao, Z., Luo, J., Chen, H., Guo, H., Yang, J., Huang, R., Pu, Q., Zhao, H., Yuan, Z., et al. (2020). Cardiac telocytes exist in the adult Xenopus tropicalis heart. *Journal of Cellular and Molecular Medicine* **24**,.

Lv, L., Guo, W., Guan, W., Chen, Y., Huang, R., Yuan, Z., Pu, Q., Feng, S., Zheng, X., Li, Y., et al. (2023). Echocardiographic assessment of Xenopus tropicalis heart regeneration. *Cell and Bioscience* **13**,.

Lynch, D. H., Ramsdell, F. and Alderson, M. R. (1995). Fas and FasL in the homeostatic regulation of immune responses. *Immunology Today* **16**,.

Lynch, K., Treacy, O., Chen, X., Murphy, N., Lohan, P., Islam, M. N., Donohoe, E., Griffin, M. D., Watson, L., McLoughlin, S., et al. (2020). TGF-β1-Licensed Murine MSCs Show Superior Therapeutic Efficacy in Modulating Corneal Allograft Immune Rejection In Vivo. *Mol Ther* **28**, 2023–2043.

Mahfouz, M. M., Li, L., Shamimuzzaman, M., Wibowo, A., Fang, X. and Zhu, J. K. (2011). De novo-engineered transcription activator-like effector (TALE) hybrid nuclease with novel DNA binding specificity creates double-strand breaks. *Proceedings of the National Academy of Sciences of the United States of America* **108**,.

Mantovani, A., Sica, A., Sozzani, S., Allavena, P., Vecchi, A. and Locati, M. (2004). The chemokine system in diverse forms of macrophage activation and polarization. *Trends Immunol* **25**, 677–686.

Mao, C. Z., Zheng, L., Zhou, Y. M., Wu, H. Y., Xia, J. B., Liang, C. Q., Guo, X. F., Peng, W. T., Zhao, H., Cai, W. B., et al. (2018). CRISPR/Cas9-mediated efficient and precise targeted integration of donor DNA harboring double cleavage sites in Xenopus tropicalis. *FASEB Journal* **32**,.

Marshall, L., Girardot, F., Demeneix, B. A. and Coen, L. (2018). Is adult cardiac regeneration absent in Xenopus laevis yet present in Xenopus tropicalis? *Cell and Bioscience* **8**,.

Marshall, L. N., Vivien, C. J., Girardot, F., Péricard, L., Scerbo, P., Palmier, K., Demeneix, B. A. and Coen, L. (2019). Stage-dependent cardiac regeneration in Xenopus is regulated by thyroid hormone availability. *Proceedings of the National Academy of Sciences* **116**, 3614–3623.

Mauduit, C., Besset, V., Caussanel, V. and Benahmed, M. (1996). Tumor necrosis factor α receptor p55 is under hormonal (follicle-stimulating hormone) control in testicular sertoli cells. *Biochemical and Biophysical Research Communications* **224**,.

McLoon, L. K. and Wirtschafter, J. (2003). Activated satellite cells in extraocular muscles of normal adult monkeys and humans. *Investigative Ophthalmology and Visual Science* **44**,.

Menegazzo, M., Zuccarello, D., Luca, G., Ferlin, A., Calvitti, M., Mancuso, F., Calafiore, R. and Foresta, C. (2011). Improvements in human sperm quality by long-term in vitro co-culture with isolated porcine Sertoli cells. *Human Reproduction* **26**,.

Milanizadeh, S., Zuwarali, K. N. N., Aliaghaei, A. and Bigdeli, M. R. (2018). Therapeutic Potential of Pretreatment with Allograft Sertoli Cells Transplantation in Brain Ischemia by Improving Oxidative Defenses. *J Mol Neurosci* **64**, 533–542.

Miller, J., McLachlan, A. D. and Klug, A. (1985). Repetitive zinc-binding domains in the protein transcription factor IIIA from Xenopus oocytes. *The EMBO journal* **4**,.

Miller, J. C., Tan, S., Qiao, G., Barlow, K. A., Wang, J., Xia, D. F., Meng, X., Paschon, D. E., Leung, E., Hinkley, S. J., et al. (2011). A TALE nuclease architecture for efficient genome editing. *Nature Biotechnology* **29**,.

Mochii, M., Akizuki, K., Ossaka, H., Kagawa, N., Umesono, Y. and Suzuki, K. ichi T. (2024). A CRISPR-Cas9-mediated versatile method for targeted integration of a fluorescent protein gene to visualize endogenous gene expression in Xenopus laevis. *Developmental Biology* **506**,.

Montarras, D., Morgan, J., Colins, C., Relaix, F., Zaffran, S., Cumano, A., Partridge, T. and Buckingham, M. (2005). Developmental biology: Direct isolation of satellite cells for skeletal muscle regeneration. *Science* **309**,.

Moore, C. and Hutson, J. C. (1994). Physiological Relevance of Tumor Necrosis Factor in Mediating Macrophage-Leydig Cell Interactions. *Endocrinology* **134**,.

Morrison, J. I., Lööf, S., He, P. and Simon, A. (2006). Salamander limb regeneration involves the activation of a multipotent skeletal muscle satellite cell population. *Journal of Cell Biology* **172**,.

Morrison, T. J., Jackson, M. V., Cunningham, E. K., Kissenpfennig, A., McAuley, D. F., O'Kane, C. M. and Krasnodembskaya, A. D. (2017). Mesenchymal Stromal Cells Modulate Macrophages in Clinically Relevant Lung Injury Models by Extracellular Vesicle Mitochondrial Transfer. *Am J Respir Crit Care Med* **196**, 1275–1286.

Mruk, D. D. and Cheng, C. Y. (2015). The mammalian blood-testis barrier: Its biology and regulation. *Endocrine Reviews* **36**,.

Musarò, A. (2014). The Basis of Muscle Regeneration. *Advances in Biology* **2014**,.

Naert, T. and Vleminckx, K. (2018a). CRISPR/cas9-mediated knockout of RB1 in xenopus tropicalis. In *Methods in Molecular Biology*, .

Naert, T. and Vleminckx, K. (2018b). CRISPR/Cas9 disease models in zebrafish and Xenopus: The genetic renaissance of fish and frogs. *Drug Discovery Today: Technologies* **28**,.

Naert, T., Tulkens, D., Edwards, N. A., Carron, M., Shaidani, N. I., Wlizla, M., Boel, A., Demuynck, S., Horb, M. E., Coucke, P., et al. (2020). Maximizing CRISPR/Cas9 phenotype penetrance applying predictive modeling of editing outcomes in Xenopus and zebrafish embryos. *Scientific Reports* **10**,.

Nahrendorf, M., Swirski, F. K., Aikawa, E., Stangenberg, L., Wurdinger, T., Figueiredo, J.-L., Libby, P., Weissleder, R. and Pittet, M. J. (2007). The healing myocardium sequentially mobilizes two monocyte subsets with divergent and complementary functions. *J Exp Med* **204**, 3037–3047.

Nenni, M. J., Fisher, M. E., James-Zorn, C., Pells, T. J., Ponferrada, V., Chu, S., Fortriede, J. D., Burns, K. A., Wang, Y., Lotay, V. S., et al. (2019). Xenbase: Facilitating the Use of Xenopus to Model Human Disease. *Front. Physiol.* **10**,.

Nguyen, T. M. X., Vegrichtova, M., Tlapakova, T., Krulova, M. and Krylov, V. (2019). Epithelial-Mesenchymal Transition Promotes the Differentiation Potential of *Xenopus tropicalis* Immature Sertoli Cells. *Stem Cells International* **2019**, e8387478.

Nieuwkoop P., F. J. (1994). *Normal Table of Xenopus Laevis (Daudin): A Systematical & Chronological Survey of the Development from the Fertilized Egg till the End of Metamorphosis*.

Oatley, J. M. and Brinster, R. L. (2012). The germline stem cell niche unit in mammalian testes. *Physiological Reviews* **92**,.

Oberpriller, J. O. and Oberpriller, J. C. (1974). Response of the adult newt ventricle to injury. *Journal of Experimental Zoology* **187**,.

O'Bryan, M. K., Gerdprasert, O., Nikolic-Paterson, D. J., Meinhardt, A., Muir, J. A., Foulds, L. M., Phillips, D. J., de Kretser, D. M. and Hedger, M. P. (2005). Cytokine profiles in the testes of rats treated with lipopolysaccharide reveal localized suppression of inflammatory responses. *Am J Physiol Regul Integr Comp Physiol* **288**, R1744-1755.

Oishi, Y. and Manabe, I. (2018). Macrophages in inflammation, repair and regeneration. *International Immunology* **30**,.

Papa, S., Vismara, I., Mariani, A., Barilani, M., Rimondo, S., De Paola, M., Panini, N., Erba, E., Mauri, E., Rossi, F., et al. (2018). Mesenchymal stem cells encapsulated into biomimetic hydrogel scaffold gradually release CCL2 chemokine in situ preserving cytoarchitecture and promoting functional recovery in spinal cord injury. *J Control Release* **278**, 49–56.

Paré, J.-F., Martyniuk, C. J. and Levin, M. (2017). Bioelectric regulation of innate immune system function in regenerating and intact Xenopus laevis. *npj Regenerative Medicine* **2**,.

Paredes, R., Ishibashi, S., Borrill, R., Robert, J. and Amaya, E. (2015). Xenopus: An in vivo model for imaging the inflammatory response following injury and bacterial infection. *Developmental Biology* **408**,.

Parks, W. C., Wilson, C. L. and López-Boado, Y. S. (2004). Matrix metalloproteinases as modulators of inflammation and innate immunity. *Nature Reviews Immunology* **4**,.

P.d, N. and J, F. (1994). *Normal table of Xenopus laevis (Daudin): a systematical and chronological survey of the development from the fertilized egg till the end of metamorphosis.*

Phipps, L. S., Marshall, L., Dorey, K. and Amaya, E. (2020). Model systems for regeneration: Xenopus. *Development* **147**, dev180844.

Piatkowski, T., Mühlfeld, C., Borchardt, T. and Braun, T. (2013). Reconstitution of the Myocardium in Regenerating Newt Hearts is Preceded by Transient Deposition of Extracellular Matrix Components. *Stem Cells and Development* **22**, 1921–1931.

Pinto, A. R., Ilinykh, A., Ivey, M. J., Kuwabara, J. T., D'antoni, M. L., Debuque, R., Chandran, A., Wang, L., Arora, K., Rosenthal, N. A., et al. (2016). Revisiting cardiac cellular composition. *Circulation Research* **118**,.

Porrello, E. R., Mahmoud, A. I., Simpson, E., Hill, J. A., Richardson, J. A., Olson, E. N. and Sadek, H. A. (2011). Transient Regenerative Potential of the Neonatal Mouse Heart. *Science* **331**, 1078–1080.

Porrello, E. R., Mahmoud, A. I., Simpson, E., Johnson, B. A., Grinsfelder, D., Canseco, D., Mammen, P. P., Rothermel, B. A., Olson, E. N. and Sadek, H. A. (2013). Regulation of neonatal

and adult mammalian heart regeneration by the miR-15 family. *Proceedings of the National Academy of Sciences of the United States of America* **110**,.

Porubska, B., Vasek, D., Somova, V., Hajkova, M., Hlaviznova, M., Tlapakova, T., Holan, V. and Krulova, M. (2021). Sertoli Cells Possess Immunomodulatory Properties and the Ability of Mitochondrial Transfer Similar to Mesenchymal Stromal Cells. *Stem Cell Rev and Rep* **17**, 1905–1916.

Poss, K. D., Wilson, L. G. and Keating, M. T. (2002). Heart regeneration in zebrafish. *Science* **298**, 2188–2190.

Qing Zhao, Irem Mertová, Aneta Wróblová, Světlana Žabková, Tereza Tlapáková, and Vladimir Krylov (2024). Immunomodulatory role of Xenopus tropicalis immature Sertoli cells in tadpole muscle regeneration via macrophage response modulation. *Stem Cell Research & Therapy* **15**,.

Rath, D., Amlinger, L., Rath, A. and Lundgren, M. (2015). The CRISPR-Cas immune system: Biology, mechanisms and applications. *Biochimie* **117**,.

Ratnayake, D., Nguyen, P. D., Rossello, F. J., Wimmer, V. C., Tan, J. L., Galvis, L. A., Julier, Z., Wood, A. J., Boudier, T., Isiaku, A. I., et al. (2021). Macrophages provide a transient muscle stem cell niche via NAMPT secretion. *Nature* **591**, 281–287.

Relaix, F., Rocancourt, D., Mansouri, A. and Buckingham, M. (2005). A Pax3/Pax7-dependent population of skeletal muscle progenitor cells. *Nature* **435**,.

Rigamonti, E., Touvier, T., Clementi, E., Manfredi, A. A., Brunelli, S. and Rovere-Querini, P. (2013). Requirement of Inducible Nitric Oxide Synthase for Skeletal Muscle Regeneration after Acute Damage. *J Immunol* **190**, 1767–1777.

Rodrigues, A. M. C., Christen, B., Martí, M. and Izpisúa Belmonte, J. C. (2012). Skeletal muscle regeneration in Xenopus tadpoles and zebrafish larvae. *BMC Developmental Biology* **12**, 9.

Rooijen, N. V. and Sanders, A. (1994). Liposome mediated depletion of macrophages: mechanism of action, preparation of liposomes and applications. *Journal of Immunological Methods* **174**, 83–93.

Sachs, L. M. and Buchholz, D. R. (2019). Insufficiency of thyroid hormone in frog metamorphosis and the role of glucocorticoids. *Frontiers in Endocrinology* **10**,.

Salvadori, L., Chiappalupi, S., Arato, I., Mancuso, F., Calvitti, M., Marchetti, M. C., Riuzzi, F., Calafiore, R., Luca, G. and Sorci, G. (2021). Sertoli Cells Improve Myogenic Differentiation, Reduce Fibrogenic Markers, and Induce Utrophin Expression in Human DMD Myoblasts. *Biomolecules* **11**, 1504.

Sanberg, P. R., Borlongan, C. V., Othberg, A. I., Saporta, S., Freeman, T. B. and Cameron, D. F. (1997). Testis-derived Sertoli cells have a trophic effect on dopamine neurons and alleviate hemiparkinsonism in rats. *Nature Medicine* **3**,.

Sanchez-Iranzo, H., Gonzalez-Rosa, J. M. and Mercader, N. (2013). Heart regeneration: dream or reality ? *European Society of Cardiology*.

Seale, P., Sabourin, L. A., Girgis-Gabardo, A., Mansouri, A., Gruss, P. and Rudnicki, M. A. (2000). Pax7 is required for the specification of myogenic satellite cells. *Cell* **102**, 777–786.

Selawry, H. P. and Cameron, D. F. (1993). Sertoli cell-enriched fractions in successful islet cell transplantation. *Cell Transplantation* **2**,.

Selawry, H. P., Kotb, M., Herrod, H. G. and Lu, Z. N. (1991). Production of a factor, or factors, suppressing il-2 production and t cell proliferation by sertoli cell-enriched preparations: A potential role for islet transplantationin an immunologically privileged site. *Transplantation* **52**,.

Sertoli cell - Wikipedia.

Session, A. M., Uno, Y., Kwon, T., Chapman, J. A., Toyoda, A., Takahashi, S., Fukui, A., Hikosaka, A., Suzuki, A., Kondo, M., et al. (2016). Genome evolution in the allotetraploid frog Xenopus laevis. *Nature* **538**,.

Shcherbo, D., Merzlyak, E. M., Chepurnykh, T. V., Fradkov, A. F., Ermakova, G. V., Solovieva, E. A., Lukyanov, K. A., Bogdanova, E. A., Zaraisky, A. G., Lukyanov, S., et al. (2007). Bright far-red fluorescent protein for whole-body imaging. *Nat Methods* **4**, 741–746.

Shi, Z., Wang, F., Cui, Y., Liu, Z., Guo, X., Zhang, Y., Deng, Y., Zhao, H. and Chen, Y. (2015). Heritable CRISPR/Cas9-mediated targeted integration in Xenopus tropicalis. *FASEB Journal* **29**,.

Shi, Z., Xin, H., Tian, D., Lian, J., Wang, J., Liu, G., Ran, R., Shi, S., Zhang, Z., Shi, Y., et al. (2019). Modeling human point mutation diseases in Xenopus tropicalis with a modified CRISPR/Cas9 system. *FASEB Journal* **33**,.

Shi, Z., Jiang, H., Liu, G., Shi, S., Zhang, X. and Chen, Y. (2022). Expanding the CRISPR/Cas genome-editing scope in Xenopus tropicalis. *Cell and Bioscience* **12**,.

Simões, F. C. and Riley, P. R. (2022). Immune cells in cardiac repair and regeneration. *Development* **149**, dev199906.

Sorokin, S. P. and Hoyt, R. F. (1992). Macrophage development: I. Rationale for using Griffonia simplicifolia isolectin B4 as a marker for the line. *Anat Rec* **232**, 520–526.

Stocum, D. L. (1992). Regeneration Redux A History of Regeneration Research: Milestones in the Evolution of a Science Charles E. Dinsmore. *BioScience* **42**,.

Suarez-Pinzon, W., Korbutt, G. S., Power, R., Hooton, J., Rajotte, R. V. and Rabinovitch, A. (2000). Testicular Sertoli cells protect islet β-cells from autoimmune destruction in NOD mice by a transforming growth factor-β1-dependent mechanism. *Diabetes* **49**,.

Shih-Lei Lai Is a corresponding authorRubén Marín-JuezPedro Luís MouraCarsten KuenneJason Kuan Han LaiAyele Taddese TsedekeStefan GuentherMario LoosoDidier YR Stainier Reciprocal analyses in zebrafish and medaka reveal that harnessing the immune response promotes cardiac regeneration. *eLife* **6**,.

Taniguchi, Y., Watanabe, K. and Mochii, M. (2014). Notochord-derived hedgehog is essential for tail regeneration in Xenopus tadpole. *BMC Developmental Biology* **14**, 27.

Tlapakova, T., Nguyen, T. M. X., Vegrichtova, M., Sidova, M., Strnadova, K., Blahova, M. and Krylov, V. (2016). Identification and characterization of Xenopus tropicalis common progenitors of Sertoli and peritubular myoid cell lineages. *Biology Open* **5**, 1275–1282.

Tripathi, H., Al-Darraji, A., Abo-Aly, M., Peng, H., Shokri, E., Chelvarajan, L., Donahue, R., Levitan, B. M., Gao, E., Hernandez, G., et al. (2020). Autotaxin Inhibition Reduces Cardiac Inflammation and Mitigates Adverse Cardiac Remodeling After Myocardial Infarction. *J Mol Cell Cardiol* **149**, 95–114.

Trivedi, A. A., Igarashi, T., Compagnone, N., Fan, X., Hsu, J.-Y. C., Hall, D. E., John, C. M. and Noble-Haeusslein, L. J. (2006). Suitability of allogeneic sertoli cells for ex vivo gene delivery in the injured spinal cord. *Experimental Neurology* **198**, 88–100.

Trounson, A. and McDonald, C. (2015). Stem Cell Therapies in Clinical Trials: Progress and Challenges. *Cell Stem Cell* **17**, 11–22.

Tseng, A. S., Adams, D. S., Qiu, D., Koustubhan, P. and Levin, M. (2007). Apoptosis is required during early stages of tail regeneration in Xenopus laevis. *Developmental Biology* **301**,.

Turek, P. J., Malkowicz, S. B., Tomaszewski, J. E., Wein, A. J. and Peehl, D. (1996). The role of the Sertoli cell in active immunosuppression in the human testis. *Br J Urol* **77**, 891–895.

Uygur, A. and Lee, R. T. (2016). Mechanisms of Cardiac Regeneration. *Developmental Cell* **36**, 362–374.

Varga, T., Mounier, R., Horvath, A., Cuvellier, S., Dumont, F., Poliska, S., Ardjoune, H., Juban, G., Nagy, L. and Chazaud, B. (2016). Highly Dynamic Transcriptional Signature of Distinct Macrophage Subsets during Sterile Inflammation, Resolution, and Tissue Repair. *The Journal of Immunology* **196**, 4771–4782.

Vegrichtova, M., Hajkova, M., Porubska, B., Vasek, D., Krylov, V., Tlapakova, T. and Krulova, M. (2022). Xenogeneic Sertoli cells modulate immune response in an evolutionary distant mouse model through the production of interleukin-10 and PD-1 ligands expression. *Xenotransplantation* **29**, e12742.

Villalta, S. A., Rinaldi, C., Deng, B., Liu, G., Fedor, B. and Tidball, J. G. (2011). Interleukin-10 reduces the pathology of mdx muscular dystrophy by deactivating M1 macrophages and modulating macrophage phenotype. *Hum Mol Genet* **20**, 790–805.

Voll, R. E., Herrmann, M., Roth, E. A., Stach, C., Kalden, J. R. and Girkontaite, I. (1997). Immunosuppressive effects of apoptotic cells. *Nature* **390**, 350–351.

Wan, E., Yeap, X. Y., Dehn, S., Terry, R., Novak, M., Zhang, S., Iwata, S., Han, X., Homma, S., Drosatos, K., et al. (2013). Enhanced Efferocytosis of Apoptotic Cardiomyocytes Through MER Tyrosine Kinase Links Acute Inflammation Resolution to Cardiac Repair After Infarction. *Circ Res* **113**, 10.1161/CIRCRESAHA.113.301198.

Wang, S. and Shi, Y.-B. (2021). Evolutionary divergence in tail regeneration between Xenopus laevis and Xenopus tropicalis. *Cell & Bioscience* **11**, 71.

Wang, M., Chen, Y., Pan, Q., Du, M., Li, Z. and Dong, H. (2021a). Co-culture of sperm with sertoli cells can improve IVF outcomes by increasing sperm motility in mice. *Theriogenology* **172**,.

Wang, J., Li, S., Li, H., Zhou, X., Wen, H. and Lai, B. (2021b). IRF4 overexpression promotes the transdifferentiation of tregs into macrophage-like cells to inhibit the development of colon cancer. *Cancer Cell International* **21**, 58.

Washburn, R. L., Hibler, T., Thompson, L. A., Kaur, G. and Dufour, J. M. (2022). Therapeutic application of Sertoli cells for treatment of various diseases. *Seminars in Cell & Developmental Biology* **121**, 10–23.

Wieczorek, D. F. (2018). The Role of Tropomyosin in Cardiac Function and Disease. In *Cardiac Diseases and Interventions in 21st Century*, p. IntechOpen.

Willsey, H. R. (2021). Whole-mount RNA in situ hybridization and immunofluorescence of Xenopus embryos and tadpoles. *Cold Spring Harb Protoc* **2021**, pdb.prot105635.

Witman, N., Murtuza, B., Davis, B., Arner, A. and Morrison, J. I. (2011). Recapitulation of developmental cardiogenesis governs the morphological and functional regeneration of adult newt hearts following injury. *Developmental Biology* **354**,.

Wright, A. V., Nuñez, J. K. and Doudna, J. A. (2016). Biology and Applications of CRISPR Systems: Harnessing Nature's Toolbox for Genome Engineering. *Cell* **164**,.

Wynn, T. A., Chawla, A. and Pollard, J. W. (2013). Macrophage biology in development, homeostasis and disease. *Nature* **496**,.

Xiao-Lin Lin, Jin-Hua Lin, Yan Cao, Han Zhang, Si-Yi He, Hai-Yan Wu, Ze-Bing Ye, Li Zheng, and Xu-Feng Qi (2024). Cardiomyocyte proliferation and heart regeneration in adult Xenopus tropicalis evidenced by a transgenic reporter line | npj Regenerative Medicine. *npj Regenerative Medicine* **9**,.

Xin, M., Olson, E. N. and Bassel-Duby, R. (2013). Mending broken hearts: Cardiac development as a basis for adult heart regeneration and repair. *Nature Reviews Molecular Cell Biology* **14**,.

Yang, S., Zhao, M. and Jia, S. (2023). Macrophage: Key player in the pathogenesis of autoimmune diseases. *Frontiers in Immunology* **14**,.

Young, J. J., Cherone, J. M., Doyon, Y., Ankoudinova, I., Faraji, F. M., Lee, A. H., Ngo, C., Guschin, D. Y., Paschon, D. E., Miller, J. C., et al. (2011). Efficient targeted gene disruption in the soma and germ line of the frog Xenopus tropicalis using engineered zinc-finger nucleases. *Proceedings of the National Academy of Sciences of the United States of America* **108**,.

Zahn, N., Levin, M. and Adams, D. S. (2017). The zahn drawings: New illustrations of xenopus embryo and tadpole stages for studies of craniofacial development. *Development (Cambridge)* **144**,.

Zaman, R. and Epelman, S. (2022). Resident cardiac macrophages: Heterogeneity and function in health and disease. *Immunity* **55**,.

Zammit, P. S., Golding, J. P., Nagata, Y., Hudon, V., Partridge, T. A. and Beauchamp, J. R. (2004). Muscle satellite cells adopt divergent fates: A mechanism for self-renewal? *Journal of Cell Biology* **166**, 347–357.

9 SUPPLEMENTAL

9.1 Pax7 CRISPR-Cas9 Knock-In Donor Plasmid Full Sequence

ORIGIN

1 ctaaattgta agcgttaata ttttgttaaa attcgcgtta aatttttgtt aaatcagctc

61 atttttttaac caataggccg aaatcggcaa aatcccttat aaatcaaaag aatagaccga

121 gatagggttg agtgttgttc agtttggaa caagagtcca ctattaaaga acgtggactc

181 caacgtcaaa gggcgaaaaa ccgtctatca gggcgatggc ccactacgtg aaccatcacc

241 ctaatcaagt tttttggggt cgaggtgccg taaagcacta aatcggaacc ctaaagggag

301 cccccgattt agagcttgac ggggaaagcc ggcgaacgtg gcgagaaagg aagggaagaa

361 agcgaaagga gcgggcgcta gggcgctggc aagtgtagcg gtcacgctgc gcgtaaccac

421 cacacccgcc gcgcttaatg cgccgctaca gggcgcgtcc cattcgccat tcaggctgcg

481 caactgttgg gaagggcgat cggtgcgggc ctcttcgcta ttacgccagc tggcgaaagg

541 gggatgtgct gcaaggcgat taagttgggt aacgccaggg ttttcccagt cacgacgttg

601 taaaacgacg gccagtgagc gcgcgtaata cgactcacta tagggcgaat tggagctcca

661 ccgcggtggc ggccgctcac ctgggagttc catgacctgt ataaaagccc ttggccttca

721 gcctcgtccc tggaatggcc ttaaaggggc ggttcacctt ttcgtcaact tttagtatgt

781 tatagaatgg ccaattctaa gcagcttttt aaatggtctt cattatttat ttttttatag

841 tttttaaact atttgacttc tgcctctttc cagctttcaa atgggggtca ctgaccccgg

901 cagccaaacc ctattgctct gtgaggctcc agttttattg ttactgttac tttttattcc

961 ttatctttct attcagcccc tctcctattc atataccagc ctctcattca aaccactccc

1021 tggttactaa ggtaatttgg accctagcaa ccagaaagct gctaaaactc caaactgcag

1081 agctgctgaa caaaaaagtg aaataacaaa aaaaaaacca aataataaaa aatgaagacc

1141 aattgcaagt tgtctcagaa tatcactctc tacatcatac taaaagctaa ctcatctcta

1201 aatataagca gctttgcagt tggtcctctg tctcatttct gatgtaaatg ataagtgttg

1261 ggttggggga taacagctag taatgtaata agcacaataa taatctaaaa attcattttt

1321 ttgttcctgt tttgcagccg ccgttgatta cctggcgaaa aatgtcagtt tgtctacgca

1381 gcgcaggatg aaactcgggg accactcggc agtactaggt ctgttacccg tggagaccgg

1441 ccaggcctac tctagaacaa aagctggtac cgggcccccc ctcgagtcca taagaaagat

1501 ataaataagc tggagagaat gcagaattgt caactagcag tgctggaatt ggggagggat

1561 gccatcccct cacttttta tttctgtgaa atagcatccc ctcagtgtgg atgcaagttt

1621 tttgaatccc ggaactgtct tttgctcctc ttcacttctg catgcaaata caatgcagag

1681 gtaaaatata atatagttaa atatataggg gattaaagga gagaaaaaat tgctgggaga

1741 gaagaagaaa agatagagaa gtgttaaaca gataaagaag gtggaggcat cagagagggt

1801 tatagagaaa aggagagaag aaaaaatgaa ggtattaaac agcagcagat taaggaatag

1861 tgagaaaatg ctttatatga aataatcttg ggtaatatag aatatgatgg ggatgtgcta

1921 tgttatgaca caatacacag aaaaggtgct ttatttgcag tagctgaatt ggtagccaag

1981 aaaagtcata agcacaattt ttatttttggg gtccctatag gtcacatatg taaatatggt

2041 tatgggaggg atgcaccaca cagagcatcc ctccactttt tttactccaa ttcaagcact

2101 gggaatgaga tatgcttcat tagcacctaa acatttgaca atgaccaatg tgaatgttag

2161 cgaccatatt tgcgtccttt tgtgaccaaa tggcatatgt gaacattcct agtgtatgta

2221 ataaaatttt gcaacaaaat atttaaaaac tccagagcag atgcttaact tagtcatgta

2281 atattcgcca gcaaatgagt atacctctat ttttaacatc acttgtgatt tttttagtaa

2341 cattcccacc tttagtattt ccagattgaa attatcatac ccccccattc tttaatatag

2401 ggaacactgt accagtgggt ctgggattat ttgtccatat attgcaatat atccaagctg

2461 accaactgtc tcaaagtcac ccctggtctg gccaataaaa cacaaacatt ctagcagaaa

2521 gtaaagctgg ccatagatgt tgagattttt aaaagatcag atcctgatcg tgagaccacg

2581 atcttctcag aacgatcgta cgatcgtacg aatctaccat caactaaaaa gaccaattta

2641 ccaggaaaac aaaggggagc tgcctgcttg gccctgcaaa catagagaga ttgcactggg

2701 gccgacaaag atttttgac ctggccgatc aatttcccga cagatgtcgg ccgaaaaatc

2761 gtaagatgta cgatcgttcg aataccacta accgcacgat aatttcgaag gattggtcgg

2821 gcttccctaa aatcggtcgt tcggcaagaa gaatcgtcgc gtctatgggg accttaagtg

2881 tacttgcttt ccaaggttaa aaattgttac ctttttatac gacactgcat ggatcacctg

2941 aaagcaggtt gggagctaca acatggaact agccactgtt cctttatatg gttatcacta

3001 cccaatttta aataattaaa ctggagttta ttgatggtgt gaccacaaaa ttgatacaga

3061 taaagacata ctgtatatat tgcgttatat gacaaataca gtaacaccac attactattt

3121 taaattatat ataaaataat attaatatat ctggggacat aaaatgtggc ttcttaaaca

3181 ttggggtgac actgatgaga ttatttggta aatgtttgat gctagctaac cattgtttgg

3241 ttcatttgtg tgattcaaaa gtggcaaaga atgacaccta gatgatgcca aattaaggat

3301 ttactagtaa ccacaattct ttaaactgtt acaaagtgtt tggaccagca actgaattgc

3361 actgtaaatt accacatcag ggtctccggg gtcaacgctg ctaagcaatg gactggaaaa

3421 tttgtgacat tgagtttttg gaataactgg gaatgctgga taactctttg ggtaaagcta

3481 tggaacaaaa gtaccagcat gaactaagaa atgactgtca cagcacaaca tcaaacacaa

3541 tgcaagacaa aggttctctg cttttgcctt acttgacaga aaaagtaagc tctaggttca

3601 tcgcatgcag acagcagcaa tacatgacat atataaaggc tggctctttt ctcccttcca

3661 ttgaactgaa acttccactc agtcagactt gcggggatcc tccgctagcg ctaccggtcg

3721 ccaccatggt gggtgaggat agcgtgctga tcaccgagaa catgcacatg aaactgtaca

3781 tggagggcac cgtgaacgac caccacttca agtgcacatc cgagggcgaa ggcaagccct

3841 acgagggcac ccagaccatg aagatcaagg tggtcgaggg cggccctctc cccttcgcct

3901 tcgacatcct ggctaccagc ttcatgtacg gcagcaaaac ctttatcaac cacacccagg

3961 gcatccccga cttctttaag cagtccttcc ctgagggctt cacatgggag aggatcacca

4021 catacgaaga cgggggcgtg ctgaccgcta cccaggacac cagcctccag aacggctgcc

4081 tcatctacaa cgtcaagatc aacggggtga acttcccatc caacggccct gtgatgcaga

4141 agaaaacact cggctgggag gccagcaccg agatgctgta ccccgctgac agcggcctga

4201 gaggccatag ccagatggcc ctgaagctcg tgggcggggg ctacctgcac tgctccctca

4261 agaccacata cagatccaag aaacccgcta agaacctcaa gatgcccggc ttctacttcg

4321 tggacaggag actggaaaga atcaaggagg ccgacaaaga gacctacgtc gagcagcacg

4381 agatggctgt ggccaggtac tgcgacctgc ctagcaaact ggggcacagc tccggactca

4441 gatctcgact agataactga tcataatcag ccataccaca tttgtagagg ttttacttgc

4501 tttaaaaaac ctcccacacc tccccctgaa cctgaaacat aaaatgaatg caattgttgt

4561 tgttaacttg tttattgcag cttataatgg ttacaaataa agcaatagca tcacaaattt

4621 cacaaataaa gcatttttt cactgcattc tagttgtggt ttgtccaaac tcacccgggg

4681 caggttagaa tttcatcttc tttaatatat aacaggaatg cctgaggtac acagagaacc

4741 catacaggcg gcaggtagcg agacccccg ctgctggtca tcagtgcaat gcaaacatct

4801 gtagcacgga caggataaaa caggtattga ttcatcttcc tactctacca cataatatag

4861 ctgaataaat tatagcggga ttatatatat gtatatatat atatacaggc gtacgagcgc

4921 gcactcgtgg ggcaaggtgg ctgtgggtca gatacagagg cggaactggg tggatggaat

4981 gttatctagt tctagttaag tggctccttg gatgtgaatt agaacaagca agtccatgtt

5041 agaagtcaaa tacatacgca gaagggtaca atgccggatc tacattcgac agaatttttt

5101 gcagaagtat aaaaaaaagg cttaatgtcc gtatgtgcac tgagcataca gagggggttc

5161 cttcgggggt cttgggttgg gatgcttcca tggaatgcaa agtcaccata gtctcttaat

5221 ccttgttgag gcttcgtcct ccgaattgcc ttaaaggggc ggttcacctt aaatttaact

5281 tttagtgtgt tatagaatgc atatagaata ctaagcaact tttcaattgg tcttcattat

5341 gtatttctta tagttttctt cttccccggc agccaaaccc tattgctctg tgaggctcca

5401 gttttattgt tattgttact ttttattact tatctttata ttcagttccc tctcctattc

5461 atatacgagt ctcattcaaa ccactccctg gttgctaagg tcatttggac cctagcaacc

5521 agagagctgc tataactcta aactggagag tcgctaaaca attactgaaa tcattaaaaa

5581 aactacaaat aataaataat gaagaccaat tgcaagtggt ctcggaatat tactctctac

5641 atcatactac ccctttagca gttcagccca taggttatac aaaaacatct ccaatacagt

5701 cgatacaaac ctggggtaat tataggaatc tgattgtgct tctttaaccc tttcttcctc

5761 tgctaacgat attttaaata tacttttttc ttttttttaa tttgggattt tctatgtaca

5821 ttttcagaca acaccactcc atgaatttac atgaaactta ctatacatct gtcaatatta

5881 ctgctcacaa gaaaacttca aatcaatcgt ctcactggaa tgattcggga ctttctttca

5941 catagaggga atcacaaggt ccgtatttac atcattgttg gccgcgactt ccaatgtcac

6001 aatgagtgac ccaatacgcg tgtgtccgac aacacaacta tttctacgtt taaggggccc

6061 attagtcaca gtcaagtttt ttagtttttt ttcatggacc tctcggaacc atttggcgag

6121 tcctggcttc ccgaccaggg aggggacagt catcgacaag acatattttt tttattaaag

6181 aaaggtgacc tggtaaaaca ttctgaatgt gggcgttggt ccgaagaatc agaatatctg

6241 tatcagataa tatatgtatc agaatacatc cttgaggtcc tttgaggaat gtgcaggaca

6301 tggaatcccc acagaggggc gccaaagatg aagatgtgta caatgacatc acgtgatatc

6361 acatgttcgt attggctggc cgtacaccca atcggatccc gcagttgaga ctacaaacat

6421 aacctgtatc tcagatttca agtggggtgc ttgaaatgag cctttacaag gcgaataaaa

6481 tatgtaacca atcagaagct gtagataaca gggggcgggg cttcccaatc tgcattgtgg

6541 gtttcctggc caactacatt tcagtcatgg cgcaaagttt atggtttatc gttttccatg

6601 atatctgatc ccttgaactg taatttccac catgaaatcg atataaggtt catatctgag

6661 attcgcaagt ctccgttggt cctttaacgt ttactccaaa ttatgttttt tggctgtgga

6721 aaaaaaaatc aagaaaaaaa agaccaataa aatgagtttt tcttcttact acccggagct

6781 tattatactg ggggatcagc atcacaagtc agaagcgatt ggtccccccа aaacttcagt

6841 ttgtcaccgt gaagtggcag gaaatttgcc aaaattgttt ttttttttt ttaaaaaagt

6901 gcaggaagca actcctggca accgccggac gcctggggtg gcagggagtt agaaggcgga

6961 tagcggagaa gcaccttgat attgtggccc tgaagcaaga tggcggaatg gacaggtctc

7021 agaagatgga tacagccgct ctgattggca gaggattccc ttggctcccg ggctgcagtc

7081 aaactctgag tccggacctg tacagctcgt ccatgccgtg ggtgtggcag caggcgctga

7141 aggactccag gagcaccatg tggtcgcggg cctcgttgcg gtccttgctg atcttggtct

7201 gagtgctcag gtagtggttg atggggatca gcacggggcc gtcgcccagg ggcacgttgg

7261 tctggtagtg gtcggccagc tgcacgccgc cgccctcgat gttgtggcgg gtcttgaagt

7321 tagcctccag gccgttgttg gccttgtcgg ggcggatgta cacgttgtgg ctgttgaagc

7381 tgtactccag cttgtggccc aggatgttgc cgtcctcctt gaagtccttg cccttcagct

7441 cgatgcggtt caccagggtg tcgccctcga acttcacctc gccgcgggtc ttgtacttgc

7501 cgtcgtcctg gaactggatg gtgcgctcct ggatgtagcc ctcgggcatg gcgctcttga

7561 agaagtcgtt catcttcatg tgctcggggt agcgggcgaa gcactggatg ccgtagcaga

7621 gggtggtcac cagggtgggc cagggcacgg gcagcttgcc ggtggtgcag atgaacttga

7681 tctccagctt gccgtagtcg gcgtcgccct cgccctcgcc gcgcacgctg aacttgtggc

7741 cgtgcacgtc gccgtccagc tcgatcagca cgggcacgat gccggcgaac agctcctcgc

7801 ccccgctcat gaattctggg ccaggattct cctcgacgtc accgcatgtt agcagacttc

7861 ctctgccctc gatatcgtag gcctggccgg tctccacggg taacagacct agtactgccg

7921 agtggtcccc gagtttcatc ctgcgctgcg tagacaaact gacatttttc gccaggtaat

7981 caacggcggc tgcaaaacag gaacaaaaaa atgaattttt agattattat tgtgcttatt

8041 acattactag ctgttatccc ccaacccaac acttatcatt tacatcagaa atgagacaga

8101 ggaccaactg caaagctgct tatatttaga gatgagttag cttttagtat gatgtagaga

8161 gtgatattct gagacaactt gcaattggtc ttcatttttt attatttggt ttttttttg

8221 ttatttcact tttttgttca gcagctctgc agtttggagt tttagcagct ttctggttgc

8281 tagggtccaa attaccttag taaccaggga gtggtttgaa tgagaggctg gtatatgaat

8341 aggagagggg ctgaatagaa agataaggaa taaaaagtaa cagtaacaat aaaactggag

8401 cctcacagag caatagggtt tggctgccgg ggtcagtgac ccccatttga aagctggaaa

8461 gaggcagaag tcaaatagtt taaaaactat aaaaaaataa ataatgaaga ccatttaaaa

8521 agctgcttag aattggccat tctataacat actaaaagtt gacgaaaagg tgaaccgccc

8581 ctttaaggcc attccaggga cgaggctgaa ggccaagggc ttttatacag gtcatggaac

8641 tcccaggtga aagcttatcg ataccgtcga cctcgagggg gggcccggta cccagctttt

8701 gttcccttta gtgagggtta attgcgcgct tggcgtaatc atggtcatag ctgtttcctg

8761 tgtgaaattg ttatccgctc acaattccac acaacatacg agccggaagc ataaagtgta

8821 aagcctgggg tgcctaatga gtgagctaac tcacattaat tgcgttgcgc tcactgcccg

8881 ctttccagtc gggaaacctg tcgtgccagc tgcattaatg aatcggccaa cgcgcgggga

8941 gaggcggttt gcgtattggg cgctcttccg cttcctcgct cactgactcg ctgcgctcgg

9001 tcgttcggct gcggcgagcg gtatcagctc actcaaaggc ggtaatacgg ttatccacag

9061 aatcagggga taacgcagga aagaacatgt gagcaaaagg ccagcaaaag gccaggaacc

9121 gtaaaaaggc cgcgttgctg gcgtttttcc ataggctccg ccccccctgac gagcatcaca

9181 aaaatcgacg ctcaagtcag aggtggcgaa acccgacagg actataaaga taccaggcgt

9241 ttcccccctgg aagctccctc gtgcgctctc ctgttccgac cctgccgctt accggatacc

9301 tgtccgcctt tctcccttcg ggaagcgtgg cgctttctca tagctcacgc tgtaggtatc

9361 tcagttcggt gtaggtcgtt cgctccaagc tgggctgtgt gcacgaaccc cccgttcagc

9421 ccgaccgctg cgccttatcc ggtaactatc gtcttgagtc caacccggta agacacgact

9481 tatcgccact ggcagcagcc actggtaaca ggattagcag agcgaggtat gtaggcggtg

9541 ctacagagtt cttgaagtgg tggcctaact acggctacac tagaaggaca gtatttggta

9601 tctgcgctct gctgaagcca gttaccttcg gaaaaagagt tggtagctct tgatccggca

9661 aacaaaccac cgctggtagc ggtggttttt ttgtttgcaa gcagcagatt acgcgcagaa

9721 aaaaaggatc tcaagaagat cctttgatct tttctacggg gtctgacgct cagtggaacg

9781 aaaactcacg ttaagggatt ttggtcatga gattatcaaa aaggatcttc acctagatcc

9841 ttttaaatta aaaatgaagt tttaaatcaa tctaaagtat atatgagtaa acttggtctg

9901 acagttacca atgcttaatc agtgaggcac ctatctcagc gatctgtcta tttcgttcat

9961 ccatagttgc ctgactcccc gtcgtgtaga taactacgat acgggagggc ttaccatctg

10021 gccccagtgc tgcaatgata ccgcgagacc cacgctcacc ggctccagat ttatcagcaa

10081 taaaccagcc agccggaagg gccgagcgca gaagtggtcc tgcaacttta tccgcctcca

10141 tccagtctat taattgttgc cgggaagcta gagtaagtag ttcgccagtt aatagtttgc

10201 gcaacgttgt tgccattgct acaggcatcg tggtgtcacg ctcgtcgttt ggtatggctt

10261 cattcagctc cggttcccaa cgatcaaggc gagttacatg atcccccatg ttgtgcaaaa

10321 aagcggttag ctccttcggt cctccgatcg ttgtcagaag taagttggcc gcagtgttat

10381 cactcatggt tatggcagca ctgcataatt ctcttactgt catgccatcc gtaagatgct

10441 tttctgtgac tggtgagtac tcaaccaagt cattctgaga atagtgtatg cggcgaccga

10501 gttgctcttg cccggcgtca atacgggata ataccgcgcc acatagcaga actttaaaag

10561 tgctcatcat tggaaaacgt tcttcggggc gaaaactctc aaggatctta ccgctgttga

10621 gatccagttc gatgtaaccc actcgtgcac ccaactgatc ttcagcatct tttactttca

10681 ccagcgtttc tgggtgagca aaaacaggaa ggcaaaatgc cgcaaaaaag ggaataaggg

10741 cgacacggaa atgttgaata ctcatactct tccttttca atattattga agcatttatc

10801 agggttattg tctcatgagc ggatacatat ttgaatgtat ttagaaaaat aaacaaatag

10861 gggttccgcg cacatttccc cgaaaagtgc cac

//

9.2 *MMP7* CRISPR-Cas9 Knock-In Donor Plasmid Full Sequence

ORIGIN

1 ctaaattgta agcgttaata ttttgttaaa attcgcgtta aatttttgtt aaatcagctc

61 atttttaac caataggccg aaatcggcaa aatcccttat aaatcaaaag aatagaccga

121 gatagggttg agtgttgttc cagtttggaa caagagtcca ctattaaaga acgtggactc

181 caacgtcaaa gggcgaaaaa ccgtctatca gggcgatggc ccactacgtg aaccatcacc

241 ctaatcaagt tttttggggt cgaggtgccg taaagcacta aatcggaacc ctaaagggag

301 cccccgattt agagcttgac ggggaaagcc ggcgaacgtg gcgagaaagg aagggaagaa

361 agcgaaagga gcgggcgcta gggcgctggc aagtgtagcg gtcacgctgc gcgtaaccac

421 cacacccgcc gcgcttaatg cgccgctaca gggcgcgtcc cattcgccat tcaggctgcg

481 caactgttgg gaagggcgat cggtgcgggc ctcttcgcta ttacgccagc tggcgaaagg

541 gggatgtgct gcaaggcgat taagttgggt aacgccaggg ttttcccagt cacgacgttg

601 taaaacgacg gccagtgagc gcgcgtaata cgactcacta tagggcgaat tggagctcca

661 ccgcggtggc ggccgccagc ttttaactgg ggcaacactg agtatatttt ggtgcaacat

721 acaaatgttt ccctgtacat attggctggt tttgcatata agactccctt aagtcataaa

781 cttttacagg tttaatatgc aacagagaat agcaaggctg ttagttacag ttgcacagag

841 ctggtattca tacagcaggt cattctgact gcagctaatc atttgaatga atgacatata

901 ctatagatca gtgatcccca gccagtggct ctggggcaac atgttgctcc ccaacacctt

961 ggatgttgct ctcagtggcc tcaaagtagg tgcttgtttt tgaattcctg gcttggaggc

1021 aagtgctgat tgcataaaac ccagtgtgaa gcctaactga accttctata ggctgccact

1081 ccacataggg gccaataacc aattatagct cttatttgca ccccaggaac ttttttccct

1141 gcttgtgttg ctcctcaaca cattttcat ttgaatgtgg ctcacgggta taaaaggttg

1201 gggatccctg ctatagactg tatatatgca gccatacata tccctgatgg tcctttcttt

1261 tggcaggttt taatctgttc ctagtggctg cgcatgaatt tggccattct ctgggactcg

1321 atcattctac tgacccacga gccttgatgt tcccgaccta ccattatgtg gacacgcagg

1381 cctttcgttt gtcccaagat gacatcaacg gaatacagtc aatatatgga agaaggcaat

1441 ctagaacaaa agctggtacc gggcccccccc tcgagtccat aagaaagata taaataagct

1501 ggagagaatg cagaattgtc aactagcagt gctggaattg gggagggatg ccatcccctc

1561 actttttat ttctgtgaaa tagcatcccc tcagtgtgga tgcaagtttt ttgaatcccg

1621 gaactgtctt ttgctcctct tcacttctgc atgcaaatac aatgcagagg taaaatataa

1681 tatagttaaa tatatagggg attaaaggag agaaaaaatt gctgggagag aagaagaaaa

1741 gatagagaag tgttaaacag ataaagaagg tggaggcatc agagagggtt atagagaaaa

1801 ggagagaaga aaaaatgaag gtattaaaca gcagcagatt aaggaatagt gagaaaatgc

1861 tttatatgaa ataatcttgg gtaatataga atatgatggg gatgtgctat gttatgacac

1921 aatacacaga aaaggtgctt tatttgcagt agctgaattg gtagccaaga aaagtcataa

1981 gcacaatttt tattttgggg tccctatagg tcacatatgt aaatatggtt atgggaggga

2041 tgcaccacac agagcatccc tccacttttt ttactccaat tcaagcactg ggaatgagat

2101 atgcttcatt agcacctaaa catttgacaa tgaccaatgt gaatgttagc gaccatattt

2161 gcgtcctttt gtgaccaaat ggcatatgtg aacattccta gtgtatgtaa taaaattttg

2221 caacaaaata tttaaaaact ccagagcaga tgcttaactt agtcatgtaa tattcgccag

2281 caaatgagta tacctctatt tttaacatca cttgtgattt ttttagtaac attcccacct

2341 ttagtatttc cagattgaaa ttatcatacc cccccattct ttaatatagg gaacactgta

2401 ccagtgggtc tgggattatt tgtccatata ttgcaatata tccaagctga ccaactgtct

2461 caaagtcacc cctggtctgg ccaataaaac acaaacattc tagcagaaag taaagctggc

2521 catagatgtt gagattttta aaagatcaga tcctgatcgt gagaccacga tcttctcaga

2581 acgatcgtac gatcgtacga atctaccatc aactaaaaag accaatttac caggaaaaca

2641 aaggggagct gcctgcttgg ccctgcaaac atagagagat tgcactgggg ccgacaaaga

2701 ttttttgacc tggccgatca atttcccgac agatgtcggc cgaaaaatcg taagatgtac

2761 gatcgttcga ataccactaa ccgcacgata atttcgaagg attggtcggg cttccctaaa

2821 atcggtcgtt cggcaagaag aatcgtcgcg tctatgggga ccttaagtgt acttgctttc

2881 caaggttaaa aattgttacc tttttatacg acactgcatg gatcacctga aagcaggttg

2941 ggagctacaa catggaacta gccactgttc ctttatatgg ttatcactac ccaattttaa

3001 ataattaaac tggagtttat tgatggtgtg accacaaaat tgatacagat aaagacatac

3061 tgtatatatt gcgttatatg acaaatacag taacaccaca ttactatttt aaattatata

3121 taaaataata ttaatatatc tggggacata aaatgtggct tcttaaacat tggggtgaca

3181 ctgatgagat tatttggtaa atgtttgatg ctagctaacc attgtttggt tcatttgtgt

3241 gattcaaaag tggcaaagaa tgacacctag atgatgccaa attaaggatt tactagtaac

3301 cacaattctt taaactgtta caaagtgttt ggaccagcaa ctgaattgca ctgtaaatta

3361 ccacatcagg gtctccgggg tcaacgctgc taagcaatgg actggaaaat ttgtgacatt

3421 gagtttttgg aataactggg aatgctggat aactctttgg gtaaagctat ggaacaaaag

3481 taccagcatg aactaagaaa tgactgtcac agcacaacat caaacacaat gcaagacaaa

3541 ggttctctgc ttttgcctta cttgacagaa aaagtaagct ctaggttcat cgcatgcaga

3601 cagcagcaat acatgacata tataaaggct ggctcttttc tcccttccat tgaactgaaa

3661 cttccactca gtcagacttg cggggatcct ccgctagcgc taccggtcgc caccatggtg

3721 ggtgaggata gcgtgctgat caccgagaac atgcacatga aactgtacat ggagggcacc

3781 gtgaacgacc accacttcaa gtgcacatcc gagggcgaag gcaagcccta cgagggcacc

3841 cagaccatga agatcaaggt ggtcgagggc ggccctctcc ccttcgcctt cgacatcctg

3901 gctaccagct tcatgtacgg cagcaaaacc tttatcaacc acacccaggg catccccgac

3961 ttctttaagc agtccttccc tgagggcttc acatgggaga ggatcaccac atacgaagac

4021 gggggcgtgc tgaccgctac ccaggacacc agcctccaga acggctgcct catctacaac

4081 gtcaagatca acggggtgaa cttcccatcc aacggccctg tgatgcagaa gaaaacactc

4141 ggctgggagg ccagcaccga gatgctgtac cccgctgaca gcggcctgag aggccatagc

4201 cagatggccc tgaagctcgt gggcgggggc tacctgcact gctccctcaa gaccacatac

4261 agatccaaga aacccgctaa gaacctcaag atgcccggct tctacttcgt ggacaggaga

4321 ctggaaagaa tcaaggaggc cgacaaagag acctacgtcg agcagcacga gatggctgtg

4381 gccaggtact gcgacctgcc tagcaaactg gggcacagct ccggactcag atctcgacta

4441 gataactgat cataatcagc cataccacat ttgtagaggt tttacttgct ttaaaaaacc

4501 tcccacacct ccccctgaac ctgaaacata aaatgaatgc aattgttgtt gttaacttgt

4561 ttattgcagc ttataatggt tacaaataaa gcaatagcat cacaaatttc acaaataaag

4621 catttttttc actgcattct agttgtggtt tgtccaaact cacccggtag atccacgtag

4681 gcacatgtaa gcttttaatc atcatttatt tatttacacg gtaccagcaa gctatacagc

4741 actttacaat aatatagcgc caaaataaaa cagaaggatt agaaggtcct gcatacaaga

4801 gcttacaatg tagcaattaa atgatgacca agctaaagca tgtgactttg caccccgggc

4861 tgcagtcaaa ctctgagtcc ggacctgtac agctcgtcca tgccgtgggt gtggcagcag

4921 gcgctgaagg actccaggag caccatgtgg tcgcgggcct cgttgcggtc cttgctgatc

4981 ttggtctgag tgctcaggta gtggttgatg gggatcagca cggggccgtc gcccaggggc

5041 acgttggtct ggtagtggtc ggccagctgc acgccgccgc cctcgatgtt gtggcgggtc

5101 ttgaagttag cctccaggcc gttgttggcc ttgtcggggc ggatgtacac gttgtggctg

5161 ttgaagctgt actccagctt gtggcccagg atgttgccgt cctccttgaa gtccttgccc

5221 ttcagctcga tgcggttcac cagggtgtcg ccctcgaact tcacctcgcc gcgggtcttg

5281 tacttgccgt cgtcctggaa ctggatggtg cgctcctgga tgtagccctc gggcatggcg

5341 ctcttgaaga agtcgttcat cttcatgtgc tcggggtagc gggcgaagca ctggatgccg

5401 tagcagaggg tggtcaccag ggtgggccag ggcacgggca gcttgccggt ggtgcagatg

5461 aacttgatct ccagcttgcc gtagtcggcg tcgccctcgc cctcgccgcg cacgctgaac

5521 ttgtggccgt gcacgtcgcc gtccagctcg atcagcacgg gcacgatgcc ggcgaacagc

5581 tcctcgcccc cgctcatgaa ttctgggcca ggattctcct cgacgtcacc gcatgttagc

5641 agacttcctc tgccctcgat atcttgcctt cttccatata ttgactgtat tccgttgatg

5701 tcatcttggg acaaacgaaa ggcctgcgtg tccacataat ggtaggtcgg gaacatcaag

5761 gctcgtgggt cagtagaatg atcgagtccc agagaatggc caaattcatg cgcagccact

5821 aggaacagat taaaacctgc caaaagaaag gaccatcagg gatatgtatg gctgcatata

5881 tacagtctat agcagggatc cccaaccttt tatacccgtg agccacattc aaatgaaaaa

5941 tgtgttgagg agcaacacaa gcagggaaaa aagttcctgg ggtgcaaata agagctataa

6001 ttggttattg gcccctatgt ggagtggcag cctatagaag gttcagttag gcttcacact

6061 gggttttatg caatcagcac ttgcctccaa gccaggaatt caaaaacaag cacctacttt

6121 gaggccactg agagcaacat ccaaggtgtt ggggagcaac atgttgcccc agagccactg

6181 gctggggatc actgatctat agtatatgtc attcattcaa atgattagct gcagtcagaa

6241 tgacctgctg tatgaatacc agctctgtgc aactgtaact aacagccttg ctattctctg

6301 ttgcatatta aacctgtaaa agtttatgac ttaagggagt cttatatgca aaaccagcca

6361 atatgtacag ggaaacattt gtatgttgca ccaaaatata ctcagtgttg ccccagttaa

6421 aagctgaagc ttatcgatac cgtcgacctc gaggggggggc ccggtaccca gcttttgttc

6481 cctttagtga gggttaattg cgcgcttggc gtaatcatgg tcatagctgt ttcctgtgtg

6541 aaattgttat ccgctcacaa ttccacacaa catacgagcc ggaagcataa agtgtaaagc

6601 ctggggtgcc taatgagtga gctaactcac attaattgcg ttgcgctcac tgcccgcttt

6661 ccagtcggga aacctgtcgt gccagctgca ttaatgaatc ggccaacgcg cggggagagg

6721 cggtttgcgt attgggcgct cttccgcttc ctcgctcact gactcgctgc gctcggtcgt

6781 tcggctgcgg cgagcggtat cagctcactc aaaggcggta atacggttat ccacagaatc

6841 aggggataac gcaggaaaga acatgtgagc aaaaggccag caaaaggcca ggaaccgtaa

6901 aaaggccgcg ttgctggcgt ttttccatag gctccgcccc cctgacgagc atcacaaaaa

6961 tcgacgctca agtcagaggt ggcgaaaccc gacaggacta taaagatacc aggcgtttcc

7021 ccctggaagc tccctcgtgc gctctcctgt tccgaccctg ccgcttaccg gatacctgtc

7081 cgcctttctc ccttcgggaa gcgtggcgct ttctcatagc tcacgctgta ggtatctcag

7141 ttcggtgtag gtcgttcgct ccaagctggg ctgtgtgcac gaacccccccg ttcagcccga

7201 ccgctgcgcc ttatccggta actatcgtct tgagtccaac ccggtaagac acgacttatc

7261 gccactggca gcagccactg gtaacaggat tagcagagcg aggtatgtag gcggtgctac

7321 agagttcttg aagtggtggc ctaactacgg ctacactaga aggacagtat ttggtatctg

7381 cgctctgctg aagccagtta ccttcggaaa aagagttggt agctcttgat ccggcaaaca

7441 aaccaccgct ggtagcggtg gttttttgt ttgcaagcag cagattacgc gcagaaaaaa

7501 aggatctcaa gaagatcctt tgatcttttc tacggggtct gacgctcagt ggaacgaaaa

7561 ctcacgttaa gggattttgg tcatgagatt atcaaaaagg atcttcacct agatcctttt

7621 aaattaaaaa tgaagtttta aatcaatcta aagtatatat gagtaaactt ggtctgacag

7681 ttaccaatgc ttaatcagtg aggcacctat ctcagcgatc tgtctatttc gttcatccat

7741 agttgcctga ctccccgtcg tgtagataac tacgatacgg gagggcttac catctggccc

7801 cagtgctgca atgataccgc gagacccacg ctcaccggct ccagatttat cagcaataaa

7861 ccagccagcc ggaagggccg agcgcagaag tggtcctgca actttatccg cctccatcca

7921 gtctattaat tgttgccggg aagctagagt aagtagttcg ccagttaata gtttgcgcaa

7981 cgttgttgcc attgctacag gcatcgtggt gtcacgctcg tcgtttggta tggcttcatt

8041 cagctccggt tcccaacgat caaggcgagt tacatgatcc cccatgttgt gcaaaaaagc

8101 ggttagctcc ttcggtcctc cgatcgttgt cagaagtaag ttggccgcag tgttatcact

8161 catggttatg gcagcactgc ataattctct tactgtcatg ccatccgtaa gatgcttttc

8221 tgtgactggt gagtactcaa ccaagtcatt ctgagaatag tgtatgcggc gaccgagttg

8281 ctcttgcccg gcgtcaatac gggataatac cgcgccacat agcagaactt taaaagtgct

8341 catcattgga aaacgttctt cggggcgaaa actctcaagg atcttaccgc tgttgagatc

8401 cagttcgatg taacccactc gtgcacccaa ctgatcttca gcatctttta ctttcaccag

8461 cgtttctggg tgagcaaaaa caggaaggca aaatgccgca aaaaagggaa taagggcgac

8521 acggaaatgt tgaatactca tactcttcct ttttcaatat tattgaagca tttatcaggg

8581 ttattgtctc atgagcggat acatatttga atgtatttag aaaaataaac aaataggggt

8641 tccgcgcaca tttccccgaa aagtgccac

//

LIST OF ATTACHED PUBLICATIONS AND MANUSCRIPTS

1. **Qing Zhao, Irem Mertová, Aneta Wróblová, Světlana Žabková, Tereza Tlapáková, and Vladimir Krylov** (2024). Immunomodulatory role of *Xenopus tropicalis* immature Sertoli cells in tadpole muscle regeneration via macrophage response modulation. *Stem Cell Research & Therapy* **15**,.

2. **Qing Zhao, Světlana Žabková, Jakub Onhajzer, Tereza Tlapáková, Vladimír Krylov**. Immature Sertoli Cells promote Heart Regeneration via Macrophage Modulation in *Xenopus tropicalis*. (Manuscript finished, to be published)